# *Production and characterization of loaded smart-microcapsules, performance evaluation and industrialization of supercritical $CO_2$ based processes*

**Ida Palazzo**

# UNIVERSITY OF SALERNO



## *DEPARTMENT OF INDUSTRIAL ENGINEERING*

*Ph.D. Course in Industrial Engineering*
*Curriculum in Chemical Engineering - XXXIII Cycle*

### *PRODUCTION AND CHARACTERIZATION OF LOADED SMART-MICROCAPSULES, PERFORMANCE EVALUATION AND INDUSTRIALIZATION OF SUPERCRITICAL CO$_2$ BASED PROCESSES*

**Supervisor**                                    **Ph.D. student**
*Prof. Ernesto Reverchon*              *Ida Palazzo*

**Scientific Referees**
*Prof. Roberta Campardelli*
*Ing. Modestino De Feo (TOTAL MS)*
*Prof. Giovanna Della Porta*

**Ph.D. Course Coordinator**
*Prof. Francesco Donsì*

# Publication List

## International Journals

1) **Palazzo I.**, Campardelli R., Scognamiglio M., Reverchon E., *'Zein/luteolin microcapsules coprecipitation with a technique assisted by supercritical fluids'*,. Palazzo I., Campardelli R., Scognamiglio M., Reverchon E., 'Zein/luteolin microcapsules coprecipitation using a supercritical fluids assisted technique, Powder Technology, 356 (2019) 899-908, doi.org: 10.1016/j.powtec.2019.09.034.

2) Gimenez-Rota C., **Palazzo I.**, Scognamiglio M., Mainar A., Reverchon E., Della Porta G., *'β-Carotene, α-Tocoferol and Rosmarinic Acid encapsulated within PLA/PLGA microcapsules to improve drug shelf-life and antioxidant activity'*, The Journal of Supercritical Fluids, 146 (2019) 199-207.

3) Tirado D.F., **Palazzo I.**, Scognamiglio M., Calvo L., Della Porta G, Reverchon, E., *'Astaxanthin encapsulation in ethyl cellulose carriers by continuous supercritical emulsions extraction: A study on particle size, encapsulation efficiency, release profile and antioxidant activity'*, The Journal of Supercritical Fluids, 150 (2019) 128-136, doi.org:10.1016/j.supflu.2019.04.017

4) **Palazzo I.**, Della Porta G., Raimondo M., Guadagno L., Reverchon E.,*' Encapsulation of Health-Monitoring Agent in Poly-Methyl-Methacrylate Microcapsules using Supercritical Emulsion Extraction'*, Journal of Industrial and Engineering Chemistry, 90 (2020) 287-299

5) **Palazzo, I.**, Trucillo, P., Campardelli, R., Reverchon, E., *'Antioxidants entrapment in polycaprolactone microparticles using supercritical assisted injection in a liquid antisolvent'*, Food and Bioproducts Processing, 123 (2020), 312-321.

6) Govoni, M., Lamparelli, E.P., Ciardulli, M.C., Santoro, Oliviero, A, **Palazzo I.**, Reverchon E., Vivarelli L., Maso A., Storni E., Donati M.E., Ruspaggiari, G., Maffulli, N., Fini, M., Della Porta G., Dallari D., *'Demineralized bone matrix paste formulated with biomimetic PLGA microcarriers for the vancomycin hydrochloride controlled delivery: Release profile, citotoxicity and efficacy against S. aureus'*, International Journal of Pharmaceutics, 582 (2020), 119322

7)  **Palazzo I.**; Lamparelli E.P.; Ciardulli M.C.; Scala P.; Maffulli N.; Reverchon E.; Santoro A., Della Porta G:, *'PLA/PLGA carriers designed for the Growth Factors sustained delivery by Supercritical Emulsion Extraction: size engineering, release profiles study and cytotoxicity evaluation'*, International Journal of Pharmaceutics, 592 (2021),120108.

# Proceedings

1) **Palazzo I.**, Ciardulli M.C., Santoro A., Maffulli N., Reverchon E., Della Porta G., Micro/nano-carriers engineering for the controlled release of bio-actives,. , 8° ISMuLT Congress 2018: 30th November-1St December 2018, Salerno, Italy.

2) Ciardulli M.C., Marino L., **Palazzo I.,** LoVecchio J., Giordano E., Selleri C., Maffulli N., Della Porta G., Tenogenic commitment of Mesenchymal Stem Cells in a 3D scaffold and dynamic culture , 8° ISMuLT Congress 2018: 30th November-1St December 2018, Salerno, Italy.

3) **Palazzo I.**, Ciardulli M.C., Santoro A., Maffulli N., Reverchon E., Della Porta G., Supercritical Emulsion Extraction technology: a case study on PLGA/PLA micro/nano-carriers engineering for the controlled release of bio-actives, 8° ISMuLT Congress 2018: 30th November-1St December 2018, Salerno, Italy.

4) Ciardulli M.C., Marino L., Lo Vecchio J., **Palazzo I.**, Santoro A., Reverchon E., Giordano E., Selleri C., Maffulli N., Della Porta G., hGDF-5 and cyclic strain controlled delivery for the tenogenic commitment of hBM-MSCs in a 3D microenviroment, 8° ISMuLT Congress 2018: 30th November-1St December 2018, Salerno, Italy.

5) **Palazzo I.**, Campardelli R., Reverchon E., Microcapsules production with supercritical fluid assisted technique: antioxidant encapsulation case study, Gricu PhD National School 2018, May 16 th -19 th 2018, Pisa, Italy.

6) Welcome Day Total PhD students - Journée d'accueil Doctorants, 8 March 2018, Paris (France)

7) Tirado D.F., **Palazzo I.,** Scognamiglio M., Calvo L., Della Porta G, Reverchon, E., The Encapsulation of Astaxanthin in Ethyl Cellulose By Continuous Supercritical Emulsions Extraction, 17th European Meeting on Supercritical Fluids - 7th European Meeting on High Pressure Technology, April 8th-9th 2019, Ciudad Real, Spain.

8) **Palazzo I.**, Ciardulli M.C., Santoro A., Maffulli N., Reverchon E., Della Porta G., *hGDF-5 encapsulation within PLGA and PLA nanocarriers using Supercritical Emulsion Extraction technique*, 17th European Meeting on Supercritical Fluids - 7th European Meeting on High Pressure Technology, April 8th-9th 2019, Ciudad Real, Spain.

9)   Giménez-Rot C., **Palazzo I.**, Scognamiglio MR, Mainar A., Reverchon E., Della Porta G., β-Carotene, α-Tocoferol and Rosmarinic Acid PLA/PLGA capsules: drug shelf-life and antioxidant activity, 17th European Meeting on Supercritical Fluids - 7th European Meeting on High Pressure Technology, April 8th-9th 2019, Ciudad Real, Spain.

10)  **Palazzo I.**, Della Porta G., Reverchon E., β-carotene encapsulation in biopolymer microspheres using supercritical emulsions extraction, Gricu 2019, July 4th -7th 2019, Mondello, Palermo, Italy.

11)  S. Orfanidis, M. Raimondo, L. Guadagno, **I. Palazzo**, E. Reverchon, A.S. Paipetis, M. Fardis, G. Papavasilliou, *Detection of the diffusion properties of the encapsulated health-monitoring agent in advanced protective coatings: A solid-state NMR study*, 10th EASN Virtual International Conference, September 2020.

12)  **I. Palazzo,** E.P. Lamparelli, E. Reverchon, N.Maffulli, A. Santoro, G. Della Porta, *PLA/PLGA nanocarriers designed for tissue engineering application and fabricated by Supercritical Emulsion Extraction*, NanoInnovation 2020, , September 15th-18th 2020, Rome, Italy.

*A mio figlio Gerardo,*
*la luce dei miei occhi,*
*il mio piccolo guerriero*

# Contents

# Figure Index

XVI

XVIII

# Table Index

# Abstract

In the last years, scientists and engineers have designed a wide range of polymeric systems capable responding to internal or external stimuli. There is a great range of responsive polymers that are sensitive to different stimuli such as light, temperature, electric field, magnetic field, pH and chemicals, etc. This kind of polymers are usually called also "smart polymers" or "intelligent polymers"; they have many applications in biology and medicine fields and can be used as sensor and biosensors, for controlled and trigger drug delivery, environmental remediation, chemo-mechanical actuators, and others.

Among several use of smart polymers, their use as micro and nano structured devices in nutraceutical and pharmaceutical field, in rigenerative medicine, in the oil-gas industry and, for example, in the lubricants field, in the *self-healing* is very interesting and still poorly investigated.

In detail, a new approach for protection of the additives from thermo-oxidative degradation was proposed, using additive loaded microcapsules produced using a supercritical techinique. These structures can allow to enhance the stability and to prolong the lifetime of the additives, reducing their volatility and reactivity and/or to maintain the additive concentration constant during operation, controlling their release. Two additives proposed by Total were studied: an antioxidant (AM) and a friction modifier (MoDTC). Spherical and regular nanocapsules with mean diameters of $195\pm12$ nm-$189\pm10$ nm and AM loading of 0.4 g- 0.73 g AM/g PMMA with EE of 57-95% were produced using Supercritical Emulsions Extraction (SEE-C) process. AM loaded microcapsules the microcapsules showed a good dispersability in base oil and the release of AM is responsive to pH level but also to temperature. Spherical and homogeneous PMMA loaded capsules were produced also using MoDTC. In this case, particles with mean diameter $187\pm23$ nm and EE of 90% were obtained.

Regarding the self-healing application, a protective coating for aerospace and automative applications with the intrinsic capability to highlight damages suffered during the operating conditions, using an efficient and green process to produce microcapsules acting as a health-monitoring visual element is proposed. SEE-C technology was used to encapsulate a health-monitoring mixture based on DiGlycidyl Ether of Bisphenol A (DGEBA), dyed with Solvent Red 242, in polymethylmethacrylate polymer (PMMA). A comparison between SEE-C and Solvent Evaporation (SE) was also carried out in term of particle size distribution (PSD), encapsulation efficiency (EE) and stability in the time (TS) of the produced microcapsules. Larger microcapsules, with the size up to 726 nm and the EE below 57% were produced using the SE technology. The best results were obtained using

SEE-C: spherical microcapsules with unwrinkled and smooth surface were obtained with mean size of 220 nm and EE up to 79 % using SEE-C. SEE-C capsules preserve their stability for the entire time frame analyzed of 30 days.

The protective coating was very sensitive in showing stress areas: impact tests carried out on strips of Carbon Fiber Reinforced Composites (CFRCs) coated with a green aqueous paint in which the SEE-C capsules were previously dispersed showed dye leaking associated with capsule breaking in the stressed areas, even using the low impact energies of 3.8 J and 4.5 J.

Controlled delivery of human growth factors is still a challenge in tissue engineering protocols, and poly-lactic acid and poly-lactic-co-glycolic acid carriers have been recently proposed for this purpose. In this study, the microencapsulation of two human growth factors, namely Growth Differentiation Factor -5 (hGDF-5) and Transforming Growth Factor β1 (hTGF-β1), by processing different emulsions using SEE-C technology. Polymer molecular weight, co-polymer ratio and surfactant amount in aqueous phases as well as phases mixing rate were varied to fabricate carriers with suitable size and loadings.

Carriers with different mean size from 0.4 ±0.09 μm up to 3±0.9 μm were obtained by SEE-C technology when processing emulsions with different formulations; carriers were also loaded with 3 μg/g and 7μg/g for hGDF-5 and hTGF-β1 and they assured both growth factors controlled release along 25 days. Carriers showed also reduced cytotoxicity when evaluated in Chinese Hamster Ovary cells (CHO-K1); interestingly, they also exhibited a reduced cytotoxicity whit respect to carriers obtained by conventional evaporation technique, and also a low reactivity on human peripheral blood mononuclear cells (hPBMCs), suggesting their safety and potential use in tissue engineering protocols.

Finally, the production of composite microspheres loaded with bioactive compounds has been another important challenge handled in this Ph.D. work. In particular, astaxanthin and beta-carotene were selected in this framework for their nutraceutical properties. The main outcome of this investigation was not only the improvement of the bioavailability, but also the protection of the antioxidant activity and shelf life of the bioactive compound. Defined and spherical particles were produced by means of the SEE-C technique using Ethyl Cellulose, PLA and PLGA as carriers.

In detail, the SEE-C technology was used to encapsulate astaxanthin in ethyl cellulose (EC), obtained particles with mean size of 363 nm and encapsulation efficiency up to 84%. β-Carotene (β-CA) was encapsulated into poly-lactic-co-glycolic acid (PLGA) and poly-lactic acid (PLA) carriers using SEE-C. α-Tocoferol (α-TOC) and Rosmarinic Acid (RA) were proposed as excipients to improve the formulation. PLA and PLGA carriers with sizes ranges between 1.5±0.5 μm and 0.3±0.07 μm were fabricated with encapsulation efficiencies between 50-80%. The co-encapsulation of α-TOC

with β-CA gained to prolonged drug shelf life. Both systems preserved their antioxidant activity against light, heat and oxygen.

In conclusion, the SEE-C technique was successfully applied for production of smart microcapsules in several fields, demonstrating to be an attractive and available process from an industrial point of view.

# Abstract

Negli ultimi anni, scienziati e ingegneri hanno progettato un'ampia gamma di sistemi polimerici in grado di rispondere a stimoli interni o esterni. Esiste una vasta gamma di polimeri reattivi che sono sensibili a diversi stimoli come luce, temperatura, campo elettrico, campo magnetico, pH e sostanze chimiche, ecc. Questo tipo di polimeri sono solitamente chiamati anche "polimeri smart" o "polimeri intelligenti", hanno molte applicazioni nei campi della biologia e della medicina e possono essere utilizzati come sensori e biosensori, per la somministrazione controllata di farmaci, risanamento ambientale, attuatori chemio-meccanici ed altro.

Tra i vari utilizzi dei polimeri intelligenti, molto interessante è il loro impiego come dispositivi micro e nano strutturati in campo nutraceutico e farmaceutico, nella medicina rigenerativa, nell'industria oil-gas; ad esempio, nel campo dei lubrificanti e del *self healing* essi sono ancora poco investigati.

In dettaglio, in questo lavoro di tesi è proposto un nuovo approccio per la protezione degli additivi dalla degradazione termo-ossidativa, utilizzando microcapsule caricate con additivi e prodotte utilizzando una tecnica supercritica. Queste strutture possono consentire di aumentare la stabilità e prolungare la vita degli additivi, riducendo la loro volatilità e reattività, mantenendone costante la concentrazione durante il funzionamento e controllandone il rilascio. Sono stati studiati due additivi proposti da Total: un antiossidante (AM) e un modificatore di attrito (MoDTC). Nanocapsule sferiche e regolari con diametri medi di $195\pm12$ nm-$189\pm10$ nm, con rapporto g AM/g PMMA 0.4- 0.73 ed EE del 57-95% sono state prodotte utilizzando il processo di estrazione con emulsioni supercritiche (SEE-C). Le microcapsule caricate con AM hanno mostrato una buona disperdibilità nell'olio base e il rilascio dell'additivo risulta sensibile alla variazione di pH ma anche di temperatura. Capsule sferiche ed omogenee caricate in PMMA sono state prodotte anche utilizzando MoDTC. In questo caso sono state ottenute particelle con diametro medio $187\pm23$ nm ed EE del 90%.

Per quanto riguarda l'applicazione *self healing*, è stato proposto un rivestimento protettivo per applicazioni aerospaziali con la capacità intrinseca di evidenziare i danni subiti durante le condizioni operative, utilizzando un processo efficiente e *green* per produrre microcapsule che fungono da elemento visivo di monitoraggio dello stato di usura. La tecnologia SEE-C è stata utilizzata per incapsulare una miscela di monitoraggio a base di diglicidil etere di bisfenolo A (DGEBA), tinto con Solvent Red 242, in polimetilmetacrilato (PMMA). È stato inoltre effettuato un confronto tra la tecnica SEE-C e la tecnica convenzionale di evaporazione del Solvente (SE) in termini di distribuzione granulometrica (PSD), efficienza di incapsulamento (EE) e stabilità nel tempo (TS) delle

microcapsule prodotte. Microcapsule più grandi, con dimensioni fino a 726 nm e EE inferiori al 57% sono state prodotte utilizzando la tecnologia SE. I migliori risultati sono stati ottenuti utilizzando la tecnica SEE-C: sono state ottenute microcapsule sferiche con superficie liscia, dimensione media di 220 nm ed EE fino al 79%. Le capsule SEE-C conservano la loro stabilità per l'intero arco temporale analizzato di 30 giorni.

Sono stati effettuati test di impatto eseguiti su strisce di compositi rinforzati con fibra di carbonio (CFRC) rivestiti con una vernice acquosa in cui le capsule SEE-C sono state precedentemente disperse. Il rivestimento protettivo è risultato sensibile ai test di impatto e ha consentito di mostrare le aree di stress che hanno evidenzito perdite di colorante associate alla rottura della capsula nelle aree sollecitate, anche utilizzando le energie a basso impatto di 3,8 J e 4,5 J.

La somministrazione controllata di fattori di crescita umana è ancora una sfida nei protocolli di ingegneria tissutale e recentemente sono stati proposti a questo scopo carrier di acido polilattico (PLA) e acido polilattico-co-glicolico (PLGA). In questo studio è stato proposta la microincapsulazione di due fattori di crescita umani, il fattore di crescita differenziale-5 ($h$GDF-5) e il fattore di crescita trasformante β1 (hTGF- by1), elaborando diverse emulsioni utilizzando la tecnologia SEE-C. Il peso molecolare del polimero, il rapporto del copolimero e la quantità di tensioattivo nelle fasi acquose nonché la velocità di miscelazione delle fasi sono stati variati per fabbricare carrier con dimensioni e carichi adeguati.

Con la tecnologia SEE-C sono stati ottenuti carriers di dimensioni medie da $0.4 \pm 0.09$ μm fino a $3 \pm 0.9$ μm utilizzando emulsioni con formulazioni diverse; le microcapsule sono state inoltre caricatie con 3 μg/ge 7 μg/g di $h$GDF-5 e $h$TGF-β1 e hanno assicurato il rilascio controllato di entrambi i fattori di crescita per 25 giorni. I carrier hanno anche mostrato una ridotta citotossicità quando sono stati messi a contatto con cellule ovariche di criceto cinese (CHO-K1), ridotta citotossicità rispetto ai vettori ottenuti con la tecnica di evaporazione convenzionale, e anche una bassa reattività sulle cellule mononucleate del sangue periferico umano ($h$PBMC), suggerendo la loro sicurezza e il potenziale utilizzo nei protocolli di ingegneria tissutale.

Infine, la produzione di microsfere composite caricate con composti bioattivi è stata un'altra importante sfida affrontata in questo lavoro di dottorato. In particolare, in questo campo sono stati selezionati astanxantina e beta-carotene per le loro proprietà nutraceutiche. Il principale risultato di questa indagine non è stato solo il miglioramento della biodisponibilità, ma anche la protezione dell'attività antiossidante e della durata di conservazione del composto bioattivo. Particelle definite e sferiche sono state prodotte mediante la tecnica SEE-C utilizzando etilcellulosa, PLA e PLGA come carriers polimerici.

In dettaglio, la tecnologia SEE-C è stata utilizzata per incapsulare l'astaxantina in etilcellulosa (EC), ottenendo particelle con dimensione media

di 363 nm ed efficienza di incapsulamento fino all'84%. Il β-carotene (β-CA) è stato incapsulato in PLGA e PLA utilizzando la tecnicas SEE-C. L'α-tocoferolo (α-TOC) e l'acido rosmarinico (RA) sono stati proposti come eccipienti per migliorare la formulazione. Particelle di dimensioni comprese tra $1.5 \pm 0.5$ μm e $0.3 \pm 0.07$ μm sono state prodotte con efficienze di incapsulamento tra il 50 e l'80%. La co-incapsulazione di α-TOC con β-CA ha consentito di prolungare la durata di conservazione del farmaco. Entrambi i sistemi hanno conservato la loro attività antiossidante preservando il principio attivo dalla degradazione di luce, calore e ossigeno.

In conclusione, la tecnica SEE-C è stata applicata con successo per la produzione di microcapsule intelligenti in diversi campi, dimostrandosi un processo interessante dal punto di vista industriale.

# Introduction

Polymers are present in the objects we use in everyday life and they have been used to improve the quality of life for ages. In the years, scientists and engineers have designed a wide range of polymeric systems capable of undergoing changes responding to internal or external stimuli. In particular, stimuli-responsive polymers (SRPs) are synthetic macromolecules that undergo changes in their properties in response to a defined external stimulus. There is a great range of responsive polymers that are sensitive to different stimuli (triggers) such as light (Jiang et al., 2006), temperature (Heskins and Guillet, 1968), electric field (Asaka and Oguro, 2000) , magnetic field (Xulu et al., 2000), pH (Feil et al., 1992, Dai et al., 2008), chemicals, etc. Additionally, SRPs can be designed that exhibit responses to more than one type of stimuli, a combination of two or more single stimuli, such as temperature and pH-responsive systems or light and temperature responsive polymers (Almeida et al., 2012). The types of responses associated with the stimuli also can vary greatly, including structural changes, sol-gel transitions, changes in optical properties, solubility changes, micelle formation, etc (Kumar et al., 2007). The behavior of SRPs is comparable to that of certain natural macromolecules (such as proteins, DNA and RNA) (Kauffman, 1988). This kind of polymers are usually also called "smart polymers" or "intelligent polymers" because they are systems capable of undergoing changes responding to internal or external stimuli (Aguilar and San Román, 2014, Faisant et al., 2006). The changes mainly include structure and property variations and for this reason, chemists have produced synthetic polymers or modified natural polymers with well-controlled polymer composition, architecture, and predictable property upon exposure to different stimuli. One important feature of this type of material is reversibility, for example the ability of the polymer to return to its initial state upon of a counter-trigger. In nature, biopolymers such as proteins and nucleic acids are all basic stimuli-responsive components of living organic systems and often remain stable over wide ranges of external variables, but undergo drastic conformational changes abruptly at given critical points (Kumar et al., 2007). Due to the controlled properties brought about by

minor environmental changes, stimuli-responsive polymers can be potentially utilized in many fields. Such intelligent polymers have found many applications in the fields of biology and medicine and can be used as sensor and biosensors (Hu and Liu, 2010), for controlled and trigger drug delivery (Bajpai et al., 2008), environmental remediation (Parasuraman and Serpe, 2011), chemo-mechanical actuation (Ma et al., 2013, Zhao et al., 2014) and for many other applications (Koerner et al., 2004, Wang et al., 2004). Biocompatible polymers with stimuli-responsive behavior are very useful also in bio-separation and bio-catalysis (Sharma et al., 2003). A surface grafted with stimuli-responsive polymers has been highlighted for its interfacial and wetting applications. For example, a smart surface with reversible, switchable wettability could be potentially used in controlled transportation of fluids and water-proof coatings (Xin and Hao, 2010, Xia et al., 2009). Stimuli-responsive polymers based on catalytic systems have been widely employed as the recyclable catalyst for organic synthesis. Stimuli-responsive polymers have been mainly emphasized for their potential applications in nanoscience, nanotechnology, and nanomedicine (Kumar et al., 2007, Almeida et al., 2012). Currently, the most exciting innovations using smart polymers have been introduced in the biomedical field (Almeida et al., 2012).

Stimuli-responsive polymers also find application in regenerative medicine. In this regard, they can be classified into polymers for the design of smart surfaces, and polymers that undergo sol–gel transitions for injectable implants. Smart surfaces may be used as supports or scaffolds, with excellent controllability of surfaces properties, that can, in turn, be used for adsorption and desorption of biomacromolecules and cells. It is known that cell behavior and attachment is greatly influenced by the wettability of a surface, and that biomacromolecules have higher affinity for hydrophobic surfaces. Therefore, depending on the application, stimuli-responsive polymers grafted on surfaces provide possibilities to design scaffolds for tissue engineering.

Cells in tissues grow in a rather complex fashion, surrounded by an extracellular matrix (ECM) that plays an essential role as a support. In addition, ECM elicits a wide range of biological signals and releases various biological factors, controlling both cell behavior and proliferation. In order to build viable cell sheets for tissue engineering, synthetic materials should mimic functionalities, similar to ECM. Thus, the use of stimuli-responsive polymers to design smart surfaces as ECM biomimetic materials to be used as scaffolds for the growth of new cells and tissue engineering is currently a fast growing research area. In order to advantageously replace other existing materials and allow the growth and proliferation of cell sheets, smart surfaces should display reversible changes in their affinity for biomolecules and their cell adhesion properties, as well as provide sustained release of biomacromolecules. Although polymer substrates have been used previously

XXX

in cell culture (with polystyrene, for instance), the use of stimuli-responsive polymers represents a gentler alternative to mechanical or enzymatic digestion (protease) for cell detachment procedures needed in these systems. It guarantees the collection of intact cell sheets using a noninvasive cell recovery method, and these cell sheets can then be implanted in the body for tissue engineering applications.

The immobilization and programmed release of biologically active agents is desirable in order to promote cell adhesion and direct cell behavior. Such molecules can be hosted on smart surfaces via electrostatic interactions, conjugation, or encapsulation. Release of proteins was shown using ionic strength-sensitive (Anikin et al., 2005) and thermo-responsive systems (Nath and Chilkoti, 2003, Comolli et al., 2009, Kim and Lee, 2009, Frey et al., 2003, Hyun et al., 2004, Cunliffe et al., 2003).

Most of these systems are used exclusively for in vitro cell cultures, followed by cell desorption: for in vivo use, surgery must be performed to implant the cell sheets. To avoid this, a class of materials known as injectable implants is used. These systems are based on the gelation of a polymer solution upon injection into the body, and can promote cell delivery or other useful therapeutic agents such as growth factor.

The basis for using injectable polymers is that the matrix temporarily replaces damaged tissue, allowing proliferation and growth of cells until a new cell sheet or extracellular matrix is produced on site. Among the physiological stimuli used for gelling, temperature is the most studied and the most advantageous for in vivo application, due to its ease of use.

Mesenchymal stem cells embedded in the copolymer solution were able to differentiate into chondrocytes (cells found in cartilaginous matrix) in vitro.

Self-healing materials represent a new paradigm of active and responsive materials (Guadagno et al., 2011, Wu et al., 2008). Self-healing has received much interest in intelligent material science because they play a critical role in determining the security, reliability and long-term durability of materials. The self-healing in materials is different from the traditional methods of material repair, including welding and patching. They do not require reliable detection techniques or a special technique for mending materials. Such recovery can occur autonomously or be activated after an application of a specific stimulus (e.g., heat and radiation). One of the most promising and useful approaches to prepare self-healing materials is the incorporation of healing agents into the material, which endows the material with the ability to heal after a damage event.

Structural health monitoring (SHM) concerns the process of activating damage detection and a characterization strategy for engineering structures. In particular, SHM aims at developing new methodologies to determine the structural integrity of aeronautical components. It is worth noting that the growing use of composite materials for which the damage originates and

evolves in a different way than in the homogeneous ones, requires new techniques aimed at assessing the performance of the most crucial components to be developed. Several process strategies have been proposed. Conductive nanoparticles based on carbon, incorporated in coatings or bulk materials have been proposed to confer self-sensing to the materials and for the damage monitoring at nano/micro-scale level (Guadagno et al., 2011, Hargou et al., 2013). Another approach is related to capsule-based strategies in which a chromophore is contained that is capable of revealing the damage.

The potential for oil-gas industrial applications of stimuli-responsive polymers are not as widely investigated (Wever et al., 2011). The oil-gas industry or petroleum industry, which includes the global processes of exploration, production, transportation, refining, and petrochemical synthesis represents the world's largest industry. Today, it is still the primary source of energy in the world. Indeed, petrochemicals, chemicals derived from the petroleum or natural gas, play a very important role in today's chemical industry. Plastics, fertilizer, solvent, pharmaceuticals, and other chemical products mainly come from petrochemical feedstocks.

Aside from relying on new and sophisticated electronics, simulation tools, new metallic alloys, the utilization of new high performance, "smart" polymers and multifunctional materials can be fundamental for the improvement of oil-gas industry. The rapid progress of design and synthesis of new stimuli-responsive polymers with controlled properties offers a wide range of possible applications. The industry already widely uses polymers as pipes, coatings, thermosets, thermoplastics, elastomers, and calls them "non-metallics." Their performance and failure is widely studied due to their importance as components such as hoses, pipes, packers, liners, coatings, and parts in blow-out preventers (BOP), completion tools, and subsea engineering components. A main advantage is their lack of corrosive parts.

Recently, stimuli-responsive polymers have been reported for enhanced oil recovery (EOR) processes (Philippova and Khokhlov, 2010). With precise property-control upon minor environmental changes, smart polymers can have great potential in other areas of oil-gas production such as drilling fluids, stimulation, flow-assurance, anti-corrosion, anti-scaling, asphaltene control, polymeric cements, coatings, de-emulsification, etc.

Despite the numerous review papers published recently on stimuli-responsive polymer and their use in several fields, the topic specifically on stimuli-responsive polymers and their application for oil-gas industry has been less studied (Morgan and McCormick, 1990, ShamsiJazeyi et al., 2014).

Nowadays, a significant interest in incorporating micronutrients (bioactive compounds) into functional food and beverage products has increased to benefit human health and wellness through the diet (Handford et al., 2014). These micronutrients include vitamins, minerals, flavors, antioxidants, antimicrobials, polyphenols, probiotics, prebiotics and

XXXII

preservatives. Some of these micronutrients are essential for human well-being (such as vitamins), whereas other substances derived from food sources provide health benefits in addition to diet (*nutraceuticals*) (Joye et al., 2014, Handford et al., 2014). Various bioactive compounds have been obtained from natural sources, for examples vegetables, fruits, legumes, oil and have shown beneficial effects on human health including antioxidant, anti-inflammatory, and antibacterial activities (Recharla et al., 2017). A recent tendency is the recovery of these bioactive compounds also from wastes derived by food industry. Indeed, the processing of plant foods results in the production of a large volume of by-products that is still rich in bioactive compounds that can be recovered. These residues could be an alternative source for obtaining natural antioxidants, which are considered completely safe in comparison with synthetic ones (Murthy and Naidu, 2012, Lafka et al., 2007, Balasundram et al., 2006, Guamán-Balcázar et al., 2019, Meneses et al., 2015).

However, bioactive compounds cannot be incorporated in their pure state into commercial food products, due to their susceptibility to physical, chemical and enzymatic degradation (Coronel-Aguilera and San Martín-González, 2015). Furthermore, the performance of these substances can be affected by light, heat, water and oxygen exposure, compromising their activity and shelf-life (Handford et al., 2014). Solid formulations consisted of the incorporation of bioactive compounds in polymeric matrices are gaining increasing interest by food industry, representing a suitable method to stabilize and protect the bioactive compound from environmental conditions (Champagne and Fustier, 2007, Franceschi et al., 2008, Janiszewska-Turak, 2017, de Paz et al., 2012, Priamo et al., 2011, Guamán-Balcázar et al., 2019).

Conventional methods, including emulsion/solvent evaporation, thermal gelation, hot homogenization technique, coacervation, spray drying, freeze-drying, antisolvent precipitation, in situ polymerization, jet milling have been used to obtain particle size reduction, solid dispersions and encapsulation of active principles in different carriers. However, these strategies are not always suitable or feasible and may show some drawbacks (Campardelli et al., 2015), such as the production of coarse particles with broad particle size distribution, the degradation of the product due to mechanical or thermal stresses, or its contamination with organic solvents or other toxic substances, low loading efficiencies and difficulty in scale up (Martín and Cocero, 2008, Temelli, 2018). In particular, emulsification and solvent evaporation need a large use of heavy and toxic organic solvents; furthermore, to reduce the residual organic solvent below the safety limits, many downstream processes, such as additional drying step, have to be performed. Even spray drying has some limitations: uses of large amount of toxic organic solvents, high temperatures to remove solvents, possible

degradation of the active product due to the thermal stress and production of particles with wide particle size distribution.

In recent years, the application of supercritical-carbon dioxide (SC-CO$_2$) based processes has attracted great attention as a valid alternative to traditional techniques (Cocero et al., 2009, Campardelli et al., 2015). These SC-CO$_2$ based techniques have been successfully applied in several fields: among them, micronization, membranes, scaffold production (Cocero et al., 2009, Campardelli et al., 2015, Baldino et al., 2014a, Baldino et al., 2014b, Reverchon and Della Porta, 2003, Prosapio et al., 2015, Franceschi et al., 2008, Adami et al., 2017, Adami et al., 2012, Adami and Reverchon, 2012, Martin et al., 2013, Meneses et al., 2015, Reverchon et al., 2015, Wu et al., 2009). Among the SC-CO$_2$ based processes, Continuous Supercritical Emulsion Extraction (SEE-C) process has been applied to produce nanocarriers, such as polycaprolactone, poly(L-lactide) and polylactic-co-glycolic acid, but, also, to prepare particles encapsulating magnetite, proteins, peptides and drugs (Campardelli et al., 2015, Reverchon et al., 2015, Reverchon et al., 2009). In SEE process, the SC-CO$_2$ was used for the selective extraction of the organic phase from a single or double emulsion producing nano and microparticles and microcapsules. A solute is dissolved in a suitable solvent to form a solution; the solution is then dispersed into an immiscible or partially miscible liquid to form an emulsion. Extracting selectively the solvent from the oil phase of the emulsion, the SEE-C process produces an aqueous colloidal suspension of particles. SC-CO$_2$ extraction has a relatively faster extraction rate compared to extraction rates of other conventional techniques (processing in minutes instead of several hours), and this allows the formation of relatively smaller particles, with narrow size distributions, and very small solvent residues.

In these fields, the SEE-C process may be an efficient alternative for the production of formulations based on active compounds loaded in different carrier matrix in order to develop new smart micro and subcapsules able to response to external stimuli such as pH, mechanical stress and biological environment. The challenge is to apply the SEE-C process in a very interesting domain, as industrialization one.

## *Aim of the thesis*

The purpose of this PhD work is to adopt a process based on SCF, capable of producing smart microcapsules for different fields of industrial application. The supercritical emulsion extraction process, recently proposed in the literature, has been successfully applied to the production of biopolymeric microparticles and microspheres for the encapsulation of different drugs, proteins, growth factors. Light sensitive drug delivery

devices was also produced with this technique. In particular, Titanium oxide (activated by UV light) and Gold (activated by NIR irradiation) nanoparticles were loaded in PLA nanocomposite devices for photodynamic therapy of cells and photothermally controlled drug delivery respectively. However, submicro and nanocapsules using smart polymers have not yet been produced with this technique. For this reason, a part of the work will be focused on the optimization of the process condition for the production of monodisperse submicro and nanospheres of different smart polymer. The production of smart microcapsules is poorly investigated and discussed in SEE-C literature. Therefore, this Ph.D. work regards the recent advances in the application of this supercritical fluid technology for the production of new solid formulations that can be applied in several industrial fields, in particular regenerative medicine, pharmaceutical, oil-gas industries and self healing materials for aereospace applications.

This Ph.D. work has been supported and granted by Total, a French multinational integrated oil and gas company and one of the seven "Supermajor" oil companies in the world. Its businesses cover the entire oil and gas chain, from crude oil and natural gas exploration and production to power generation, transportation,refining, petroleum product marketing, and international crude oil and product trading. Total is also a large  scale chemicals manufacturer. In the frame of the research collaboration between Total and the Department of Industrial Engineering (DIIN) of the University of Salerno, a part of this work of thesis has concerned the development of microcapsules formulations using additives proposed by the Company, in order to scale up SEE process for industrialization purposes. Due to secrecy agreements, these active substances are presented using acronyms and no further detailed information is reported. Two different additives are tested on behalf of Total: monoalkyl amine ethoxylated (AM, used to control the acidity of the lubricant oil) and MoDTC (a friction modifier). For each of these additives, a systematic study is performed to optimize SEE-C process conditions aimed at the specific targets requested by the Company. In particular, the Chapter III of this work of thesis presents the results achieved in the frame of this research collaboration, which are aimed to validate the SEE-C industrialization.

To investigate in depth the applicability of SEE-C process in the development of new and smart microcapsules formulations in the fields of self-healing materials, the encapsulation of a structural health monitoring agent will be proposed. This fields of application was not explored in SEE-C literature and in general in processes based on SCF, for this purpose a comparison between SEE process and conventional solvent evaporation will be performed.

Another aspect still poorly explored in SEE-C literature regards the application of this well-known technology in a smart research field, like the

regenerative medicine one. Therefore, the aim of this part of Ph.D. work has been to test the applicability of the SEE-C process in the production of complex nanodelivery devices formulations based on the encapsulation of growth factors for cells differentiation in biodegradable, biocompatible matrices, like PLA and PLGA. A series of tests will be performed to study the role of the *carrier* in influencing PSD, morphology, solid state, and, particularly the growth factors encapsulation efficiency. Growth factors will be encapsulated in PLGA and PLA particles which will be tested in citoxicity assay.

Another application of the SEE-C technology regards new research field, like the nutraceutical one. Therefore, the aim of this part of Ph.D. work has been to test the applicability of the SEE-C process in the production of nutraceutical formulations based on the dispersion of bioactive compounds, such as beta-carotene and astaxanthin, in matrices like PLA, PLGA and Ethyl Cellulose. For these systems, in addition to the improvement of bioavailability, the most important aspect has concerned the role of the *carrier* in protecting the antioxidant activity of the bioactive compound.

# Chapter I
# Stimuli-Responsive Polymeric Carriers and their potential application

## I.1 Classification of Stimuli-Responsive Polymers

Based on the material state, stimuli-responsive polymers can be in solution, in solid state, as film, or as gel. Stimuli-responsive polymers can be divided into the single-stimuli responsive polymers, dual-stimuli responsive polymers, and multiple-stimuli responsive polymers based on the number of stimuli. The most commonly used classification of stimuli-responsive polymer is based on stimuli that could be either reversible or irreversible.

### *I.1.1 Single Stimuli-Responsive Polymers*

The stimuli could be grouped into three major categories: (1) physical, (2) chemical, and (3) biochemical stimuli (**Figure I.1**) (Cabane et al., 2012). Every category has several types of stimuli as subgroups.

Physical stimuli (light, temperature, ultrasound, magnetic, mechanical, electrical) usually modify chain dynamics, i.e. the energy level of the polymer/solvent system, whereas chemical stimuli (solvent, ionic strength, electrochemical. pH) modulate molecular interactions, between polymer and solvent molecules, or between polymer chain. Biological stimuli (enzymes, receptors) are related to the actual functioning of molecules: enzymatic reactions, receptor recognition of molecules.
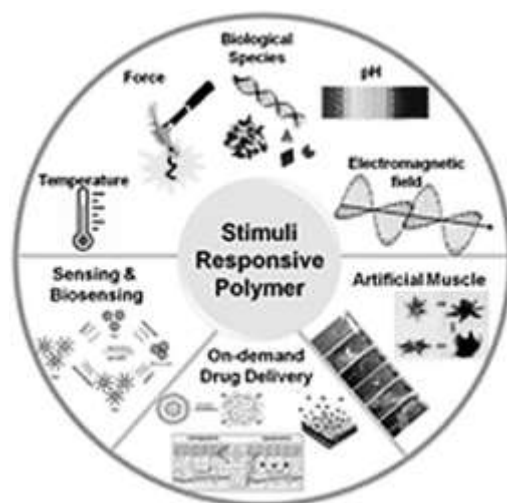
**Figure I.1** *Classification of single stimuli responsive polymers (Cabane et al., 2012).*

*Physical Stimuli-Responsive Polymers*

Physical stimuli mainly include temperature, light, electrical potential, electromagnetic field, and pressure or mechanical stress. Among these, temperature-responsive, light-responsive and mechanical stress responsive are polymers more commonly studied.

*Temperature- Responsive Polymers*

Temperature-responsive polymers have attracted great interest in bioengineering and biotechnology fields, because when a diseases occurs, changes in temperature generally manifest (Zhang et al., 2006b). Normally, these copolymers are characterized by a critical solution temperature around which the hydrophobic and hydrophilic interactions between the polymeric chains and the aqueous media abruptly change within a small temperature range. This induces the disruption of intra- and intermolecular electrostatic and hydrophobic interactions and results in chain collapse or expansion (a volume phase transition). Typically, these polymer solutions possess an upper critical solution temperature (UCST) above which one polymer phase exists, and below which a phase separation appears. Alternatively, polymer solutions that appear as monophasic below a specific temperature and biphasic above it generally possess a so-called lower critical solution temperature (LCST).

The temperature-responses of these thermo-sensitive polymers are highly reversible, which make them excellent candidates for smart devices and catalytic systems.

Poly(N-isopropylacrylamide) (PNIPAM) is one of the most well-known polymers with LCST behavior. Poly(N,N-diethylacrylamide) (PDEAAM), poly(N-vinylcaprolactam) (PVCL), poly(2-isopropyl-2-oxazoline) (PIOZ), and poly(vinyl methyl ether) (PVME) are also thermo-sensitive polymers with the phase transition temperature at 33 °C, 32 °C, 48 °C, and 35 °C, and for most of these polymers, their LCST are also dependent on the molecular weight ($M_w$) and solution concentration (Dimitrov et al., 2007).

The study of thermo-sensitive polymers featuring a UCST is mainly focused on the zwitterionic polymers because of their biocompatibility and other special solution properties. Poly(sulfobetaine)s are one of the most well-studied zwitterionic polymers. They are insoluble or hardly soluble in water; however the problem could be resolved by the addition of salt.

Similarly, poly(3-[N-(3-methacrylamido-propyl)-N,N-dimethyl]-ammonio propionate sulfonate) exhibited a UCST behavior in water due to the strong intermolecular attraction, and the result showed that the UCST of the PSPP increased with the molecular weight of the polymer (Huglin and Radwan, 1991).

Aside from these temperature-responsive polymers derived from well-known thermo-sensitive monomers, other TSPs were also synthesized to other different applications.

Block copolymers based on the amphiphilic balance were also reported for their temperature responsive micellization. For example, due to the amphiphilic balance, a block copolymer poly(ethylene oxide)-b-poly(propylene oxide) (PEO-b-PPO) also exhibits temperature sensitivity in aqueous solution. As a substituent of PPO blocks hydrophobic groups, like poly(1,2-butylene oxide) (PBO), poly(L-lactic acid) (PLLA), and (DL-lactic acid-co-glycolic acid) (PLGA) were also utilized to copolymerize with PEO to form thermo-sensitive block copolymers (Li et al., 1997, Jeong et al., 1997). One application of thermo-sensitive polymers is their role in fabricating thermally controlled reversible surface wetting behavior. Moreover, fabrication of a temperature sensor is another interesting application of thermo-sensitive polymers.

*Light-Responsive Polymers*

During the last decade, studies on light-responsive polymers (LRP) have been particularly interesting due to their precise time and site control. Light responsive polymers show great potential interest in applications such as controlled drug delivery (Alvarez-Lorenzo et al., 2009), self-healing material (Burnworth et al., 2011), reversible wettability (Lim et al., 2006), and recycleable catalyst (Yang et al., 2013).

Based on the reversibility of photo-induced structural changes, light-responsive polymers could be divided into reversible LRPs and irreversible LRPs. Chemically speaking, reversible LRPs are the polymers containing

photochromic moieties with reversible structural change, usually from structrual isomerization; whereas irreversible LPRs are the polymers with photochromic moieties with irreversible structural changes, mostly chemical bond breakage.

There are mainly two types of reversible LRPs: the first kind is one with photo-induced structure-isomerization units. Some organic dyes, such as azobenzene, spiropyran, dithienylethene, and N-salicyliden-aniline, undergo a reversible structure isomerization upon light irradiation with a specific wavelength range (Liu and Chiu, 2010, del Barrio et al., 2010, Akiyama et al., 2014). The process is usually accompanied with a color change as well as polarity changes. As a result, the polymer containing these kinds of photochromic units will undergo a solubility change in a specific solvent upon irradiation. Azobenzene is one of the most well-studied photochromic molecules because of its reversible photo-isomerization depending on the wavelength of light source.

The molecular shapes and sizes can be altered simply by UV or visible light irradiation. Another interesting study utilizing azobenzene group is the reversibility on surface wettability.

Using 7-[(trifluoromethoxyphenylazo)phenoxy]pentanoic acid as the photo-switcher, Lim and coworkers fabricated a nano-porous organic-inorganic hybrid multilayer film by layer-by-layer technique. Upon UV or visible light irradiation, the obtained film could be reversibly switched between superhydrophobic and superhydrophilic surface. Based on multi-azobenzene sugar alcohol derivatives, another group also developed a material with reversible adhesion (Akiyama et al., 2014).

As another kind of reversible LRPs, polymers with photo-induced cross-linking units are mainly focused on the polymers bearing coumarin groups. The coumarin groups will undergo photo-dimerization through a cyclo-addition reaction upon UV irradiation at>310 nm, and the obtained cyclobutane bridges could be cleaved by UV light at <260 nm (Trenor et al., 2004). It is a common knowledge that micelles from the self-assembly of amphiphilic block copolymer may not be stable because physical interactions could be easily affected by concentration, temperature, pH, and salt concentration. In such cases, the photo-induced reversible cross-linking based on coumarin group is particularly advantageous.

The coumarin moieties can be introduced into the hydrophobic block of the amphiphilic polymers. The self-assembled micelles from these polymers could be intermolecularly cross-linked by photodimerization of coumarin side groups. With this concept, Jiang et al. and Babin et al. fabricated both core-cross-linked polymer micelles and shellcross- linked reverse polymer micelles, and they demonstrated that the cross-linking process is completely reversible by simply shining light of different wavelengths (Jiang et al., 2007, Babin et al., 2008).

Irreversible light-responsive polymers are generally the polymers with photo-cleavable groups at the backbone or side chains. The covalent bond will be broken into two parts, and the process is irreversible. As the most well-known photocleavable group, o-nitrobenzyl (ONB) based fraction has been extensively studied in polymeric systems. Insertion of the o-nitrobenzyl groups to the polymer backbone, especially as the linker of two blocks of the polymers, will result to a photocleavable polymer (Theato, 2011).

*Electronically Responsive Polymers*

Electronic stimuli such as electrical potential or voltage could provide a simple, quick, and effective manner to control polymer property and morphology. All the conducting polymers, including polyanilines, polypyrroles, polythiophenes, poly(carbazole) and their derivatives, are electronic-potential responsive or semiconductor polymers. They show electrochromic effects, especially in thin film form (Meng and Li, 2013).

Electrical and electrochemical stimuli are widely used in research and applications, due to their advantages of precise control via the magnitude of the current, the duration of an electrical pulse or the interval between pulses (Mendes, 2008). Typical electrically responsive polymers are conducting polymers, as for example polythiophene (PT) or sulphonated-polystyrene (PSS), which can show swelling, shrinking or bending in response to an external field (Koo et al., 2008). There are different effects upon electrochemical stimulation: (a) an influx of counter ions and solvent molecules causes an increase in osmotic pressure in the polymer, resulting in a volumetric expansion, (b) control of the loading/adsorption of polyelectrolyte on to oppositely charged porous materials, (c) formation and swelling of redox-active polyelectrolyte multilayers. For example, when an electrochemical stimulus is applied to multilayer polyacrylamide films, the combined effects of $H^+$ ions migrating to the region of the cathode and the electrostatic attraction between the anode surface and the negatively charged acrylic acid groups lead to shrinking of the film on the anode side.

A possible application of electrically conducting polymers is in controlled wetting behavior of conducting surfaces (electro-wetting), sensors and actuators. In electro-wetting, it is possible to apply this film to oil-water separators to prepare produced oil for transport or for oil-spill clean-up. For sensors, these materials can often be electrochromic, potentiodynamic, semi-conducting (resistance), and even fluorescent. This means that they can be associated with certain analyte sensitivity (composition of produced oil, gas detection, and refined petroleum products). As actuators, they may be useful for the preparation of mechanical movements in micro-electromechanical systems (MEMS) or valves. An increasing electro-optical application is in the use of downhole sensors and optics in drilling tools and operations. Coil wire substitutes, energy generation, and maintaining conductivity pathways

are some of the increasing environment in monitoring the "health" downhole. However, this is also associated sometimes with high temperature and high pressure (HTHP) conditions and brine or high salt concentrations which are already corrosive and destructive.

*Magnetic Fields Responsive Polymers*

Magnetic field responsive polymers are generally obtained by incorporating colloidal magnetic particles (Zrínyi, 2000) or carbon nanotubes (Kimura et al., 2002) into the polymer materials. Combination of magnetic and elastic properties leads to a number of striking phenomena which are exhibited when applying magnetic fields.

The nano-composite shows great potential in various applications with high elasticity, giant deformational effect, anisotropic elastic, and swelling properties, along with the instant response to magnetic field. Magnetic field polymer composite gels were obtained by incorporating magnetic nanoparticles into the cross-linked PNIPAAm-co-poly(vinyl alcohol) gels. The polymer gels are randomly dispersed in solution when no magnetic field is applied. They rapidly aggregate in a non-uniform magnetic field, while they can form a straight chain-like structure when applying a uniform magnetic field. Due to the enhanced physical and mechanical properties, magnetic field polymer composite shows great potential in pharmaceutics, cosmetics, paint production, and perhaps oil-gas industry. The elastic modulus of a magnetic poly(dimethylsiloxane) (mPDMS) was measured under a uniform magnetic field at 293 K (Filipcsei et al., 2007). It is apparently seen that the field-free modulus of the material increases with the concentration of the filler particles. Two kinds of experimental arrangements were used, depending on the direction of the field to the mechanical stress. It shows that there is a slight increase in the modulus as the increase of external magnetic field. Possible applications are in the area of magnetic field controlled surfaces and phase behavior. The magnetic field can be used to provide mechanical stress or control the deposition of coagulated materials with magnetic particle content. Much like the light responsive applications, this property can be limited to the field gradient of the electro-magnetic generating device and can be very local. Another use of the magnetic field effect is in heating. More recently, magnetic nanoparticle materials have been used in conjunction with magnetic imaging systems.

*Pressure- or Mechanical-Stress Responsive Polymers*

Pressure or mechanical force can also act as an external stimulus to trigger changes on density and/or structure of the polymer, which will, then, produce property modifications (Genzer and Efimenko, 2000). For example, Zhang et al. reported a particularly interesting mechanically sensitive

polymer film (Zhang et al., 2005). The elastic polyamide film exhibited a triangular netlike structure, with average side length of 200 mm and fiber diameter of 20 mm. The contact angle of water on this polyamide film was measured to be 151°. The average side length of the triangular structure of the polyamide film would be 450 mm, when the film was biaxially extended to greater than 120%. At the same time, the water droplet will spread out into the space among the fibers, and polymer film will become superhydrophilic with the measured contact angle around 0°. Considering industrial processes, especially for many processes in the petroleum industry, pressure or/and mechanical force is always one of the most important parameters to control. Therefore, the industrial applications of these polymers are particularly promising. For example, pressure-sensitive adhesives including acrylic polymer, styrene acrylic polymers, and carboxylated styrene-butadiene latex, are already commercially available. They are designed for either permanent or removable applications. Safety label for power equipment, automative interior trim assembly, and sound/vibration damping films are examples of permanent applications. Removable adhesives are designed as a temporary bond, which can be removed after months or years. They are currently used as surface protection films, masking tapes, and price marking labels. Pressure changes can also be associated with flow behavior. It is possible to conceive of coatings that can be triggered to have a different wetting behavior in pressurized fittings or pipes that changes its wetting behavior at critical limits. Autonomic trigger of pressure response can also result in changes in dimensionality or trigger shape-memory function hence application in valves and membranes, e.g., valve regulation and produced water purification and filtration.

*Chemical Stimuli-Responsive Polymers*

Chemically-dependent stimuli comprise pH, redox, ionic strength and solvent.

*pH-Responsive Polymers*

The common feature of pH-responsive polymers is the presence of ionizable functional groups in their chemical structures, which are capable of donating or accepting protons upon environmental pH changes (**Figure I.2**) (Liu and Urban, 2010).

7
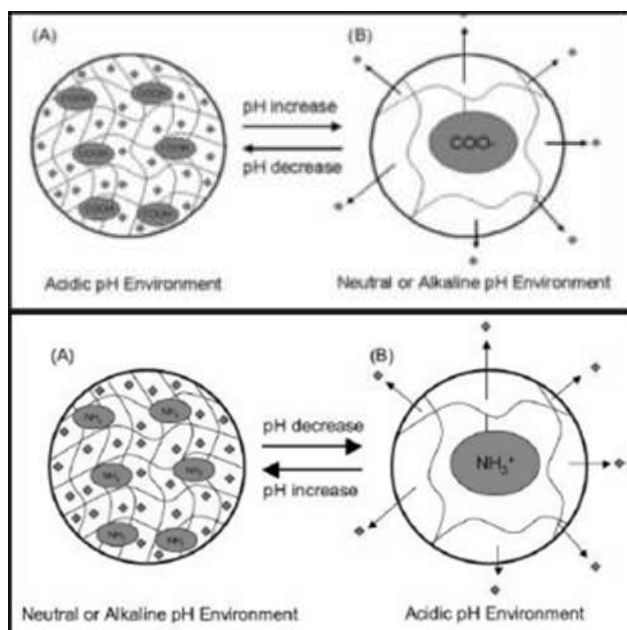
**Figure I.2** *Behavior of pH responsive polymers (Liu and Urban, 2010)*

Electrostatic repulsions between generated charges, cause the alternations of the hydrodynamic volumes of polymer chains, which is capable of extending or collapsing. There are basically two types of pH-responsive polyelectrolytes: weak polyacids and weak polybases (Gil and Hudson, 2004).

The representative acidic pendent group of weak acid is the carboxylic acid. Poly(acrylic acid) (PAA) and poly(methacrylic acid) (PMAA) with pKa values around 5 release protons and extend polymer chains under basic pH values (Li et al., 2008). On the other hand, weak bases accept protons and swell under acidic conditions. The amine and amino groups in polyallyamine (PAM) and poly(N,N'-dimethyl aminoethyl methacrylate) (PDMAEMA), respectively, are responsible for these transitions. Based on such a simple concept, pH-sensitive polymers are designed for many potential applications.

pH is an important environmental parameter for biomedical applications, because pH changes occur in many specific or pathological compartments. For example, there is an obvious change in pH along the gastrointestinal tract from the stomach (pH = 1–3) to the intestine (pH = 5–8), chronic wounds have pH values between 7.4 and 5.4, and tumor tissue is acidic extracellularly. Therefore, unlike temperature changes, this property can be exploited for a direct response at a certain tissue or in a cellular compartment.

In the oil-gas industry field, one study showed that the sulfonated elastomeric polymers, which were copolymers of isoprene and sodium

styrene sulfonate or terpolymers of isoprene, styrene, and sodium styrene sulfonate, could be used as viscosification agents when added to oil-based drilling fluids. They exhibited excellent performance to maintain pressure, cool drill bits, and lift cutting from the holes in the drilling operation, even at a high temperature (Turner et al., 1984). Another possible application is as fluid additives that can be triggered by changes in the pH condition of the whole fluid base resulting in a reversibility of function or phase, e.g., anti-scaling, emulsification, or amphiphilicity, and coagulation function. This means that such polymers are pH sensitive, and that pH control of the matrix is critical to keeping these additives stabilized or destabilized at a particular point in drilling (upstream) or transport (midstream).

### Redox-Responsive Polymers

Polymers containing labile groups present a beneficial opportunity to develop redox-responsive biodegradable or bioerodible systems. Acid labile moieties inside polyanhydrides, poly(lactic/glycolic acid) (PLGA), and poly(b-amino esters) (PbAEs) induce redox responsiveness (Shenoy et al., 2005). Disulfide groups have also been used to induce redox responsiveness, because they are unstable in a reducing environment, being cleaved in favour of corresponding thiol groups(Cerritelli et al., 2007). Polymers with disulfide cross-links degrade when exposed to cysteine or glutathione, which are reductive amino-acid based molecules (Matsumoto et al., 2009). Another typical redox responsive polymer is poly(NiPAAm-co-Ru(bpy)3), which can generate a chemical wave by the periodic redox change of Ru(bpy)3 into an oxidized state of lighter colour. This redox reaction alters the hydrophobic and the hydrophilic properties of the polymer chains and results in swelling and deswelling of the polymer.

### Ionic Strength-Responsive Polymers

The responsiveness to ionic strength is a typical property of polymers containing ionisable groups. These polymer systems exhibit unusual rheological behaviour as a result of the attractive Coulombic interactions between oppositely charged species, which may render the polymer insoluble in deionized water, but, soluble in the presence of a critical concentration of added electrolytes, where the attractive charge/charge interactions are shielded. Therefore, changes in ionic strength cause changes in the length of the polymer chains, the polymer solubility and the fluorescence quenching kinetics of chromophores bound to electrolytes (Liu et al., 2012).

*Solvent-Responsive Polymers*

Generally, macromolecular chains usually exhibit a coil-like conformation in solution, rather than adopting a stretching conformation. However, the polymer brush or polymer segment will present itself in a more stretched form in a better solvent, and shrink to some degree in a non-solvent. As a result, the block copolymers or mixed polymer brushes with different polarities or solubilities will display them with different conformations and hence different properties.

The study of solvent-responsive polymers is mainly focused on the polymer brush due to its switchable surface properties. Based on the phase separation of different blocks, the surface properties of block copolymer brushes will be different when exposing to the solvents with different affinities to each block. A tri-block copolymer poly(styrene-block-2-vinylpyridine-block-ethyleny oxide) (PS-b-P2VP-b-PEO) is a representative example of such a material to tune the balance among steric, electrostatic, and hydrophobic forces by exposing the polymers to different external solvents (Gras et al., 2007, Xu et al., 2006).

Another interesting study regarding the solvent-sensitive polymer brush is the utilization of water and air as alternating external stimuli instead of two different solvents. An amphiphilic block copolymer containing poly(styrene), poly(4-octylstyrene), or polyisoprene as the hydrophobic segment, and poly(2,3-dihydroxylpropyl methacrylate) as the hydrophilic segment was grafted onto the surface. The contact angle measurement indicated a hydrophobic surface due to the enrichment of the hydrophobic segment, but the hydrophilic groups dominated when soaked in water. Drying could be utilized to recover the hydrophobic surface (Mori et al., 1994). Similarly, polymer rearrangement and replacement of the hydrophobic groups at the top surface with hydrophilic groups when soaked in water were also demonstrated by several other groups (Senshu et al., 1999).

In general, the stimuli provided by a change in solvent property or ionic strength can mediate the wetting and miscibility of polymeric films and additives. The different grades of produced oil and the mitigation of asphaltene, paraffins, or control of ions produced from the formation are of specific importance. Typically, produced oil is a water in-oil emulsion and varies from location, geography and formation to give light, medium, and heavy oil. The presence of sulfur, salts, asphaltene, and bitumen gives each type of oil its specific grade for refining. Solvent and ionic strength responsive polymers can be used to aid in the viscosity reduction and demulsification leading to efficient transport of produced oil without necessitating heating. In more upstream applications, such stimuli response or even lack of stimuli-response can be used to control the drilling fluid rheological behavior or deposition of additives to their intended role. Together with temperature, high ionic strength or brine condition can pose

challenges in the rheological properties. Other important additive functions are fluid-loss agents, binders, weighting agents, and drag reducers. Of particular importance in hydraulic fracturing may be in hydrogel formation or a curing step in resin-coated proppants. Guar, which is a medium common for gelation in drilling and hydraulic fracturing fluids, is particularly sensitive to ionic strength. Therefore, stimuli responsive polymers that can be made, superior to guar in terms of pH and ionic strength control are always of high interest.

### Biochemical Stimuli Responsive Polymers

The biochemical stimuli responsive polymers are mainly the polymer materials responding to biochemicals, and hence exhibited great potential application in bio-related fields, especially in controlled drug delivery or gene delivery (Ganta et al., 2008).

The blood glucose level is one of the important criteria for a healthy body. A patient suffering diabetes mellitus needs an extra supply of insulin via periodic injection, while this treatment could not allow the blood glucose level to be maintained in a normal range. The glucose responsive polymer system could probably provide a self-regulating insulin release system depending on the glucose concentration in the blood. To achieve this target, several strategies including the ones based on pH-sensitive polymer hydrogel or glycopolymers were developed.

In nature, bacteria located mainly in the colon produce special enzymes, including reductive enzymes (e.g. azoreductase) or hydrolytic enzymes (e.g. glycosidases) that are capable of degrading various types of polysaccharides, such as pectin, chitosan, amylase/amylopectin, cyclodextrin and dextrin (Chambin et al., 2006). In most enzyme-responsive polymer systems, enzymes are used to destroy the polymer or its assemblies. The largest advantage of enzyme responsive polymers is that they do not require an external trigger for their decomposition, exhibit high selectivity and work under mild conditions. For example, polymer systems based on alginate/chitosan or DEXS/chitosan microcapsules are responsive to chitosanase (Itoh et al., 2006), and azoaromatic bonds are sensitive to azoreductase. In this respect, they have great potential for in vivo biological applications. However, the main disadvantage is the difficulty of establishing a precise initial response time.

For inflammation-responsive systems, the reactive oxygen metabolites (oxygen free radicals) released by polymorphonuclear (PMN) leukocytes and macrophages during the initial phase of inflammation are the stimuli. Such chemical mediators have been successfully used as stimuli for responsive drug delivery. For example, in vivo implantation experiments revealed that hyaluronic acid (HA) cross-linked with glycidylether can degrade in response to inflammation (Nobuhiko et al., 1993).

A possible application of biologically stimuli responsive polymers for the oil-gas production is in controlling bacterial colonies of biofilm formation as biocides or biostats that can mitigate problems with microbial corrosion (MIC) and in decreasing biogenic $H_2S$ generation. Certain metabolites produced by these organisms can trigger specific action or function by these polymers resulting in their mitigation. They can also have possible uses in aiding bio-remediation by triggering environments or media conducive for enzymatic action of helpful microbes (bacteria eating oil).

## I.1.2 Dual-Stimuli Responsive Polymers

There are several types of dual-stimuli responsive polymers. Theoretically, any combination of two single-stimulus responsive polymers is considered as a dual-stimuli responsive polymer. For example, temperature-responsive polymers are combined with other stimuli, like light, pH, and magnetic field (Dimitrov et al., 2007).

### Combination of Thermo- and Light-Responsive Properties

Recently, Jochum and Theato published a good review on the temperature- and light-responsive polymers, considering the most important dual-stimuli responsive polymers. Most of the polymer materials are simply based on the copolymerization of thermo-sensitive monomers and light-sensitive monomers. For example, a block copolymer with PNIPAM as the thermo-sensitive block and spiropyran groups as the light-sensitive block was fabricated. The block copolymers could be used as temperature sensor due to the temperature-responsive linear and reversible bathochromic/hypochromic shift of the absorption spectra within a wide temperature range under UV irradiation. Another interesting study with great potential use in oil-gas industry is the utilization of light- and temperature-responsive polymers to afford a stimuli-responsive emulsion with n-dodecane as the oil phase. Perrin et al. fabricated an amphiphilic photo-responsive polymer based on azobenzene-modified poly(acrylate), and it could play as the surfactant of the emulsion foams. The stability of the emulsion foams can be triggered by both temperature and light: starting from a cold sample, the foam stability could be decreased with increasing temperature or upon UV irradiation, and no foam would be created during this process. Then, the foamability could be recovered by simply decreasing temperature, and this can be cycled for several times. Foams have also been used for drilling, fracturing, and enhanced oil recovery (EOR). Therefore, foam control can be utilized towards these applications (Salonen et al., 2010).

*Combination of Thermo- and pH- Responsive Properties*

Utilization of temperature and pH as the solution variables have been of great scientific and technological interest because these factors are readily modified in a typical system (Dimitrov et al., 2007). The pH-responsive properties are always associated with the polyelectrolytes. The presence of charges along the polymer chains will lead to complex intra- and inter-molecular interactions, and it will always have a strong impact on the structural, dynamic, and rheological properties of the system.

Recently, strategies such as modification of pH are employed to tailor the temperature of induced phase transition (PT) for different applications. It is well known that the incorporation of different amounts of charged monomers is an efficient way to modulate the PT temperature (Li et al., 2002). The hydrogen-bonding interactions play an important role in the system of a pH-tunable PT temperature. For example, carboxylic groups could form hydrogen bonds with the amide groups of the PNIPAM structures, which are used to modify the LCST of the polymers (Salgado-Rodríguez et al., 2004).

One interesting study with great potential in oil-gas industry based on the combination of pH- and thermo- responsive polymers is their role as shear-thickening materials (Bokias et al., 2000). The block copolymers have two characteristic: (1) they featured a thermosensitive N-isopropylacrylamide backbone, and (2) the polymers bear a high fraction of hydrophobic side groups, and the solubility is ensured by the equal number of positive charges. Their phase behavior is governed by the competition between the hydrophobic alkyl groups and hydrophilic character of the charge. The hydrophilic character of a positive charge will prevail over the hydrophobic contribution of the alkyl chains when the alkyl groups are not long enough. The hydrophobic character of the dodecyl groups will be strong enough to prevail over the hydrophilic character of the charges.

*Dual-Responsive Polymers with Other Combinations*

Dual-responsive polymers with other combinations are also possible to construct novel smart materials for real applications. For example, the nano-composite with the combination of thermo-responsive property and magnetic-field responsive property are potential tools for protein separation (Ding et al., 2000), and even as an artificial muscle (Zrínyi, 2000).

### I.1.3 Multi-Stimuli Responsive Polymer

The current study on multi-stimuli responsive polymers is mainly focused on responsive nanoparticles, and they are mainly used in drug delivery systems. Cheng et al. reviewed the recent progress of the dual and multi-

stimuli responsive polymeric nanoparticles for programmed site-specific drug delivery (Cheng et al., 2013). The multi-stimuli responsive nanoparticles or micelles are mainly self-assembled micelle from the linear block copolymers, and the stimuli are the combinations of temperature, pH, redox agent and magnetic field (Zhuang et al., 2013).

Recently, covalently stable polymer nanoparticles are also reported based on a thermosensitive hyperbranched polymer (Zhang et al., 2013). Until now, the potential industrial applications of the multi-stimuli responsive polymer nanoparticles are still rarely investigated.

While multi-responsive polymers can be quite complicated to quantify their response or even define structure-composition-property relationships, it should be noted that many factors for oil-gas production are complex and interdependent in the environment. From the upstream side, the demands for new materials will ever increase with deep see drilling, high temperature-high pressure (HTHP) conditions, high brine concentration, different formation erosion, and the demands of directional drilling. As such it is early to dismiss the potential of multi-stimuli responsive materials in some of the technical challenges that are yet to come.

## I.2 Perspectives of application for stimuli-responsive polymers

Responsive polymer materials can adapt to surrounding environments, regulate transport of ions and molecules, change wettability and adhesion of different species on external stimuli, or convert chemical and biochemical signals into optical, electrical, thermal and mechanical signals, and vice versa. These materials are playing an increasingly important part in a diverse range of applications, such as drug delivery, diagnostics, tissue engineering and 'smart' optical systems, as well as biosensors, microelectromechanical systems, coatings and textiles. Currently, the major application of stimuli-responsive polymers is in the biomedical field, especially in the controlled-drug delivery system (Ganta et al., 2008). Several stimuli, such as pH, magnetic field, light, and temperature could be utilized to trigger the release of the encapsulated cargos, such as drugs. Light is a particularly interesting stimulus due to the precise time and site control, while the utilization of the near IR light is preferred over UV or visible light considering real-time application. The responsive properties of smart polymer are relevant to many biotechnological and biomedical applications (Mendes, 2008, Bajpai et al., 2008, Alexander and Shakesheff, 2006), because these polymers can undergo dynamic changes in accord with changes in living systems. Several key aspects have attracted interest in stimuli-responsive polymers. First, the possibility of tuning and switching adhesion between stimuli-responsive materials and proteins and cells has been explored for the control of cell (Lutolf et al., 2003) and protein (Alarcón et al., 2005, Ionov et al., 2009) adhesion, and used for tissue engineering and bioseparation. Second, the

possibility of exposing and masking functional moieties at the biointerface is very important for the presentation of regulatory signals and concomitant modulation of biomolecule activity for cell research and bioengineering.

Polymer materials, obtained either from natural polymers or from bio-based or petroleum based feedstocks, have been used in oil-gas industry (Lai et al., 2013).

Recently, polymer scientists and engineers tried to bridge the gap between the oil-gas industry and stimuli-responsive polymers. Zwitterionic water-soluble polymers with pH-response behaviors have been demonstrated to serve as efficient oil/water surfactants and fluid viscosifiers (Morgan and McCormick, 1990). The hydrophobically decorated polyelectrolytes with both solvent- and pH-response were demonstrated as smart materials for water control and hydraulic fracturing in the EOR process. In fracking industry, the reversible gels are also utilized to deliver the propants into a tight formation, which will help the oil release process.

Considering the rapid progress of stimuli-responsive polymers with numerous emerging and exciting studies, they should be explored for many potential applications in the oil-gas industry aside from the EOR process. From upstream, midstream, and downstream, the needs are enormous and challenging. The nano-sensors based on stimuli-responsive polymer could probably be used to monitor the temperature, pH, or pressure of the pipeline and oil reservoir (Shiraishi et al., 2009). The smart surface, typically with reversible super-hydrophobic- super-hydrophilic transformation, may be applied in the controlled fluid transportation. The oil-water foamability controlled by light and temperature may show great promise in the oil recovery process (Salonen et al., 2010). The shear-thickening materials based on hydrophobically modified water-soluble stimuli-responsive polymers might be useful in terminating unwanted flow or sealing unwanted channels (Bokias et al., 2000). It is true that the cost of the stimuli-responsive polymer would be a big challenge for their real applications in oil gas industry. There are always possibilities, such as using small amount of expensive polymers as additives in cheaper materials, small amount of stimuli-responsive polymer as highly effective material, or producing low-cost stimuli-responsive polymers. Currently, more efforts are still needed from polymer scientists and petroleum engineers working together to apply these possible techniques to improve operations and cost-effectiveness in the oil-gas industry.

Reconstructable polymer surfaces form a toolbox for the rapidly developing field of smart coatings (Urban, 2006). The structure of the coatings can be programmed in the formulation. After deposition, external stimuli affect the phase separation of the ingredients to self-assemble into a coating with programmed properties. Coatings with self-healing capabilities fall in the category of smart coatings with a programmed structure and response (Urban, 2009). A multilayered LbL system made up of

polyelectrolytes and a corrosion inhibitor could heal the corrosive area on a metal substrate and release the inhibitor during a corrosion attack. The origin of such self-healing behaviour lies in the breaking and re-establishing of polyelectrolyte complexes in response to changes in a corrosive environment (that is, high ionic strength) (Andreeva et al., 2008).

## I.3 State of art: Smart microcapsules production

Recently, stimuli-responsive nanoparticles and nanocapsules have attracted great interest because of the opportunities for their applications. Such nanosized capsules could store and protect various drugs, and release them inside cells after the capsule has been internalized. A smart drug-delivery polymeric system should undergo a complex chain of responses to survive in vivo, deliver the cargo, release the drug into the target cells, and match the desired kinetics of the release. Among the various approaches used to enhance the efficacy of chemotherapy is the use of carrier systems that release a drug in response to stimuli, such as changes in pH, glutathione concentration, or the presence of specific enzymes that are selectively encountered in relevant cell organelles. Biopolymeric capsules are reported in literature using solvent evaporation or extraction from emulsion.

Self-healing polymeric materials have a great potential to be explored and utilized in many applications such as engineering and surface coating. Various smart materials with self-healing ability and unique self-healing mechanisms have been reported in recent publications. Currently, the most widely employed technique is by embedding microcapsules that contain a healing agent into the bulk polymer matrix. When cracks develop in the polymer matrix, the curing agent is released from the microcapsules to cross-link and repair the cracks. Microencapsulation of the healing agent in the core can be achieved by in situ polymerizing of shell material and solvent evaporation of solvent from an emulsion.

The use of microcapsules encapsulation of the lubricating has been focused on encapsulation of the lubricating oil rather than additives as is this thesis work. Recently, patents of lubricant additives encapsulation are reported in literature. Monodisperse poly(methyl methacrylate) (PMMA)/additive particles were efficiently produced via dispersion polymerisation in a non-aqueous continuous phase, interfacial polymerization and internal phase separation and using inverse micelles.

Recently, there has been an increasing interest in the development of food-grade carrier systems for encapsulation and protection of nutraceuticals in order to enhance their stability. Several biopolymer-based micro/nanocarriers can be designed to preserve a bioactive compound by preventing its degradation. Encapsulating techniques include interfacial polymerization, polymerization in situ, coacervation, solvent evaporation, solvent extraction, nanoprecipitation, dispersion polymerization.

### I.3.1 Conventional techniques of microcapsules production

*Solvent evaporation/extraction of emulsions*

The solvent evaporation/extraction of emulsions allows the production of both microspheres and microcapsules of FDA approved biopolymers. This process is mainly used to produce composite particles starting from an emulsion. The polymer is dissolved in a suitable water immiscible solvent and the drug is dispersed or dissolved in this polymeric solution. The resultant solution is then emulsified in an aqueous phase to form droplets. This technique makes it possible to encapsulate hydrophilic and hydrophobic drugs using double (*water-in-oil-in-water*) and single (*oil-in-water*) emulsions respectively. The emulsion is continuously stirred and heated (at a fixed temperature) to remove the organic solvent for evaporation. At the end, microspheres can be recovered as a cake. Despite these potential advantages the solvent evaporation/extraction of emulsion technique suffers of some drawbacks. Indeed, this technology uses a simple vessel/stirrer setup, but may exhibit difficulties in producing large amounts of microspheres in a robust and well-controlled manner. Solvent evaporation may also require elevate temperatures or reduced pressures to eliminate the liquid solvent. Solvent extraction uses relatively large amounts of a second solvent and, then, the mixture of these two solvents has to be recycled. They also require long processing times (several hours) to be completed and, as a consequence, aggregation phenomena occur between the droplets producing microspheres with a larger polydispersity respect to the starting emulsions (Yang et al., 2000).

*Interfacial polymerization*

Interfacial polycondensation (IP) is a step growth polymerization of two or more monomers at the interface between two immiscible phases. This type of polymerization occurs when the monomers with different functionality are located in different phases. Often, the reaction occurs at a liquid-liquid interface. However, the polymerization can also occur at a liquid-gas or liquid-solid interphase (Morgan and Kwolek, 1959).

The IP method is suitable for a wide range of monomers and allows for the synthesis of a large variety of polymers including polyamides, polyesters, polyurethanes, polyureas, polyimides, polysulfonamides and polycarbonates (Perignon et al., 2015). It also allows for microencapsulation of various materials and for the fabrication of a variety of functional materials such as ultra thin metal-organic hybrid frameworks (Zhang et al., 2020).

Interfacial polymerization possesses several advantages over classical step-growth polymerization including high reaction rates at mild reaction

conditions and high final molecular weights. However, the control of reaction rate is very difficult with with negative consequences on the properties of the final product.

*Polymerization in situ*

In situ polymerization is a preparation method that occurs in the polymerization mixture and is used to develop polymer nanocomposites from nanoparticles. There are numerous unstable oligomers (molecules) which must be synthesized in situ (i.e. in the reaction mixture but cannot be isolated on their own) for use in various processes. The in situ polymerization process consists of an initiation step followed by a series of polymerization steps, which results in the formation of a hybrid between polymer molecules and nanoparticles. Nanoparticles are initially spread out in a liquid monomer or a precursor of relatively low molecular weight. Upon the formation of a homogenous mixture, initiation of the polymerization reaction is carried out by addition of an adequate initiator, which is exposed to a source of heat, radiation, etc. After the polymerization mechanism is completed, a nanocomposite is produced, which consists of polymer molecules bound to nanoparticles.

There are several advantages of the in situ polymerization process, which include the use of cost-effective materials, being easy to automate, and the ability to integrate with many other heating and curing methods. Some downsides of this preparation method, however, include limited availability of usable materials, a short time period to execute the polymerization process, and expensive equipment is required(Advani and Hsiao, 2012).

*Dispersion polymerization*

Dispersion polymerization is a type of precipitation polymerization, meaning the solvent selected as the reaction medium is a good solvent for the monomer and the initiator, but is a non-solvent for the polymer. In a dispersion polymerization process, the reaction mixture starts out as a homogeneous solution and the resulting polymer precipitates as spherical particles, stabilized by a steric barrier of dissolved polymer(Lok and Ober, 2011). During polymerization, polymers remain in solution until they reach a critical molecular weight (MW) and precipitate. These initial polymer particles are unstable and coagulate with other particles until they reach the stabilized particles form. At this point of the polymerization, growth only occurs by addition of monomer to the stabilized particles. As the polymer particles grow, stabilizer (or dispersant) molecules attach covalently to the surface. These stabilizer molecules are generally graft or block copolymers, and can be preformed or can form in situ during the reaction. Typically, one side of the stabilizer copolymer has an affinity for the solvent while the other

side has an affinity for the polymer particle being formed. These molecules play a crucial role in dispersion polymerization by forming a "hairy layer" around the particles that prevents particle coagulation. The final polymer particle size is determined by the inherent polymer aggregation behaviour under a given set of conditions (Kawaguchi and Ito, 2005). Dispersion polymerization can produce nearly monodisperse polymer particles of 0.1–15 micrometers (μm).

## Coacervation

Coacervation is a chemical method for producing polymer droplets in suspension based on the separation of two liquid phases into one concentrated colloidal phase, being the coacervate, and another highly dilute colloidal phase. The phase separation of a single polyelectrolyte or a mixture of polyelectrolytes from a solution and deposition of the agglomerated colloidal particles (i.e., the matrix material) on an immiscible active core results in the formation of a simple coacervate or a complex coacervate, respectively (Piacentini, 2016).

## Nanoprecipitation

Nanoprecipitation technique is based on precipitation mechanism. Polymer precipitation occurs after the addition of a non-solvent to a polymer solution in four steps mechanism: supersaturation, nucleation, growth by condensation, and growth by coagulation that leads to the formation of polymer nanoparticles or aggregates. The scale-up of laboratory-based nanoprecipitation method shows a good reproducibility. In addition, flash nanoprecipitation is a good strategy for industrial scale production of nanoparticles. Nanoprecipitation is usually used for encapsulation of hydrophobic or hydrophilic compounds. Nanoprecipitation was also shown to be a good alternative for the encapsulation of natural compounds. Process and formulation related parameters in nanoprecipitation technique have critical effect on nanoparticles characteristics (Martínez Rivas et al., 2017).

## I.3.2   Supercritical techniques

### Precipitation from Gas Saturated Solution

In this process, well known as PGSS, the supercritical fluid is dissolved in a melted solute to create a saturated solution that is then expanded to atmospheric pressure. This expansion causes a fast release of the dissolved gas producing a fast solidification of the solute in form of particles avoiding the use of organic solvents. In order to apply this technology, solids have to

be immiscible in the supercritical fluid and no thermal sensitive (Martín and Cocero, 2008, Reverchon et al., 2009).

*Rapid Expansion of Supercritical Solution*

This process, well known as RESS, consists of the saturation of the supercritical fluid with a solid solute; then, this solution is sprayed through a heated injector into a low pressure vessel producing a rapid nucleation of the substrate in form of very small particles that are collected from the gaseous stream. Depending of process parameters, such as temperature, pressure drop, type of nozzle etc., different kind of morphology can be obtained. When the supercritical solution is expanded directly in a liquid, the process is named RESOLV. These processes show some drawbacks: difficulty in controlling the particle size of the precipitates, possible coalescence of particles produced. However, the main limitation is that the application of this technique requires high solubility of the compound in the supercritical fluid to be processed (Martín and Cocero, 2008, Campardelli et al., 2015).

*Supercritical Antisolvent precipitation*

The Supercritical Anti-solvent (SAS) has been proposed using various acronyms (SEDS, ASES); but, the process is substantially the same in all cases. In SAS, the supercritical fluid is used as an anti-solvent that causes the precipitation of the solute in a liquid solvent in form of empty shells (balloons), micro and nanoparticles depending of the operating conditions investigated. The key phenomena of SAS process are the jet break-up at the exit of the nozzle, the high-pressure vapor-liquid equilibrium and mass transfer in and out of the droplet. If the precipitation occurs from a supercritical phase, nanoparticles are obtained since droplets do not form and the material precipitates from the gas. In subcritical single-phase conditions, the droplets are formed and the competition between surface tension and jet break-up is responsible of the process evolution. The droplet expansion followed by the solute precipitation leads to the production of empty particles (ballons). At intermediate conditions (near critical point), microparticles can be produced (Campardelli et al., 2015, Reverchon et al., 2015).

*Supercritical Assisted Atomization*

The Supercritical Assisted Atomization (SAA) is a techniques that use $CO_2$ as co-solute have something in common with the micronization by spray-drying: the SCF and the solution are intimately mixed and then sprayed in a drying atmosphere. This SCF-based micronization technique is very interesting because it can be applied to water-soluble compounds

difficult to handle with the other SCF techniques without excluding the possibility of using other organic solvents. Atomization, also assisted by an inert gas, is generally used in the spray drying of solutions. The innovative aspect of the SAA process is the solubilization of SC-CO2 in the liquid solution formed by the solvent and the (solid) solute, and the subsequent atomization of the gas-solid-liquid mixture using a thin wall nozzle. The SAA process has been successfully performed using water, organic solvents with relatively low boiling points (EtOH, MeOH, acetone) and mixtures of them. Solvents with high boiling points, typically used e.g. in SAS micronization (i.e. DMSO, NMP, toluene) cannot be used because of the difficulty of removing them during precipitation. The SAA process allows the successful production of particles in the range of dimension 1-3 μm. A limitation of the SAA process that reduces the possibility to use this process for the production of devices for biomedical application is the need of elevated temperatures in the precipitation chamber, that can damage thermolable compounds.

*Supercritical Assisted Liposome formation*

The Supercritical Assisted Liposome formation (SuperLip) has used to create lipid nanovesicles, starting from the production of water nanodroplets and, then, nanosomes are formed around them. For this reason, the process consists of a first step of atomization of water based solutions directly in a supercritical solution in which phospholipids are dissolved. Then generally, ethanol is added to increase solubility of phospholipids in SC-CO2. Since micelle formation is a fast and spontaneous process, the lipids contained in the expanded liquid formed tend to organize themselves in a layer around the water nanodroplets. Studies have demonstrated that different drugs and antioxidants can be encapsulated with efficiencies around 80% (Campardelli et al., 2015).

## I.4 Supercritical Emulsion Extraction (SEE)

Recently, Supercritical Emulsion Extraction (SEE) has been proposed in literature for the production of particles with controlled size and distribution, starting from *oil-in-water (o-w)* and *water-in-oil-in-water (w-o-w)* emulsions. In this process, SC-CO2 has been proposed for the selective extraction of the oily phase of emulsions, obtaining the polymer hardening and microspheres formation. The use of supercritical fluids as extraction media is a promising alternative for the formation of microparticles of active principles and pharmaceutical excipients. There are two main reasons for using this technique. Firstly, the selective solvating power of supercritical fluids makes it possible to extract the organic solvent from emulsions and produce microspheres. Secondly, the favorable mass transfer properties and

high solubility of solvents in the supercritical fluid make the solvent removal rapid and efficient with low level of residual solvent as requested by the authorities. The process layout of SEE has been first proposed by Chattopadhyay et al. (Chattopadhyay and Gupta, 2003, Chattopadhyay et al., 2006, Chattopadhyay et al., 2007), obtaining particles of nanometric and micrometric size with narrow particle size distribution. Particularly, they used SC-$CO_2$ to eliminate the organic solvent from *o-w emulsions* for the preparation of drug microparticles of megestrol acetate, griseofulvin and cholesterol acetate, or for the formation of biopolymer particles charged with ketoprofen and indometacin. It has been reported that the mean diameter of the particles ranged between 0.1 and 2 μm and the residual solvent was less than 50 ppm.

In the apparatus used by Chattopadhyay et al. for the precipitation of particles the extraction of the solvent from emulsions was carried out in an electrically heated stainless-steel extraction column. The SCF fluid delivery system consisted of a liquid $CO_2$ pump which provided SC-$CO_2$ to the bottom of the extraction column through a frit. The emulsion was delivered from the top countercurrently, using an HPLC pump, and was injected through a capillary nozzle, which broke the emulsion into droplets, thereby increasing its surface area of contact with SC-$CO_2$. After the contact with SC-$CO_2$, an aqueous particles suspension was formed at the bottom of the column and removed through a needle valve. The effluent SC-$CO_2$ was vented from the top of the column. The pressure inside the column was maintained constant using a backpressure regulator valve.

A different process layout for the extraction of the emulsion organic phase using SC-$CO_2$ was also proposed by Della Porta and Reverchon (Della Porta et al., 2010, Della Porta and Reverchon, 2008). The apparatus proposed by Della Porta and Reverchon for the precipitation of particles in the supercritical fluid extraction operated in batch mode. The emulsion was placed into a cylindrical stainless steel vessel. SC-$CO_2$, delivered using a high pressure diaphragm pump, was bubbled into the extraction vessel, through a cylindrical stainless steel porous dispenser located at the bottom of the extractor. The dispenser maximizes the contact between the two phases during the extraction. Temperature was controlled using an air-heated thermostated oven. The pressure inside the reactor was controlled by a micrometric valve located downstream the extractor. A separator located downstream the extractor was used to recover the liquid solvent extracted and the pressure in the separator was regulated by a backpressure valve. At the exit of the separator, a rotameter and a dry test meter were used to measure the $CO_2$ flow rate and the total quantity of $CO_2$ delivered, respectively. When the extraction process was complete, the microspheres suspension produced was removed from the bottom of the extractor vessel for analysis and further processing.

Mazzotti and co-workers (Kluge et al., 2009a, Kluge et al., 2009b) also proposed the use of SC-$CO_2$ for the production of particles of pure PLGA and PLGA loaded with lysozyme or ketoprofen through supercritical fluid extraction of emulsions. Particles with average sizes ranging between 0.1 μm and a few μm with very narrow size distributions were produced. In the layout proposed by Mazzotti and co-workers for supercritical fluid extraction of emulsions $CO_2$ was drawn from a dip tube cylinder and pre-cooled in a pressure module before being delivered to the reactor by a piston pump. The stream then passed a backpressure regulator above the desired reactor pressure, to reduce stream fluctuations generated by the piston pump. The emulsion was delivered to the reactor by an HPLC pump. Both streams were mixed at the inlet of the reactor in a two substance nozzle. The reactor was kept at the operating temperature by a thermostat. The particles were formed by solvent extraction from the organic emulsion droplets and remained suspended in the continuous water phase throughout the whole process. The product suspension accumulated at the bottom of the reactor was withdrawn through an outlet at the bottom of the reactor. The off-gas stream left the reactor through an outlet at the top. The pressure inside the reactor was controlled by a backpressure regulator located downstream, through which the off-gas stream was expanded to atmospheric pressure and was vented.

It has been shown that the average size of particles is clearly related to the average size of droplets in the original emulsion. The size of the emulsion droplets mainly depends on the mixing rate or the degree of homogenization and the concentration of surfactant or polymer. Generally, a high degree of homogenization, higher concentrations of surfactant and lower concentrations of polymer tend to produce smaller droplets. Therefore, precipitation of particles with different sizes can be accomplished by varying the emulsion formulations and by optimization of the solvent-surfactant system.

The SCF-based emulsion extraction is beneficial compared to the traditional emulsion evaporation/extraction. Indeed, SEE process combines the advantages of traditional emulsion based technology, namely control of particle size and surface properties, with the advantages of supercritical fluid extraction process, such as higher product purity and shorter processing times. Due to the enhanced mass transfer of SC-$CO_2$, this process has a relatively faster extraction rate compared to other conventional techniques (processing in minutes instead of several hours) and, thus, adds to the formation of relatively smaller particles with narrow size distributions. In the SEE process, microparticles aggregation phenomena are not observed, due to the presence of the external water phase, immiscible with SC-$CO_2$, which prevents their aggregation. High product purity and low content of residual solvents may be achieved at the same time, at moderate operating temperatures and with reasonable $CO_2$ consumption. One of the major limitation of the SEE process, in these discussed configuration, is that the

process remains intrinsically discontinuous, sharing this inconvenient with traditional solvent evaporation/extraction processes. Indeed, a batch of emulsion can be treated for each run with problems of repeatability of the batches and reduction of the process yield, due to the material lost. For this reason Della Porta and Reverchon (Della Porta et al., 2011b) suggested also the possibility of a continuous process layout (SEE-C) where the SC-$CO_2$ is continuously contacted with an emulsion in a column to extract the organic solvent without interacting with dispersant phase. At the bottom of the column, a suspension of microstructured particles can be continuously collected. The SEE-C continuous layout has been used during this PhD thesis.

### I.4.1   SEE-C Apparatus

Process equipment consists of a high pressure packed column where gas and liquid phases (SC-$CO_2$ and emulsion) are contacted counter currently and mass transfer between the two phases is improved by the internal packing elements. A schematic representation of SEE-C process is illustrated in **Figure I.3c**.

The SEE-C apparatus mainly consists of a 1680 mm long column with an internal diameter of 13.11 mm. The column is packed with stainless steel packings 4 mm nominal size with 1889 $m_{-1}$ specific surface and 0.94 voidage (0.16-inch Pro-Pak, Scientific Development Company, State College, PA, USA), and is formed by five AISI 316 cylindrical sections connected by 4-port elements. The extraction stages are three. The apparatus is thermally insulated by ceramic cloths and its temperature is controlled by six controllers (Series 93, Watlow, Milan, Italy) inserted at different heights of the column. SC-$CO_2$ is fed at the bottom of the column by a high-pressure diaphragm pump (mod. Milroyal B, Milton Roy, Pont Saint-Pierre, France) at a constant flow rate. The emulsion is taken from a reservoir and delivered from the top of the column, using a high pressure piston pump (mod. 305; Gilson, Villiers-le-Bel, France), at a constant flow rate. Particles formation in emulsion is achieved by removal of the internal organic oil phase from the emulsion droplets by extraction using SC-$CO_2$. A separator located downstream the top of the column is used to recover the extracted "oily" solvent and the pressure in the separator is regulated by a backpressure valve (26-1700 Series, Tescom, Selmsdorf, Germany). At the exit of the separator, a rotameter (mod. N5-2500, ASA, Sesto San Giovanni, Italy) and a dry test meter (mod. LPN/S80AL class G2.5, Sacofgas, Milan, Italy) are used to measure the $CO_2$ flow rate and the total amount of $CO_2$ delivered, respectively. The microspheres suspension is continuously removed from the bottom of the extraction column by decompression, using a needle valve (mod. SS-31RS4, Swagelok, Brescia, Italy). .

The start-up of the extraction process begins delivering SC-$CO_2$ from the bottom of the column until the operating pressure is reached. Then, the emulsion delivery is started at the top of the column. At the end of each run, the column is washed with distilled water to eliminate any processing residue from the packing surface. Finally, a washing step is always performed to recover the carriers still retained in the column packing elements. Normally, 70% of the overall polymer used in the emulsion is recovered for each run as a result of the loss of emulsion/suspension caused by dead-volumes of SEE apparatus. The organic solvent recovered is less than 50% in weight of the solvent loaded in the emulsion, because it is partially loss in the gas stream at the exit of the separator located at the top of the column. After the SEE-C experiment, particles are recovered from the suspension and separated from the surfactant by centrifugation with a large volume of distilled water at a rotation speed of 6500 rpm for about 30 min. Then, the supernatant is discharged and particles are re-suspended in pure water, recovered by membrane filtration and dried at air for further processing.

### I.4.2 Definition of SEE-C operative conditions

SEE-C operating conditions of pressure and temperature were chosen to allow the selective extraction of organic solvent from the oily phase of the emulsion. Considering the high pressure vapor-liquid equilibrium diagram (VLE) of the system ethyl acetate/$CO_2$, pressure and temperature conditions were chosen at 8 MPa and 312K to selectively extract the organic solvent from the oily phase of emulsion (see **Figure I.3b**), adapted from (Chrisochoou et al., 1995). Indeed, adopting these operative pressure and temperature, the approximately operative point in the steady state operation) is indicated as the blue dot in **Figure I.3b** and it is located outside the miscibility hole of the system ethyl acetate (EA) plus $CO_2$. Therefore, the complete miscibility of the ethyl acetate in dense carbon dioxide can be assumed. This temperature is also compatible with the glass transition temperatures of the selected polymers. At these operative conditions the solubility of the external phase in SC-$CO_2$ is extremely small (Sabirzyanov et al., 2002, Sovova et al., 1997) and a selective extraction of the oily phase of the emulsions can be obtained. The counter-current operation in the packed column is also favored by large density differences between the two phases (liquid and SC-$CO_2$) involved in the process, since it allows the counter-current flow inside the column. In the case of a supercritical fluid, the lower is the pressure the lower is the fluid phase density and the larger is the density difference at a fixed temperature. At 38°C and at 80 bar, a large difference in density between the emulsion and SC-$CO_2$ is obtained, because densities are about 993 kg/m3 and 304 kg/m3, respectively. These conditions assured enough difference in density to properly operate the counter-current

flows (McBride-Wright et al., 2015). Another important operating parameter, to be taken into account when operating with a continuous extraction tower, is the liquid to gas ratio (L/G). Difficult separations are characterized by a very low L/G ratios; it means that high quantities of SC-$CO_2$ are necessary per unit of liquid treated to obtain the desired extraction efficiency (Brunner, 2009). However, it is not possible to decrease freely the L/G ratio since, when very large flow rates of the gas stream are used, the liquid is entrained by the gas and flooding occurs determining the failure of the process. In this thesis, L/G ratio was fixed at 0.1, as a consequence of a previous optimization of the tower fluid dynamics (Falco et al., 2012b). A $CO_2$ flow rate of 1.2 kg/h and an emulsion flow rate of 2.4 mL/min were used according to the previous discussion.

Another relevant process parameter in the continuous operation is the time required to obtain steady state conditions in the column. Indeed, during the continuous operation, mass transfer between the two phases is activated, but, variations in the top and bottom product composition can be observed until steady state conditions have been obtained. Therefore, the SEE-C performance evaluations were always performed after reaching the steady state conditions. This initial phase of the process is also important to wet the column packing with the surfactant, that favors particles slipping on the packing surface. Indeed, the use of packed towers is commonly not suggested for processes involving the presence of a solid phase that could cover the packing surface, producing a reduction of the mass transfer and, then, the blockage of the column. However the dimensions of the microparticles produced in this work are always in the micronic and submicronic range; therefore, tend to remain suspended in the falling liquid film inside the column.

Operating in this manner, also very low solvent residues (less than 500 ppm) were measured in the recovered suspension, that are significantly lower than those that can be found after the conventional liquid emulsion extraction (LEE) (Della Porta et al., 2011a, Gimenez-Rota et al., 2019).
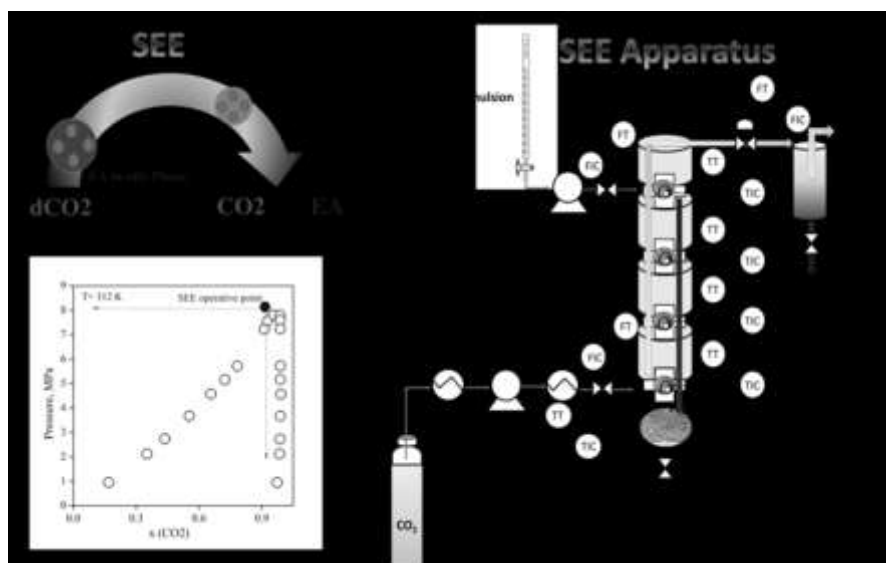
**Figure I.3** *Schematic illustration of SEE process with the representation of droplet (in emulsion) shrinkage and polymer particle formation after the oily phase extraction by dense-$CO_2$ (a). Vapour Liquid Equilibrium (VLE) at high pressure for the system EA-$CO_2$ at 312 K adapted by Chrisochoou et al., (1995); the blue dot approximatively indicates the operative point, neglecting the water phase that is immiscible in $CO_2$ in the same conditions (b). SEE apparatus layout with the packed column operating in counter-current mode; other legends: $CO_2$ supply; chiller used for $CO_2$ cooling; diaphragm pump used for high pressure $CO_2$; heater used for SC-$CO_2$ heating; emulsion supply; piston pump used for the emulsion; TT-TIC, temperature control; FT-FIC, flow rate control; BPR, back pressure regulator; separator used for $CO_2$ and solvent recovery; suspension recovery (c).*

# Chapter II
# Analytical methods

## II.1     Analyses on morphology

### *II.1.1  Field Emission Scanning Electron Microscope*

The morphology of the powder was observed by a field emission-scanning electron microscope (FESEM, mod. LEO 1525, Carl Zeiss SMT AG). SEE powders were dispersed on a carbon tab previously stuck to an aluminum stub (Agar Scientific, Stansted) and coated with gold (layer thickness 250Å) using a sputter coater (mod. B7341, Agar Scientific Stansted). Approximate composition of particles was observed using FESEM coupled with an energy dispersive X-ray spectroscopy (EDX, INCA Energy 350).

### *II.1.2 Transmission Electron Microscope*

The morphology of the encapsulated additives was assessed by Transmission Electron Microscope (TEM FEI Tecnai electron microscope operating at 200 KV). An aqueous suspension of capsules was centrifuged at 6500 rpm for 10 min. After that, the supernatant was removed.

For sample preparation, a drop of concentrated suspension was placed on a copper grid for 60 seconds. The drop is then dried with a filter paper. A drop of coloring agent is placed on the grid and left for 30 seconds; the excess amount is removed with filter paper.

## II.2     Particle size distribution (PSD)

Droplets Size Distributions (DSD) and Particles Size Distributions (PSD) were by the dynamic laser scattering (DLS) method using a Nanosizer (NanoZS Malvern Instrument, UK) equipped with a He-Ne laser operating at 4.0 mW and 633 nm, for measuring the hydrodynamic diameter of the particles. To performe these measurements, droplets and microcapsules

suspension were suspended in a dispersant solvent, which varies depending on the analyzed solute. In this PhD thesis, water was used as dispersant solvent. The distributions proposed in this work are the mean of 13 measurements produced in triplicate using DLS analysis.

The shrinkage factor percentage (SF%) was calculated as indicated in equation 1:

$$\% \text{ Shrinkage} = (1 - \frac{carriers\ mean\ size}{droplets\ mean\ size}) \times 100 \qquad (eq.1)$$

## II.3    Analyses on solid state

### II.3.1  Differential Scanning Calorimetry

The thermal behavior of powders was measured by a Differential Scanning Calorimeter (DSC, model TC11, Mettler Toledo, Inc., Columbus, USA), using Mettler STARe system. Fusion temperature and enthalpy were calibrated with an indium standard (melting point, 156.6°C, enthalpy of fusion 28.52 J/g). 3 mg of the sample were accurately weighed, crimped into an aluminum pan that was heated from 25 to 350°C under a nitrogen purge (flow rate 50 mL/min), at 10°C/min.

### II.3.2  Fourier Transform Infrared (FTIR)

The measurement of FTIR spectra was carried out with a FTIR spectrophotometer (IR-Tracer100, Shimadzu). The powder samples were ground and mixed thoroughly with small amount of potassium bromide (KBr) and pressed to 10 tons for 10 minutes in a manual press. The scan analysis was performed at 25°C, in a scan wavenumber ranging between 4000 and 450 cm$^{-1}$ at a resolution of 1 cm$^{-1}$; 32 scan signals were averaged to reduce the noise of measurements.

### II.3.3 Coating Procedure

A "K303 MULTICOATER" surface coating applicator, from RK Printcoat Instrument, was used to produce uniform resin coating on CFRCs panels.
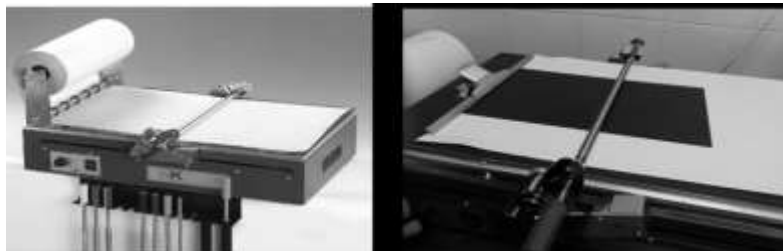
**Figure II.1**: *Setup for the coating procedure*

Controlled speed and pressure ensure repeatability of results. The panel (carefully cut to 30 x 140 mm) is deposited on the multicoater and clamped with a vice, in order to avoid movement during the covering. After tightening, the appropriate head is applied.

## II.3.4 Impact Tester - Impact resistance test

Impact Tester is a widely used tool in the paint and plastics industry. In both fields, impact resistance is measured by a weight that falls from a controlled height. For plastic materials, the strength is increased until structural failure occurs. In the case of a painted surface, the failure will appear as a crack in the paint film. The impact tester creates a deformation in the surface that can also be used to measure the flexibility of a paint.

The prepared specimens were subjected to mechanical stress by a manual impactor, fixing two impact energies, respectively 3.8 J and 4.5 J.

## II.3.5 Oil dispersability Test

The dispersability of produced microcapsules in base oil was evaluated adding in 5gr of base oil the necessary amount of microcapsules to obtain a total AM content of 5%. The suspension was put in agitation at 300 rpm for 16 h. The obtained suspension was left at ambient condition without any agitation for the rest of the time of observation.

## II.3.6 AM activated acid release test

Release tests at acid conditions were performed suspending microspheres (20 mg) containing AM in of distilled water acidified with sulfuric acid up to the desired level of acidity. Methyl orange was used as pH indicator. This indicator is at acid pH and turned to pale yellow in condition of nutral or basic pH. The release of AM was detected as a variation of the color of the release medium as a consequence of the pH neutralizing effect of the additive. The release tests were conducted at different temperatures in the range 25-80 °C. At the end of the release tests the microcapsules degradation was also observed using FESEM analysis.

## II.4    Loading efficiency and dissolution tests

### II.4.1  Spectophotometer UV-vis

Active principle (additives or SHM) loading in SEE microcapsules was evaluated by UV-vis spectrophotometer (model Cary 50, Varian, Palo Alto, CA), measuring the absorbance in correspondence of active principle characteristic wavelength. The carriers used for SEE-C encapsulation experiments is not visible at these wavelengths by spectrophotometer. Then the absorbance was converted into active principle concentration, using a calibration curve. Each analysis was performed in triplicate and the results were expressed as the mean value. The loading or encapsulation efficiency (EE) is calculated as the ratio of the effective loading to the theoretical loading, according to equation (2):

$$EE = \frac{effective\ loading}{theoretical\ loading} \times 100 \qquad (eq.2)$$

where the theoretical loading is the mass ratio of active principle/carrier (w/w) in the emulsion injected into the SEE-C plant and the effective loading is the actual mass ratio of active principle/carrier (w/w) in the SEE capsules.

The encapsulation efficiency was measured dissolving about 5 mg of washed microspheres in a solvent and measuring the absorbance of the solution at active principle characteristic wavelength. Using the calibration curve, the amount of additive dissolved in the solution was calculated. In **Table II.1**, the characteristic wavelength of active principles used and the solvent used for calibration curve were reported.

**Table II.1** *Characteristic wavelength of active principles studied.*

| Active compound | Wavelength | Solvent |
|:---:|:---:|:---:|
| AM | 255 | Ethyl acetate |
| MoDTC | 280 | Ethyl acetate |
| Epoxy resin | 536 | Acetone |
| Astaxanthin | 470 | Acetone |

The same instrument was used to perform the shelf life assay on capsules containing β-CA and β-CA with α-TOC. In the first case, by quantifying the remaining β-CA in the capsules compared with the pure compound after exposed to UV radiation (λ=254 nm) for 1 hour a day for 10 days. In the second case, by measuring the remaining encapsulated β-CA after 2 years of storage at 4ºC in the dark. In both shelf life studies, samples were solved in

acetone and the amount of active β-CA was measured at 450 nm using the spectrophotometer UV-vis.

## II.4.2  High Performance Liquid Chromatography

The study of active principles like β-carotene (β-CA), α-Tocoferol (α-TOC) and rosmarinic acid (RA) was performed in an Agilent HPLC-UV/vis (High Performance Liquid Chromatography, Hewlett-Packard model G131-132). equipped with a Waters Spherisorb ODS-2 (Ø 5 μm 150x4.6 mm) column. The mobile phase used was 80:20 Methanol:Water acidified 0.1% acetic acid; the flow rate was of 1 mL/min. The injection volume was 20 μL in every test and the detection wavelength of: 450 nm for β-CA, 292 nm for α-TOC and 330 nm for RA. A calibration curve was built for each compound. The encapsulation efficiency percentage (EE%) was calculated as amount (mass) measured/amount (mass) loaded x100. All of the analyses were performed in duplicate.

## II.4.3      Enzyme Linked Immunosorbent Assay for growth factors release study and encapsulation efficiency

Growth factors release profiles were monitored in vitro suspending about 5 (±0.3) mg of carriers in 0.5mL of Minimum Essential Medium Alpha (α-MEM) plus 0.1% w/w Tween 20, placed in an incubator at 37°C, and stirred continuously at 100 rpm. Every 24 hours, the samples were centrifuged at 12000 rcf for 10 min and the supernatant completely removed and replaced with fresh media to maintain sink conditions. The concentration of the released peptides were then measured with an Enzyme Linked Immunosorbent Assay (ELISA, Cloud-Clone Corp., USA). Release experiments were performed in duplicate (N=2) and the curve describes the mean profile was calculated as ng of growth factor released from 100mg of polymer versus time.

Encapsulation Efficiency (%) was defined as the ratio between loaded peptides in the emulsion and the recovered one per g of polymer; this value is expressed as a percentage. This characterization was performed by the Department of Medicine, Surgery and Dentistry "Scuola Medica Salernitana", University of Salerno.

## II.4.4.     Cells isolation and harvesting

Chinese Hamster Ovary Cells sub-clone K1 (CHO-K1, ATCC® CCL-61™) were seeded in 96-well plates at a density of 10.000 cells/well and cultured in HAM's F12 medium supplemented with 10% FBS and 1%

penicillin/streptomycin (50 U/mL). Cells were then incubated in a humidified atmosphere containing 5% $CO_2$ and 95% air.

Human Peripheral Blood Mononuclear Cells (hPBMCs) were obtained from three healthy donors (age 25-40 years) and separated by Ficoll-Hypaque gradient density (Sigma-Aldrich) following standard techniques (Santoro et al., 2008). All donors gave their written informed consent in accordance with the Declaration of Helsinki for the use of their residual blood for research purposes, with approval from the University Hospital of Salerno Institutional Review Board. After isolation, cells were re-suspended in RPMI medium, supplemented with 10% heat-inactivated FBS, 10 mg/mL L-glutamine, and penicillin/streptomycin (50 U/mL). Cells were then seeded in 96-well plates at a density of 10.000 cells/well and incubated in a humidified atmosphere containing 5% $CO_2$ and 95% air. This characterization was performed by the Department of Medicine, Surgery and Dentistry "Scuola Medica Salernitana", University of Salerno.

### II.4.5 MTT assay for cytotoxic activity

Cell viability was analyzed using the MTT assay. Briefly, cells were treated with decreasing amounts of growth factor loaded and unloaded PLGA and PLA carriers; pure growth factors were also tested at different concentrations for 24 and 48h. All carriers were suspended in culture medium using ultrasound in ice-cold (Elmasonic P, Elma Schmidbauer GmbH, DE).

At the end of the treatments, 3-(4,5-Dimethylthiazol-2-yl)-2,5-diphenyl-tetrazolium bromide (MTT) was added (1 mg/mL) to each well and then incubated at 37°C for an additional 4 h. Plates were centrifuged at 300 g for 10 min and the supernatants completely removed. Formazan products were dissolved in 100 µL of dimethyl sulfoxide (DMSO). Absorbance was determined at 490 nm using a microplate reader (Infinite F200 PRO, Tecan Group Ltd., SW). All assays were performed in triplicate (N=3). For the MTT assay on hPBMCs, three independent experiments were performed in triplicate, each one on a single subject (N=3). Cell viability was calculated as the percentage of the control group, considered as 100%. The percentage viability of cells was calculated according to equation (3):

$$\% \text{ Cell viability} = \frac{Abs\ of\ sample - Abs\ blank}{Abs\ of\ control - Abs\ blank} \times 100 \qquad (eq.3).$$

This characterization was performed by the Department of Medicine, Surgery and Dentistry "Scuola Medica Salernitana", University of Salerno.

## II.5    Antioxidant activity

### II.5.1  DPPH method

DPPH$^+$ (2,2-diphenyl-1-picrylhydrazyl) is a stable free radical that assumes a purple color in solution, with an absorption band around 517 nm. When this radical reacts with a hydrogen donor, the reduced form of DPPH is formed and a discoloration of the violet color is obtained. The spectrophotometric method described in literature (Brand-Williams et al., 1995) with minor modifications was used to study the reduction of DPPH and, hence, the antioxidant capacity.

Regarding β-CA, firstly, a calibration curve was performed monitoring the antioxidant activity of pure compound. 1.5 mL of β-CA solution were added to 1.5 mL of 0.1 mM DPPH both dissolved in mixture of AC:ET (1:7) and then kept in the dark for 18 hours at room temperature. The biopolymer capsules were solved in 0.5 mL acetone first and then 3.5 mL of ET was added; the mixture was centrifuged at 6500 rpm for 30 min. 3 different concentrations of the supernatant were prepared. Finally, 1.5 ml of these solutions were added to 1.5mL of 0.1 mM DPPH. The antioxidant activity was measured 18 hour at 517nm. The DPPH inhibiton percentage (%) was defined as in eq. (4):

$$DPPH\ inhibition\ (SA)\ \% = \ 100\ x\ \frac{(Abs\ DPPH - Abs\ sample)}{Abs\ DPPH} \quad \text{(eq. 4)}$$

where Abs sample is the absorbance measured for the sample solution with DPPH after the reaction and Abs DPPH is the absorbance of DPPH solution. The theoretical inhibition percentage was calculated for each concentration of capsules and a theoretical inhibition curve was built for each product. The theoretical IC50 was compared with the IC50 obtained experimentally.

For astaxanthin antioxidant activity measurement, 1 mL of a methanolic solution of the sample (powder) was added to 3 mL of a freshly prepared methanolic solution containing $1x10^{-4}$ M DPPH. As blank (negative control) was used the DPPH solution. Before measuring the absorbance of the solution, this mixture was then kept at room temperature in a dark chamber for 18 h.

# Chapter III
# SEE microcapsules formulations for Total

## III.1 Agreement with Total

Some microcapsules formulation have been studied as proposed by Total MS within the research project "Production and characterization of microcapsules loaded with different additives, performance evaluation and industrialization of supercritical $CO_2$ based processes". The french company Total funded the research project supporting this Ph.D. work with the aim to invest in SEE-C plant for additive loaded microcapsules engineering using SCFs. As part of the agreement between the company and the Department of Industrial Engineering (DIIN) of the University of Salerno, this part of thesis was focused on the development of formulations based on additive directly proposed by Total for its world-wide partners, in order to scale up the process for industrialization. This section, due to secrecy agreements, will be presented using acronyms and no further detailed information will be reported.

Investigations and studies were performed on additive encapsulation previously tested using traditional techniques by other groups of research with no satisfying results. These additives were:

- ❖ AM
- ❖ MoDTC.

First, for each compound a feasibility study was carried out in order to investigate the kind of polymer that can be used for the applicability of SEE-C process. Then, SEE-C operative conditions was optimized to reach the targets requested by Total. A series of characterization analyses was performed according to methods suggested by Total and by our analytical

experiences. Finally, grams of powders were produced by SEE and sent to the company for further industrial considerations.

## III.2   Introduction

The protection of lubricant oils additives from thermo-oxidative degradation still remains a hard challenge for lubricants formulators. During usage, lubricating oils undergo changes termed degradation and contamination, which render them ineffective for further application. Lubricating oil goes through normal degradation and about 50% of the oil is consumed in the process. The rest of the oil picks up a number of contaminants from the working environment, such as, residual components of engine fuels, solids from wear processes along with corrosion products and dirt, soot, combustion products etc (Tripathi and Vinu, 2015).

Degradation involves changes in the desired viscometric properties of oil as a result of alteration in the lubricating oil molecular structure caused by cracking, isomerization and polymerization reactions prompted by high temperatures in the running engine. The overall effect of this degradation is the formation of low molecular weight compounds and oxidation products which include polymerized or condensed molecules called gum and sludge (Diphare et al., 2013).

Lubricant additives play a critical role in preventing lubricant degradation. Additives are synthetic chemicals used to improve different lubricant parameters, they can boost existing properties, eliminate adverse characteristics, or introduce new properties in the base oil. The additives are essentially sacrificial in their role of protecting the base oil because the additives will degrade first while minimizing any degradation to the base oil molecular properties (Rizvi, 2003, Minami, 2017, Hsu, 2004).

After additive content is consumed by operational forces, the integrity of the hydrocarbon base oil becomes compromised because it is no longer protected by additives. At this point lubricant oxidation and the consequent 'tell-tale' discolouration commences. A time-specific delivery approach of additives using nano-structured devices could be the right answer. These structures can allow to enhance the stability and to prolong the lifetime of the additives, reducing their volatility and reactivity and/or to maintain the additive concentration constant during operation, controlling their release. The encapsulation system should be designed to react to a specific trigger (pH, temperature, mechanical stress), that activates the release of the additive, trying to meet the desired release target or release rate.

Several techniques have been developed for encapsulating active substances (spray-drying, emulsion polymerization or evaporation, phase separation, coacervation etc.).

Mitchell et al. (Mitchell et al., 2018) proposed the encapsulation of lubricant additives by dispersion polymerization in non aqueous continuous

phase. A Stabilizer, an initiator and a monomer (MMA) were dissolved in a continuous phase where an insoluble cosolvent (solvent and additive) were added. Upon stirring and heating, monomers react and cosolvent were incorporated within the growing polymer particles (PMMA). When all of the monomer has reacted, polymerization is complete. The typical conversion rate in this particular synthesis was measured to be $\sim$70%, but it is necessary remove the unreacted monomer and initiator using centrifugation steps and for each step supernatant have to be removed and the particles have to be re-suspended in fresh solvent, with high solvent use and low encapsulation efficiency. Total and ExxonMobil recent patents (Matray et al., 2015, Webster et al., 2019) proposed the encapsulation of lubricant additives by interfacial polymerization technique. In this case, during the polymerization occurs the reaction of the monomers dissolved in the continuous phase and the dispersed oil phase and the formation of polymer structure which incorporated the additive. Long process time were necessary to prepare the oil phase, for the polymerization and cooling steps, moreover filtration cycles with strong recycle of solvent were used.

The George Washington University (Hsu and Zhao, 2017) proposed internal phase separation as encapsulation methods for microencapsulation of chemical lubricant additives using polymers as polymethylmetacrylate and polystyrene. ExxonMobil (Calcavecchio et al., 2015) also proposed the encapsulation of additives for lubricant oil in inverse micelles. These micelles are aggregates of surfactant molecules dispersed in a liquid colloid. They suffer of a strong instability because their stability was concentration dependent.

Therefore, all these techniques require large amounts of solvents or surfactants and lead to a final product containing some residues. They also show low encapsulation efficiency especially in the case of liquid cores and it is difficult to control capsule size at micrometric and submicrometric range and encapsulated additive concentration (Mishra et al., 2013).

In this PhD project the production of micro-capsules has been performed using innovative processes based on the use of supercritical $CO_2$.

The microcapsules were produced using the Continuous Supercritical Emulsion Extraction process (SEE-C). Microcapsules are produced starting from an emulsion; generally speaking for microcapsules production a double emulsion was prepared. In this case the additive (oil phase, $O_1$) was dispersed in the oil phase formed by the selected polymer, dissolved in an appropriate organic solvent, (oil phase, $O_2$). The $O_1/O_2$ emulsion was, then, emulsified in an external water phase, W, obtaining the final $O_1/O_2/W$ phase. To obtain microcapsules the selective extraction of the $O_2$ organic solvent is necessary. During the extraction of the solvent the polymer precipitates incorporating the $O_1$ phase and producing microcapsules. This extraction was performed using supercritical $CO_2$ as extracting solvent, tunable with pressure and temperature. In a continuous tower, packed with packing

elements, a counter-current extraction of the solvent form the emulsion is obtained, allowing the continuous production of microcapsule suspension, recovered at the bottom of the tower.

Microparticles, produced using SEE process, were characterized in terms of morphology, particle size distribution and additive encapsulation efficiency.

**Materials**

Carbon dioxide, $CO_2$, purity 99.9% was provided by Morlando Group (Naples, Italy). Ethyl acetate (EA) of purity 99.9% was supplied from Carlo Erba Reagents (Milan, Italy). Eudragit polymer (EPO, ERL, ERS; Eudraguard) were supplied by Evonik Industries, Germany. Poly-methyl methacrylate (PMMA MW: 15,000-97,000 g/mol, Sigma-Aldrich, Italy), Polystyrene (PS, Sigma-Aldrich, Italy), Ethyl cellulose (EC, viscosity 100 cps in 40/40 toluene/ethanol, 455 kDa, Sigma-Aldrich, Italy), Polycaprolactone (PC, Sigma-Aldrich, Italy), Tween 80 (Sigma-Aldrich, Italy), Methyl orange (Sigma-Aldrich, Italy ) were used as received. AM and MoDTC additives were send by Total MS. Base oil at different viscosity for dispersability test on capsules were sent by the company.

## III.2   Compound #1: AM

The first aim of the study will be focused on the encapsulation of an additive (AM), send by TOTAL MS, that is used to control the acidity of the lubricant oil during the usage. For this reason the research was dedicated on the choice of the polymer and production of additive loaded in pH responsive microcapsules. The microcapsules will be produced using the Continuous Supercritical Emulsion Extraction process (SEE-C).

The release of the additive from microcapsules should be favored at an acidic pH (pH <4), for this reason the first phase of the study was focused on the choice of the best polymer(s) for early dissolution test of the capsules produced in acidic pH. The polymer was selected to ensure a controlled release of the AM at pH below 4.

From a bibliographic study, the focus fell on pH sensitive polymers used in drug delivery, particularly where the pH conditions are acidic. The pH sensitive polymers are polyelectrolytes that have in their structure acid or basic groups that can accept or release protons in response to pH changes in the surrounding environment This group of smart polymers changes its solubility by changing the electrical charge of the polymer molecule. Thus, the transition from a soluble state to an insoluble state is caused by the decrease of the electrical charge in the polymeric molecules. In the human body we can see remarkable changes of pH that can be used to direct therapeutic agents to a specific body area, tissue or cell compartment (Kocak et al., 2017).

Preliminary tests were performed on different pH sensible polymers poly(methyl methacrylate) PMMA, copolymers derived from esters of acrylic and methacrylic acid (Eudragit polymers) and ethyl cellulose in order to select the family of polymers more suitable for the specific application and compatible with the SEE process. Process conditions were optimized to produce microcapsules with a maximum particle mean diameter of 300 nm and with a minimum AM content of 40% w/w with respect to the polymer weight.

### III.2.1 Experimental results on AM

*Polymer selection and SEE operative parameters optimization*

In all the experiments a double $O_1/O_2/W$ emulsion was produced. 100 mL of emulsion were prepared for each run. The emulsion composition was maintained as *oil/water* 20/80 for all the experiments reported in this study; the $O_1/O_2$ ratio was changed in order to have different AM theoretical loading. The $O_1$ phase was stabilized using 2% of Tween80 as surfactant, the $O_2$ solvent was ethyl acetate in which a fixed amount (expressed as % with respect to the oil phase) of polymer was dissolved, the water phase was saturated with ethylacetate and contained 1 % of Tween 80 as surfactant. The primary $O_1/O_2$ was obtained using sonication with a high power sonication probe, at 30% of the power for 30s. The $O_1/O_2/W$ emulsion was obtained adding the primary emulsion to the water phase using a high-speed stirrer at 4000 rpm for 4 min.

SEE-C operative conditions were selected considering that according to the binary vapor-liquid equilibrium diagram (VLE) the mixture critical point for the system $CO_2$-ethylacetate is at about 80 bar at 40°C. At this condition ethyl acetate is completely miscible in SC-$CO_2$. Liquid to gas ratio, L/G, was fixed at 0.1 (mass flow ratio), as a consequence of a previous optimization of the tower fluid dynamics. A $CO_2$ flow rate of 1.4 kg/h and an emulsion flow rate of 2.4 mL/min were used.

#### *Eudragit polymers*

Tests carred out are listed in **Table III.1**. These experiments had the objective to verify the processability of Eudragit polymers using the SEE-C process.

**Table III.2** *SEE microcapsules production for the encapsulation of AM using Eudragit polymers as carrier*

| Test | Polymer in $O_2$ phase [%] | AM [%] | DM±DS [nm] |
|---|---|---|---|
| EPO_00 | 10 | --- | 601 ± 103 |
| EPO_01 | 10 | 33.3 | 659 ±193 |
| EPO_02 | 10 | 20 | 724 ± 164 |
| EU_01 | 2 | --- | 175 ± 35 |
| ERL_01_SEE | 5 | --- | 146 ± 22 |
| ERL_01_Solv | 5 | --- | 291 ± 39 |
| ERS_01_SEE | 5 | --- | 159 ± 23 |
| ERS_01_Solv | 5 | --- | 277 ± 37 |

**Eudragit EPO**

A first set of experiments was performed using Eudragit EPO as the polymer matrix for microcapsules production.

A first experiment was performed without using AM, to produce empty microcapsules. The experiment was successful and submicrometric particles with a mean diameter of 601 ±103 nm were obtained. A FESEM image of obtained particles is reported in **Figure III.1a**: spherical non coalescing particles were obtained. This result confirmed good polymer processability using SEE-C. Another experiment was performed at the same process and emulsion conditions, adding AM at 33.3% of theoretical loading with respect to the polymer content. A stable suspension was obtained also in this case with a mean diameter of 659 ±193 nm (**Table III.1**); however, looking at FESEM image, microcapsules (**Figure III.1b**) are irregular, aggregated, linked and probably AM was not entrapped. For this reason it was tried to obtain a better control of particle morphology reducing the AM content to 20% with respect to the polymer content (test EPO_02 **Table III.1**). However, the result was not different from the previous experiment, as data reported in **Table III.1** and **Figure III.1c.**

**(a)**



**(b)**



**(c)**
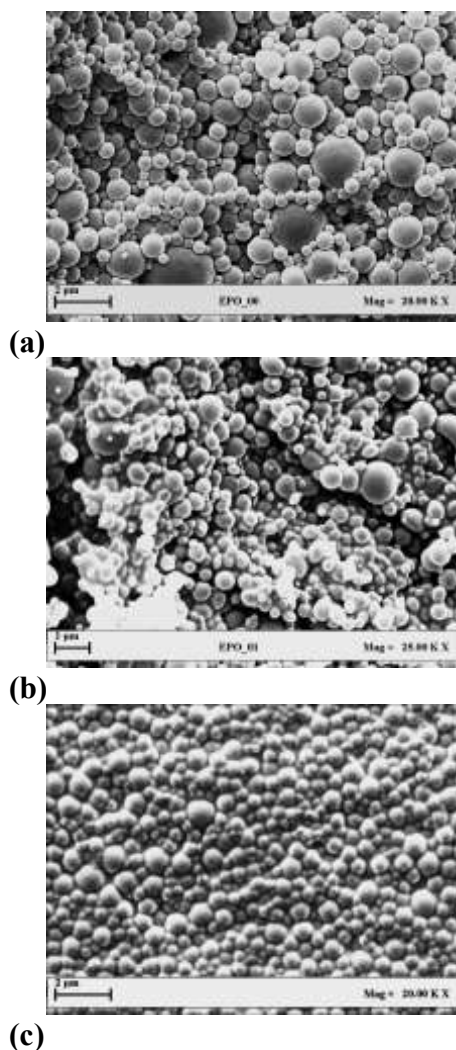
**Figure III.1** *FESEM images of SEE microcapsules produced using 10 % of Eudragit EPO in the oil phase: for only polymer (a), polymer with 33.3% of AM (b), polymer with 20 % of AM (c)*

Probably a chemical interaction between the selected polymer and AM was formed. Indeed, only the experiments for the production of loaded microcapsules were unsuccessful. A simple test was done, producing a physical mixture of Eudragit EPO and AM to understand if some reaction could develop between the two compounds and to verify incompatibility between additive and polymer. The result is reported in **Figure III.2** where it is possible to note that the physical mixture between EPO and additive showed a formation of a gel.

**Figure III.2** *Interaction between Eudragit EPO and AM*

**Eudraguard**

Other Eudragit polymers were tested. In particular, using Eudraguard, a recent pH polymer used for food application, a feasibility test was performed. Fixing the polymer concentration in oil phase at 2 % in weight, an emulsion with droplet size diameter of 659± 83 nm was obtained. The emulsion was processed using SEE-C and particles with mean size of 175 ± 35 nm were obtained. In details, in **Figure III.3** is reported FESEM image of the obtained suspension.
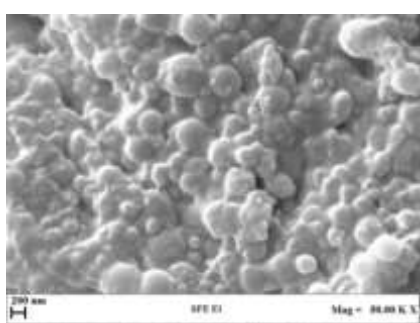


**Figure III.3** *FESEM image of obtained capsules (a) and image of emulsion and suspension using Eudraguard as polymer matrix (b)..*

As it is possibile to note from the FESEM image of **Figure III.3a**, aggregated particles were obtained. In particular, after SEE process, the obtained suspension was completely transparent (**Figure III.3b**), indeed no powder recovery was obtained. For this reason Eudraguard polymer was not a good candidate for SEE-C process and the optimization study was not conducted.

**Eudragit ERL and Eudragit ERS**

Other two Eudragit polymers were studied: Eudragit ERL and Eudragit ERS. Fixing polymer concentration at 5 % by weight in the oil phase, a feasibility test using Eudragit ERL was performed using conventional

44

method of solvent evaporation and SEE-C innovative technique but no good results were obtained in term of produced particles, as reported in the FESEM image in **Figure III.4.**
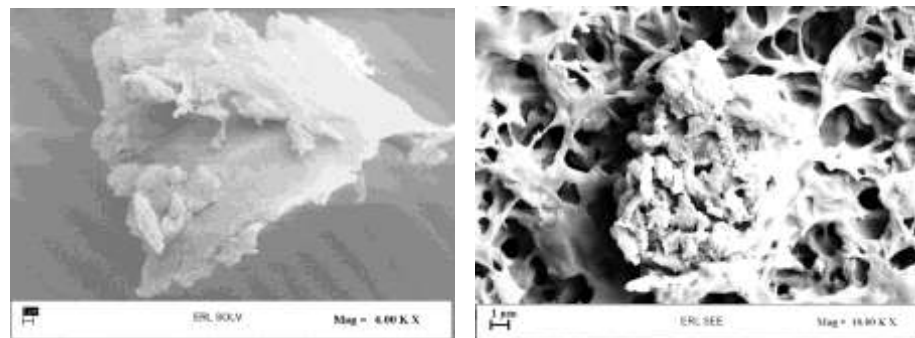


**Figure III.4** *FESEM image of the test using Eudragit ERL as polymer: conventional method (a) and SEE process (b)*

As it is possible to note from the **Figure III.4**, no particles were obtained using both methods, in fact the powders were coalescent and aggregated.

Using Eudragit ERS at the same concentration of the previous test, conventional and innovation process were performed in order to obtain a morphological comparison (**Figure III.5**).
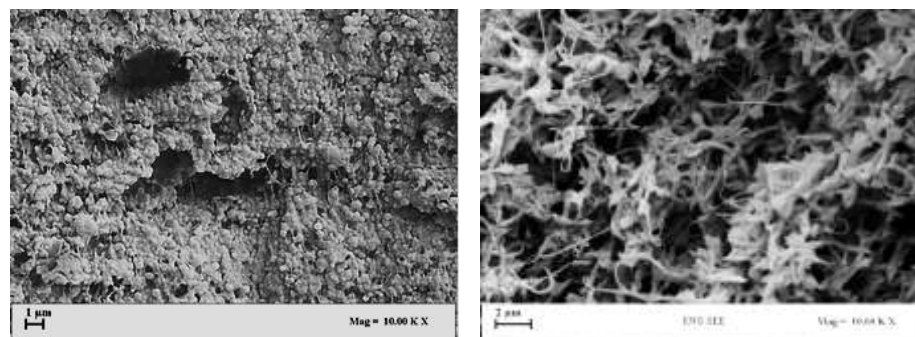


**Figure III.5** *FESEM image of obtained powder using solvent evaporation technique (a) and using SEE-C process (b).*

As reported in **Figure III.5**, using solvent evaporation techinique (a), coalescent and aggregated particles were obtained whereas using SEE-C process (b), particles were not obtained. For this reason, also in this case optimization study was not carried out.

*Ethylcellulose*

Ethyl cellulose (EC) was another polymer selected with Total as polymer for the microcapsules formation. In detail, EC is a pH sensitive polymer and

it was considered a good candidate for AM encapsulation study. First tests of empty capsules production and AM encapsulation were performed, using conventional method of solvent evaporation from emulsion. A qualitative analysis was performed based only on the morphology of obtained particles.

In particular, fixing a polymer concentration of 2.5% by weight in the oil phase, spherical particles were obtained processing only polymer, whereas when an amine content of 50% by weight respect to the polymer was added, more aggregated particles were produced (**Figure III.6**).
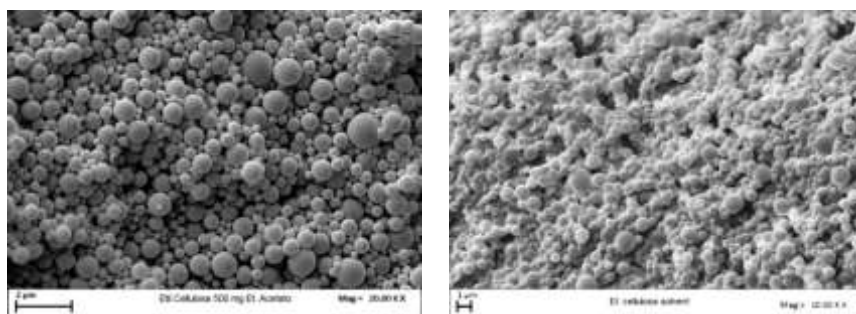


**Figure III.6** *FESEM image of obtained particles using solvent evaporation technique: empty ethyl cellulose capsules (a), ethyl cellulose loaded AM capsules (b).*

Same test for AM encapsulation was performed using the supercritical technique, and in this case aggregated and coalescent particles of AM/polymer were produced (**Figure III.7**).
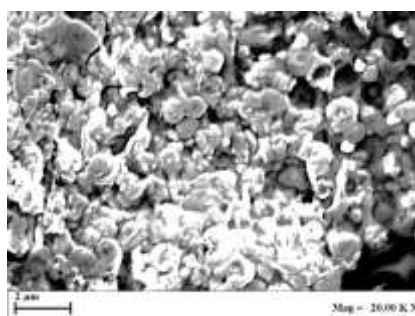


**Figure III.7** *Ethyl cellulose loaded amine capsules using SEE-C process.*

According with Total, an optimization on the EC SEE-C processability using some references of the literature (Liu et al., 2009, Prasertmanakit et al., 2009) was conducted.

In detail, the experiments were conducted by changing the polymer concentration in oily phase and the surfactant concentration in water phase: the concentration was varied from 0.1 %, 0.2 %, 0.3 % and 0.6 % for

surfactant and 1.0 %, 1.5 %, 2.0 % and 2.5 % for polymer. The experiments were repeated at least twice and the analyses were performed in triplicate, mean values and standard deviations were calculated for all data. The influence of the polymer amount in the disperse phase and the surfactant content in the continuous phase was analyzed in terms of mass recovery of the polymer, mean diameter (MD) and polydispersity index (PDI) as well as their morphology. All the formulations tested and the results obtained in terms of mean size and standard deviation are summarized in table below.

**Table III.3** *Optimization study for the production of Ethyl cellulose capsules: influence of the polymer amount in the disperse phase and the surfactant content in the continuous phase in terms of mean diameter (MD) and polydispersity index (PDI).*

| Polymer (%) | Surfactant (%) | MD (nm) | PDI |
|---|---|---|---|
| 1.0 | 0.1 | 242 ± 6 | 0.16 ± 0.02 |
|  | 0.2 | 189 ± 3 | 0.22 ± 0.04 |
|  | 0.3 | 184 ± 0 | 0.26 ± 0.01 |
|  | 0.6 | 200 ± 13 | 0.35 ± 0.02 |
| 1.5 | 0.1 | 297 ± 2 | 0.22 ± 0.02 |
|  | 0.2 | 206 ± 2 | 0.15 ± 0.00 |
|  | 0.3 | 188 ± 2 | 0.18 ± 0.02 |
|  | 0.6 | 161 ± 8 | 0.38 ± 0.05 |
| 2.0 | 0.1 | 518 ± 3 | 0.32 ± 0.05 |
|  | 0.2 | 220 ± 2 | 0.16 ± 0.05 |
|  | 0.3 | 200 ± 1 | 0.23 ± 0.01 |
|  | 0.6 | 172 ± 2 | 0.26 ± 0.01 |
| 2.5 | 0.1 | 733 ± 7 | 0.18 ± 0.04 |
|  | 0.2 | 282 ± 1 | 0.17 ± 0.03 |
|  | 0.3 | 256 ± 1 | 0.28 ± 0.08 |
|  | 0.6 | 220 ± 1 | 0.35 ± 0.01 |

As reported in **Table III.2**, at surfactant concentration of 0.1%, by increasing the polymer concentration in the oily phase from 1.0 % to 2.5 %, an increase of the fabricated carrier MD was observed from 242 nm to 733 nm. Setting the polymer concentration in the oil phase and increasing the surfactant concentration, an important reduction of nanocarriers MD from

730 nm to 150 nm was observed. However, the largest differences were found when Tween 80 concentration between 0.1% and 0.6% w/w were used, at all the polymer concentrations. In **Figure III.8** are reported the FESEM images of the tests carried out.



**0.1 % Tween 80**

**0.2 % Tween 80**

**0.3 % Tween 80**

**0.6 % Tween 80**

**0.1 % Tween 80**

**0.2 % Tween 80**

**0.3 % Tween 80**

**0.6 % Tween 80**

**0.1 % Tween 80**

**0.2 % Tween 80**

**0.3 % Tween 80**

**0.6% Tween 80**
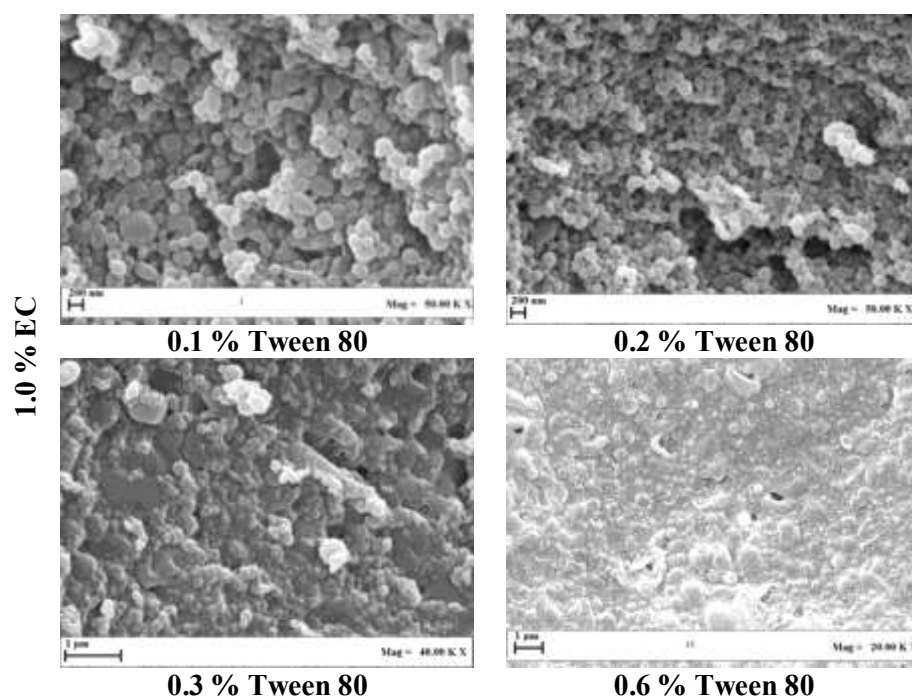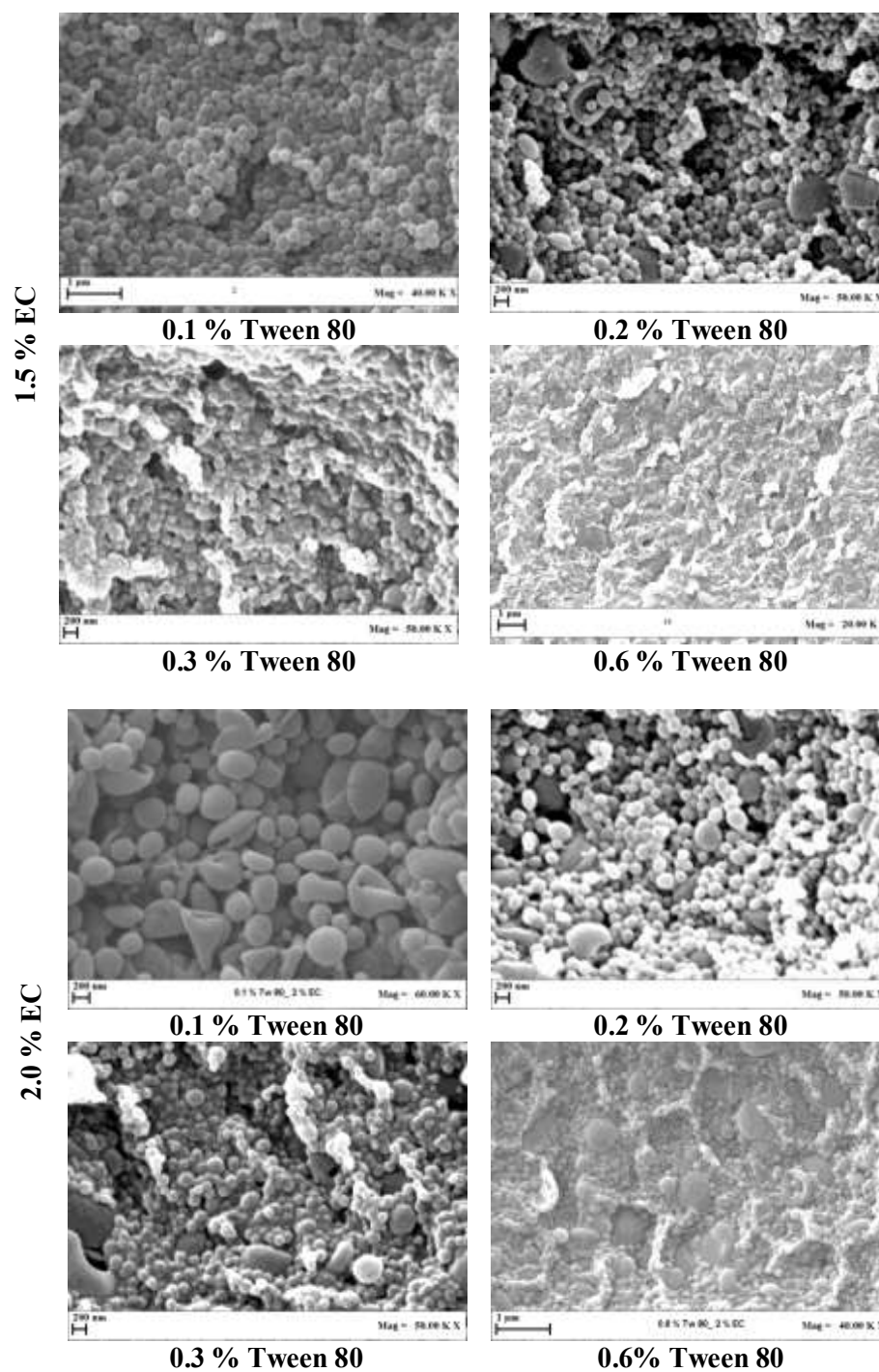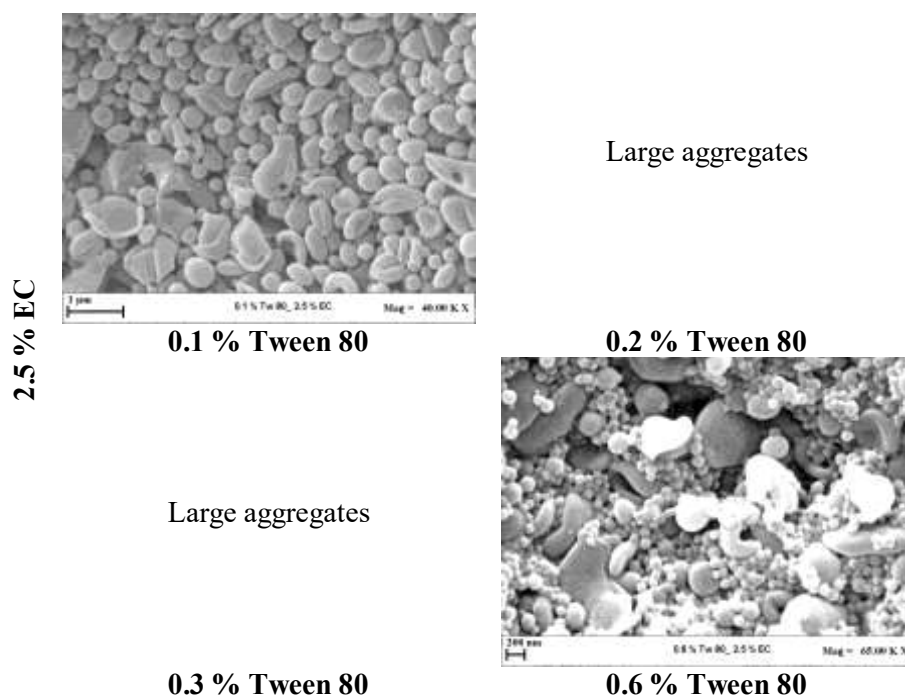
**Figure III.8** *FESEM images of Ethyl cellulose capsules at different polymer concentration in the oily phase and different surfactant concentration in the water phase.*

In general, as can be noted from FESEM images of **Figure III.8** and data in **Table III.2**, the particles obtained were spherical, some of them ellipsoidal and with PDI values from 0.15 to 0.35. Beyond 0.3% of Tween 80 in water phase, agglomeration and formation of unshaped particles were observed at all polymer concentrations. On the other hand, at lower surfactant concentrations (0.1% and 0.2%) and exceeding 1.5% w/w of EC, the formation of unshaped particles was obtained. In the **Figure III.9** is reported the behavior of the particles size diameter respect to the polymer and surfactant concentration.
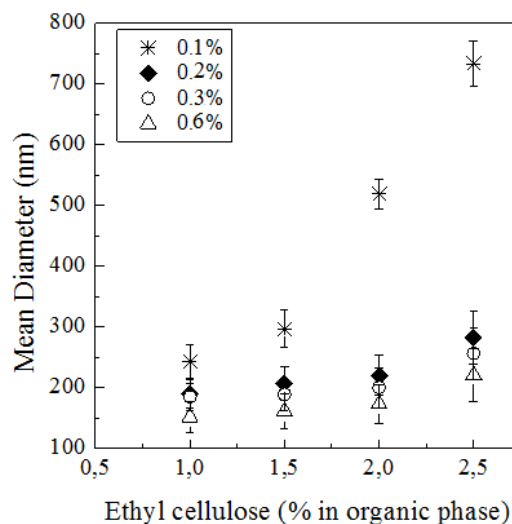
**Figure III.9** *Effect of polymer and surfactant concentration on the mean diameter of produced particles.*

In particular, as reported in the graph of **Figure III.9**, at a surfactant concentration of 0.1% mass, by increasing the polymer concentration in the oily phase from 1.0–2.5% mass, an increase of the fabricated carrier MD was observed. This behavior has already been reported in the literature and it can be explained by considering the increase of the oily phase viscosity with the polymer concentration which causes an increase of the emulsion droplet size at constant emulsion production parameters (such as rotational speed, time and emulsifier method). In **Figure III.9** is also showed that setting the polymer concentration in the oil phase and increasing the surfactant concentration, an important reduction of nanocarriers MD was observed. However, the largest differences were found between 0.1 and 0.6% mass of Tween 80 at all the polymer concentrations. The lowest difference was found at the lowest EC concentration of 1% mass and this difference became greater with the increase in the polymer fraction.

However, best result in term of mophology and MD were obtained at lower polymer concentration and lower surfactant concentration (1% EC and 0.1% Tween 80) but these results are not in target of Total requests because the recover was very slow (about 100 mg of capsules for test).

Considering these results (good morphology of ethyl cellulose particles obtained at low polymer concentration), the conditions for additive encapsulation were not optimized because the amount of additive cargo should be very low and the recovery was not in required target.

*Polymethylmetacrilate*

The processability of PMMA using supercritical $CO_2$ was already known from previous experimentations (Park and Shim, 2003). For this reason the first experiment was performed directly loading AM. SEE operative conditions were the same of the previous experiments set. Several experiments were performed to optimize the production of PMMA microcapsules loaded with AM. Experiment conditions and the relative results are reported in **Table III.3**.

**Table III.4** *SEE microcapsules production for the encapsulation of AM using PMMA as polymer carrier. *Emulsion conditions were 2000 rpm for 2 min.**Emulsion condition were 3400 rpm for 4 min.*

| Test | Polymer in O2 phase [%] | g AM/g PMMA theorical | DM±DS [nm]r | EE [%] | g AM/g PMMA effective |
|------|------|------|------|------|------|
| A1 | 5 | 1 | 189±10 | 73 | 0.73 |
| A2 | 10 | 0.5 | 247±19 | 44 | 0.22 |
| A3 | 5 | 0.7 | 195±12 | 57 | 0.40 |
| A4* | 5 | 1 | 880±217 | 47 | 0.47 |
| A5 | 5 | 3 | 162±8 | 98 | 2.94 |
| A6 | 5 | 2.4 | 180±16 | 81 | 1.94 |
| A7** | 5 | 0.75 | 267±35 | 95 | 0.71 |

For the first test (A1), PMMA was dissolved in ethyl acetate at 5% w/w with respect to the $O_2$ phase (20 g). The O1 phase, was fixed at 1 g AM/g PMMA. Stable emulsion with droplets mean size of 211±11 nm was obtained. The optical microscope image of the obtained emulsion and the relative droplet size distribution (DSD) are reported in **Figure III.10a** and **Figure III.10b**. The DSD is narrow and monodisperse, with a polydispersion index below 0.1. After SEE processing, spherical and not aggregated particles with a mean diameter of 189±10 were obtained, PSD and FESEM image and of obtained microcapsules are reported respectevly in **Figure III.10b** and **Figure III.11a**. Also microcapsules are monodispersed, with a polidispersion index equal to 0.1. This means that practically all the particles have the same dimension and it is evident also from the FESEM image. AM encapsulation efficiency was measured using a calibration curve and it was about 73%, with a AM loading respect to the polymer content of 0.73. The result obtained in this experiment matches the

required characteristics of the research study, for AM loading and microcapsules dimensions.



(a)

(b)
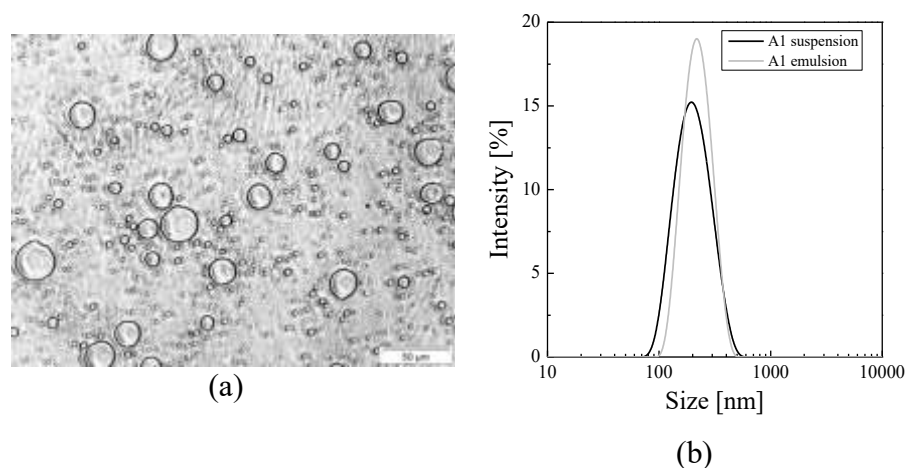
**Figure III.10** *A1 test: Optical microscope image of emulsion (a), droplets size distribution (DSD) and particles size distribution (PSD) (b).*

The effect of the operative parameters on microcapsules production were also studied and an experiment was performed increasing the amount of PMMA in the O2 phase. In particular, the A2 test of **Table III.3** was performed dissolving 10% w/w of PMMA in the O2 phase. The O1 phase was left unchanged and for this reason the total AM loading was 0.5 g AM/g PMMA. Also in this case a stable emulsion was obtained and it was successfully processed using SEE. Larger microcapsules were produced with a mean diameter of 247±19 nm, as it is possible to see in **Table III.3**. A polydispersity index of 0.15 was measured. Microcapsules were perfectly spherical and not aggregated (**Figure III.11b**). AM encapsulation efficiency was 44%, resulting in a final AM loading of 0.22 g AM/g PMMA.

(a)


(b)


(c)


(d)


(e)


(f)


(g)
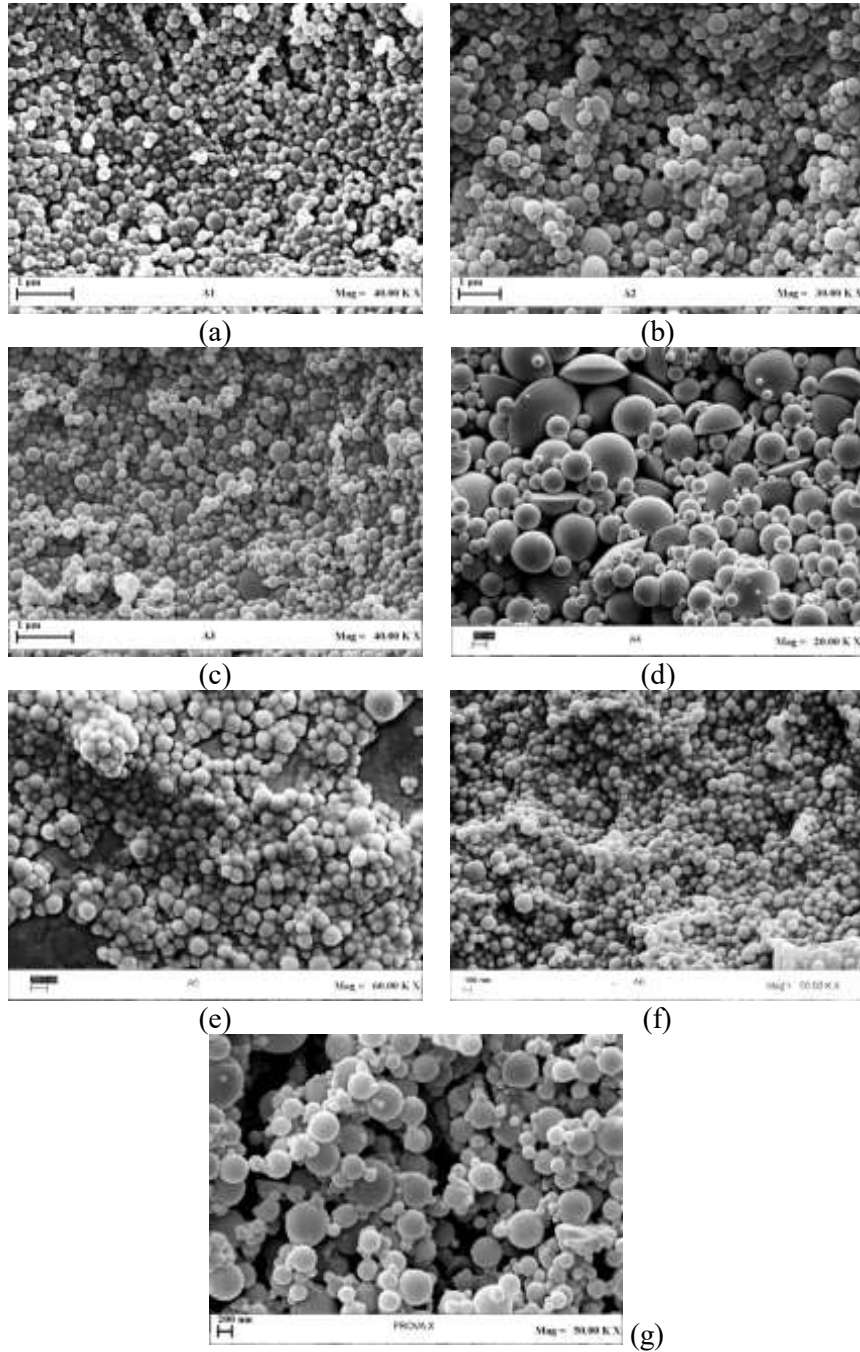
**Figure III.11** *FESEM images of AM encapsulation tests*

Another experiment was performed changing AM theorical loading. Fixing the PMMA content of the O2 phase at 5% w/w; the O1 phase, was fixed at 0.7 g AM/g PMMA. Homogeneous spherical particles were

produced also in this case, with a particles mean diameter of 195±12 nm and a polidispersity index of 0.12, indicating again a good control of particles size distribution. Results are visible in **Figure III.11c**. In this case AM encapsulation efficiency was 57%, with a final real AM loading of 0.40 g AM/g PMMA. This result suggests a decrease of AM encapsulation efficiency with the decrease of AM total loading. Also this result matches the required characteristics for this research study, regarding AM loading and microcapsules particles size diameter.

The experiment A1 was repeated changing the emulsification condition, in order to obtain larger particles and to understand how this parameter could affect microcapsules production. For this reason test A4 was performed with mild emulsification condition to allow the formation of larger water droplets and, then, larger microcapsules after SEE (see **Table III.3**). AM loading was fixed at 1 g AM/g PMMA.

In this way larger particles were obtained, as it is possible to see from FESEM image (**Figure III.11d**) and from data reported in **Table III.3**. Micrometrical particles with a mean diameter of 880±217 nm were produced and the PSD was also very wide, with a polydispersity index of 0.4. AM encapsulation efficiency was 47% resulting in a real AM loading of 0.47 g AM/g PMMA. This result seems to indicate a decrease of AM encapsulation efficiency with the increase of particle dimensions.

In the **Figure III.12** a PSD comparison of A1, A2 and A4 was reported. It is possible to note two effect: fixing the AM cargo, when the polymer amount increased (test A1 vs A2), the mean diameter of obtained particles increased and the same trend was observed changing the emulsion condition (test A1 vs A2); in particular reducing the emulsification condition a larger DSD and a consequent increasing of particles size distribution was observed.
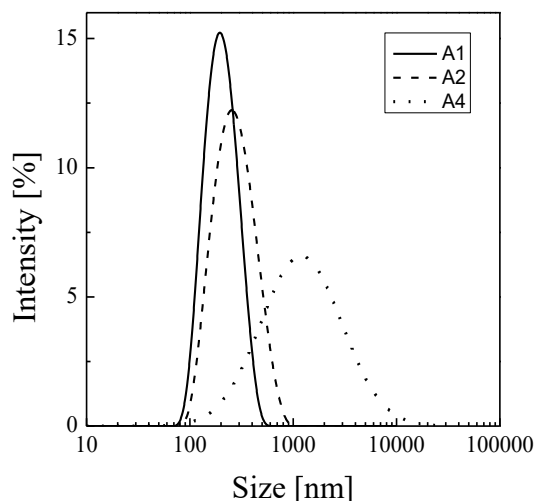
**Figure III.12** *Comparison of A1, A2 and A4 granulometric distributions: effect of polymer concentration and emulsion condition.*

Considering that it was observed that a reduction of AM total loading produced a reduction of AM encapsulation efficiency, another set of experiment was performed increasing AM/PMMA ratio from 1 to 3. All the other experiment conditions were left unchanged with respect to experiment A1, (see **Table III.3**). Using a theorical ratio AM/PMMA of 3 (test A5), a stable microcapsules suspension with a mean diameter of 162±8 nm and a narrow PSD with a polidispersity index of 0.09 was obtained. The increase of AM content produced a reduction of particle mean diameter, see **Figure III.11e**. Also encapsulation efficiency was really encouraging, AM was entrapped at 98%, obtaining a total AM loading of 2.94g AM/g PMMA. Increasing the additive theorical loading a significant increase of encapsulation efficiency was obtained. However, it was difficult to recover the particles from the water suspension probably as a consequence of their small size. From FESEM image (**Figure III.11e**) it appears also that microcapsules are not perfectly separated each other. Probably the high content of AM did not allow a complete hardening of the polymer shell of the microcapsules.

Test A6 was performed reducing AM total loading used in experiment A5, in ordert to understand if a reduction of AM loading could allow to obtain at the same time the good encapsulation efficiency of experiment A5 and also a good particles recovery. For this reason AM total loading was fixed at 2.4 g AM/g PMMA. Nanometrical capsules with a mean diameter of 180±16 nm and a polidispersion index of 0.1 were obtained also in this case; results are shown in **Figure III.11f**. Also in this case AM encapsulation

efficiency was very high, 81%, with a final AM content in microcapsules of 1.94 g AM/g PMMA. However, the problem of particle recovery from the water suspension obtained after the SEE process remained.

In **Figure III.13** a comparison of PSD varyng the ratio g AM/g PMMA from 1 to 3, was reported.
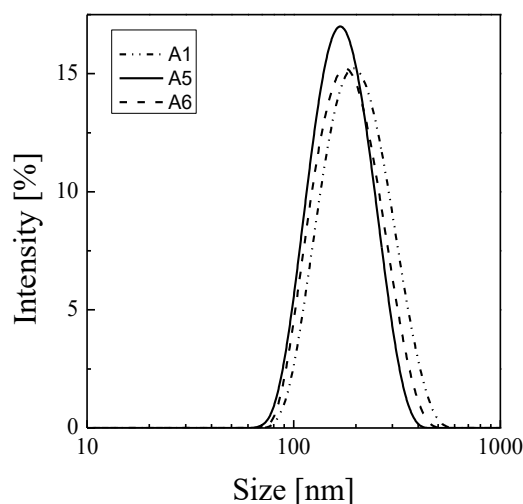


**Figure III.13** *Comparison of granulometric distributions varyng the ratio g AM/g PMMA from 1 to 3.*

Looking at the previous results of experimentation, it was possible to conclude that the best conditions found are those of experiment A1 and A3. In the first case microcapsules with a mean diameter of 189±10 nm and AM loading of 0.73 g AM/g PMMA were produced, in the second case larger particles with a mean diameter of 195±12 nm and AM loading of 0.4 g AM/g PMMA were obtained. It was also possible to note that when ratio AM/PMMA higher than 1 was tested for additive encapsulation, a sort of emulsification effect of additive was found (AM works like a surfactant) and for this reason smaller particles, higher AM EE and lower recovery were obtained, maybe due to AM presence outside the produced capsules. When mild emulsion conditions (like in A4 test) were tested, it was noted that EE decreased and particles size diamension increased. However, the low loading efficiency is more related to the low emulsion stability rather than to the production conditions of the emulsion; indeed in the literature it is generally reported that an increase in the average size of the produced capsules involves an increase in EE (Wu et al., 2017).

For this reason another test was performed using the same PMMA concentration in the oil phase ($O_2$) and an AM theorical loading of 42.8% (test A7 in **Table III.3**), but changing again the emulsion condition (3400

rpm for 4 min). This test was performed in according with the company, to obtain an increasing of AM loading and particle size dimension but at same time using a lower concentration of pure additive in respect to the test A1. Spherical and regular capsules were obtained, particles produced were characterized by a mean deameter of $267 \pm 35$ nm and AM encapsulation efficiency of 95%. A FESEM image of A7 test was reported in **Figure III.11g**. This result was very encouraging and completely satisfied the targets required by the company.

35 gr of this sample were send to Total in different step (~5gr at different time) for internal company tests.

## III.2.2 Characterization of AM microcapsules

Produced microcapsules were then characterized in terms of behavior at acid pH and oil dispersability.

### Microcapsules behavior in acid conditions

Different release conditions, in terms of temperature and pH acid values, have been considered. Tests under different pH conditions were performed to verify the efficiency of the pH activated release of AM and the ability of the released additive to neutralize pH.

Release tests at acid conditions were performed suspending capsules (20 mg) containing AM in 10 mL of distilled water acidified with sulfuric acid up to the desired level of acidity. Methyl orange was used as pH indicator. This indicator is red at acid pH and turns to pale yellow at neutral or basic pH.



**Figure III.14** *Methyl orange pH indicator color change at different pH level in water solution.*

The AM release was detected as a variation of the color as a consequence of additive pH neutralizing effect: indeed, when pure AM was added to an acid water solution, the color tuned to yellow as a consequence of the basification obtained thanks to the AM action, as it is possible to see from **Figure III.15**.
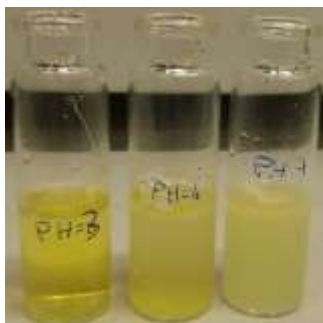
**Figure III.15** *AM mediated basification of acid water solutions*

The sample A3 (**Table III.3**), was used for release tests. This sample was obtained using PMMA at 5% in oil phase and AM theorical loading of 40%. In a release test, PMMA loaded AM microcapsules were dispersed in a water acid solution (pH 3) with methyl orange indicator. At the beginning of the release test the suspension showed an intense red color, see **Figure III.14**. The sample was left for 1 h at different release temperature: 25 °C, 80 °C and 150 °C. As shown in **Figure III.15**, AM release was evident and a color change in every temperature conditions was reported. However, the most significant effect of basification was obtained at higher temperature. These results indicated that the AM release from PMMA capsules is responsive to pH level but also temperature sensitive.
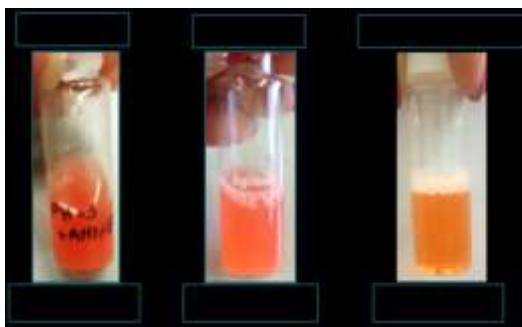


**Figure III.16** *AM release after 1 h at different temperatures.*

At the end of the release tests microcapsules degradation was also observed using FESEM.

(a)


(b)


(c)
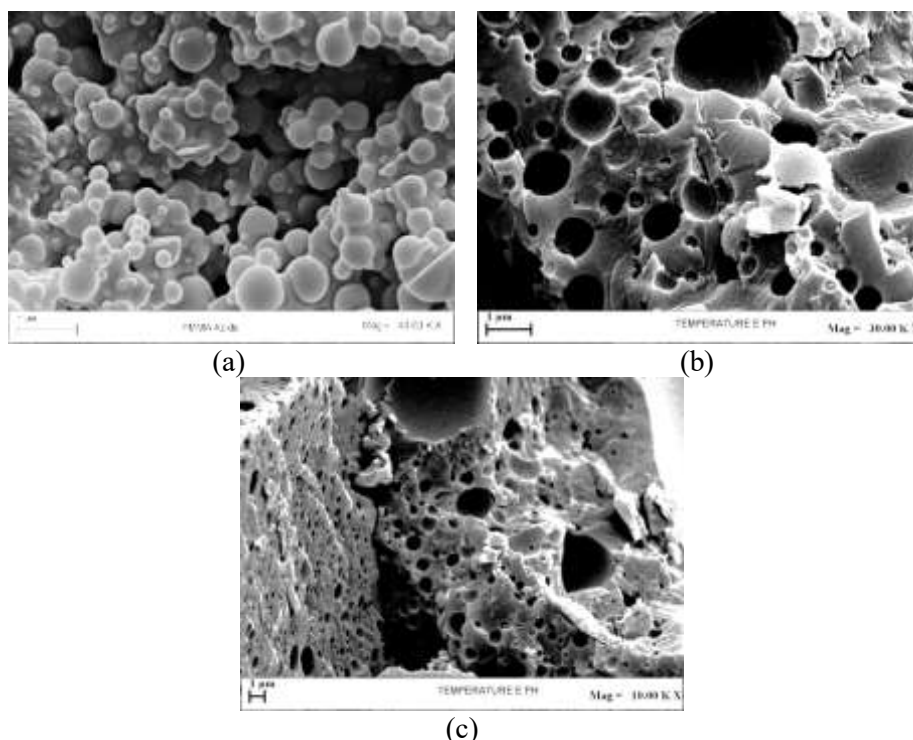
**Figure III.17** *FESEM image of PMMA loaded AM microcapsules after 1h at pH 3: 25 °C (a), 80 °C (b) and 100 °C (c).*

In **Figure III.17** it is reported, the FESEM images of the sample in acid water and after 1 h at 25 °C (**Figure III.17a**), at 80 °C (**Figure III.17b**) and at 100°C (**Figure III.17c**), in order to understand the effect of pH on polymeric structures separated form the effect of the temperature. As it is possible to see from these figures the polymer is swelled and microcapsules morphology is partially destroyed using mild temperature, but the effect is much more evident at higher temperatures, in fact the microcapsules quickly lose their spherical morphology and show a gruyere-like appearance, probably due to the release of the additive from the polymeric capsules.

*Microcapsules oil dispersability*

Microcapsules oil dispersability was an important parameter to evaluate the effectiveness of the lubricant additive encapsulation. In fact, the produced capsules must be dispersed in the base oil homogenously, without aggregation and/or sedimentation phenomena. For this reason, several tests was performed using different base oil (sent by TOTAL MS), with different viscosity proprieties.

In the first analyses, the microcapsules dispersability was measured adding microcapsules in the lubricant base oil in order to obtain a total amine

content (taking into account the encapsulation efficiency) in the prepared suspension of 5% w/w.

The suspension was agitated for 16 h at 300 rpm and the suspensions were observed in the time in order to measure their stability and the sedimentation time. As it is observed in the **Figure III.18**, the capsules dispersion was compromised in the time by elevated base oil viscosity.
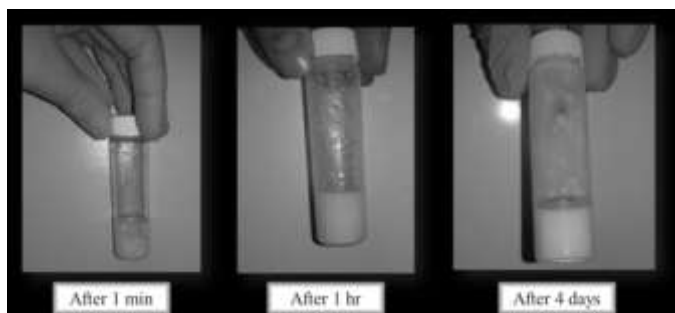


**Figure III.18** *Stability of AM capsules in the oil suspension.*

In order to increase suspension stability, tests with base oil at lower viscosity and different amine content (1%-2%-3%and 5%) were performed and reported in **Figure III.19**.



**Figure III.19** *Stability of AM capsules in the oil suspension at different concentration.*

In all cases the microcapsules showed a good dispersability in oil, the suspension turned rapidly to a milk homogeneous color.

However the internal company experiments showed that capsules dispersability was not for long time. This effect was clearly due to a difference of density of capsules and oil.

## III.3 Compound #2: MoDTC

Encapsulation of additive with specific friction modifier properties (MoDTC) was proposed by the company.
In this case, process conditions were selected to produce microcapsules with mean diameter of about 300 nm and with a minimum additive content of

40% w/w with respect to the polymer weight. For all the experiments a double $O_1/O_2/W$ emulsion was produced. The emulsion composition was maintained as oil/water 20/80 for all the experiments reported; the $O_1/O_2$ ratio was changed in order to have different additive theoretical loading. The $O_1$ phase was stabilized using 1 % of Tween80 as surfactant, the O2 solvent was ethyl acetate in which a fixed amount (expressed as % with respect to the oil phase) of polymer was dissolved, the water phase was saturated with ethylacetate and contained 0.6 % w/w of Tween 80 as surfactant. The primary $O_1/O_2$ was obtained using sonication with a high power sonication probe, at 30% of the power for 30s. The $O_1/O_2/W$ emulsion was obtained adding the primary emulsion to the water phase using a high-speed stirrer at 3300 rpm for 4 min. SEE operative conditions were the same of amine encapsulation: according to the binary vapor-liquid equilibrium diagram (VLE) at critical condition of 80 bar and 40 °C ethyl acetate is completely miscible in SC-$CO_2$. Liquid to gas ratio, L/G, was fixed at 0.1 (mass flow ratio), $CO_2$ flow rate at 1.4 kg/h and an emulsion flow rate of 2.4 mL/min were used.

Different experiments using PMMA as polymer were performed, data are reported in **Table III.4**.

**Table III.5** *SEE microcapsules production for the encapsulation of MoDTC using PMMA as polymer carrier.*

| Test | Polymer in $O_2$ phase [%] | MODTC [%] | DM±DS [nm] | EE [%] | EE after heptane [%] |
|---|---|---|---|---|---|
| **M_01** | 5 | 50 | 234±32 | ~100 | 87 |
| **M_02** | 5 | 25 | 268±50 | ~100 | 95 |
| **M_03** | 10 | 33 | 238±44 | ~100 | 67 |
| **M_06** | 5 | 31 | 206±31 | 94 | 70 |
| **M_06*** | 5 | 31 | 197±92 | 94 | 65 |
| **M_07** | 5 | 31 | 193±123 | 94 | 64 |
| **M_08** | 5 | 41 | 188±19 | ~100 | 75 |
| **M_08*** | 5 | 41 | 187±23 | 95 | 64 |
| **M_08**** | 5 | 41 | 202±25 | 94 | 69 |

*Effect of additive cargo*

First tests were carried out using the same trend of AM optimization tests. The effect of additive loading was investigated using different MoDTC cargo in the preparation of the emulsion and then increasing the polymer

concentration in oil solvent phase ($O_2$). In the first test (M_01), PMMA was dissolved in ethyl acetate at 5% w/w with respect to the $O_2$ phase (20 g). The O1 phase, was fixed to have a theorical additive load equal to 50% w/w.

FESEM images of produced particles are reported in **Figure III.20a**.

Particles of mean size of 234±32 nm and EE ~100 were produced but looking at the FESEM they appear quite aggregated.

Suggested by Total, powder was washed with a solvent able to dissolve additive and not the polymer in order to remove a possible presence of MoDTC outside the particles. Heptane was the selected solvent used. Encapsulation efficiency and morphology after heptane washing was revaluated and reported respectively in **Table III.4** and **Figure III.20b**. After heptane washing, EE of 87% were obtained: evidently, part of the additive was outside the particles and produce particles aggregation. Indeed, FESEM image of particles shows particles more separated but not not completely. In order to improve the capsules morphology, a second test was carried out using a theorical additive loading of 25% w/w. A stable emulsion was obtained and it was successfully processed using SEE-C. Larger microcapsules were produced with a mean diameter of 268±50 nm, as it is possible to see in **Table III.4**. Also in this case, microcapsules were aggregated (**Figure III.20c**) and EE was about 100%. After heptane washing, EE of 95%, correspondent to 0.47g MoDTC/g PMMA, and spherical and not aggregated capsules were obtained (**Table III.4** and **Figure III.20d**). This result matches the required characteristics for this research study.

The effect of polymer concentration was evaluated in the next test (M_03), where fixing the additive concentration as in the test M_01, the polymer concentration has been doubled. Increasing polymer concentration, no effect were observed on PSD, indeed capsules with mean size of 238±44 nm were produced and also in this case EE of about 100% were obtained (**Table III.4**). Aggregated particles were obtained as reported in FESEM image of **Figure III.20e** and also in this case the analysis after heptane washing was reported (**Figure III.20f**). As reported in Table III.4, EE was of 67% corresponded to 0.33 g of MoDTC/g of polymer.

(a)       (b)

(c)       (d)

(e)       (f)
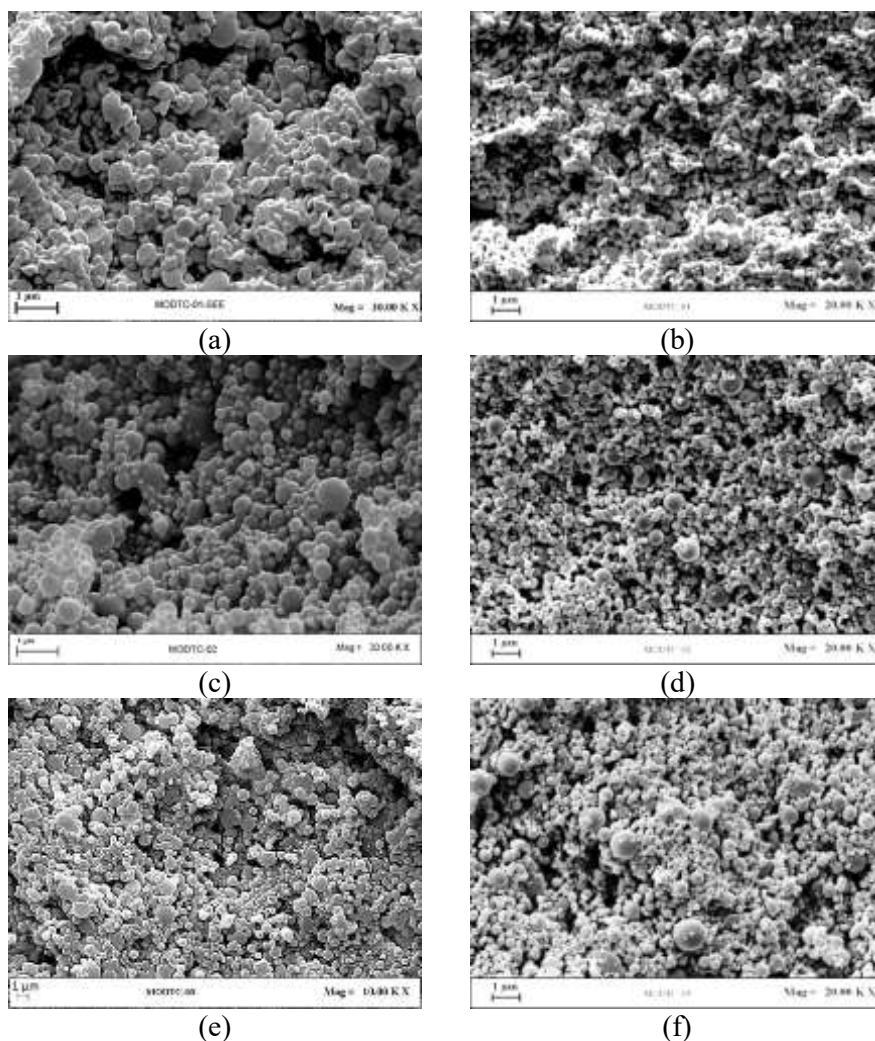
**Figure III.20** *FESEM image of PMMA loaded MODTC particles*

2 gr of tests M_02 and M_03 were sent to Total for internal company test.

*Stirring effect on the emulsion formation*

In order to obtain separated particles and increase MoDTC cargo in PMMA, other tests were performed using a theoretical loading of 31% and 41% of MoDTC in emulsion formulation and changing the emulsion parameters in terms of stirring (3300 rpm for M_06, 3000 rpm for M_06* and 2800 rpm for M_07).

In the case of M_06, spherical and homogeneous particles were obtained with mean diameter of 206±31 nm whereas in the case of M_06* and M_07

spherical but polydispersed particles were produced in both cases with PDS of 197±92 and 193±123 respectively.

Also in this case, particles were washed using heptane and the EE measured was between 64-70%: the stirring effect in the emulsion formulation had an effect on the mean particles diameter but not on the EE.

This effect was largely discussed in licterature: increasing the mixing speed generally results in decreased microsphere mean size and decreased of PDI value as it produces smaller emulsion droplets through stronger shear forces and increased turbulence (Yang et al., 2001). This effect was evident also in FESEM images of **Figure III.21**, where produced capsules of test M_06 and M_07 before and after heptane washing were reported.



| M_06 | M_06 after heptane |
| --- | --- |



| M_07 | M_07 after heptane |
| --- | --- |
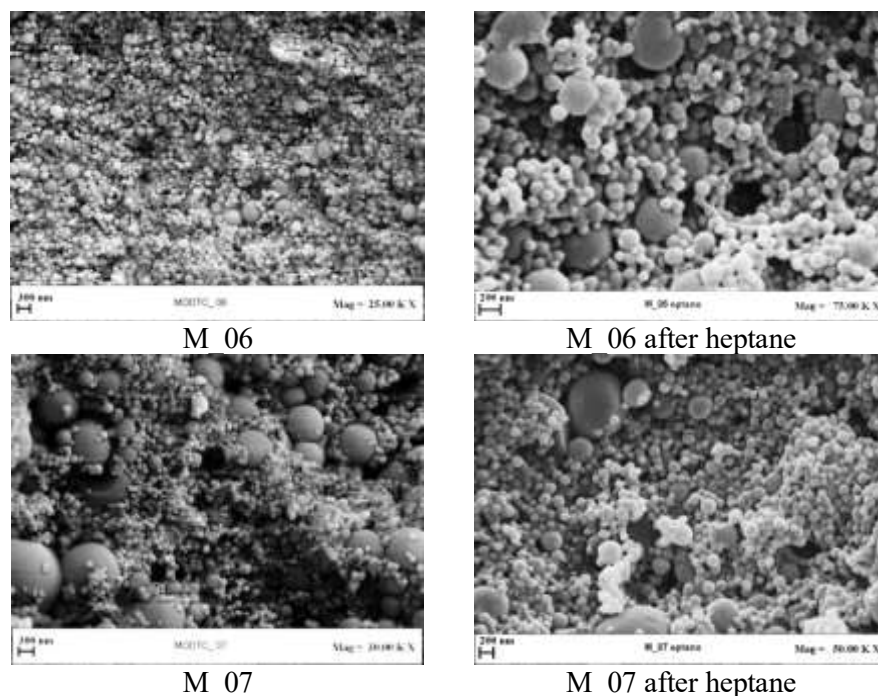
**Figure III.21** *FESEM image of M_06 and M_07, before and after heptane washing.*

*Study of surfactant effect*

Fixing the polymer concentration in the oil phase at 5% w/w and increasing the theorical additive cargo to 41% w/w respect the polymer, the effect of surfactant in the inner oily phase of emulsion was studied. In detail, the test M_08 was performed using the Tween80 at 1% by weight in the O1 phase as in the previous tests whereas the test M_08* was carried out without the surfactant and M_08** using a surfactant concentration of 0.5% by weight. Data of PSD of produced capsules were reported in **Table III.4**.

As it can see from the mean size reported in **Table III.4**, the surfactant had no effect on particles mean size, indeed PSD of 188±19, 187±23 and 202±25 nm were obtained respectively for M_08, M_08* and M_08**test, but a little effect was present on EE: considering also in this case an heptane washing, the EE increasing with the increasing of surfactant in inner oily phased of emulsion, respectively of 75%, 69% and 64% for test M_08, M-08** and M_08*. In **Figure III.22**, the FESEM images of test M_08 and M_08*, respectevly with 1% and without the surfactant use are reported.



| M_08 | M_08* |
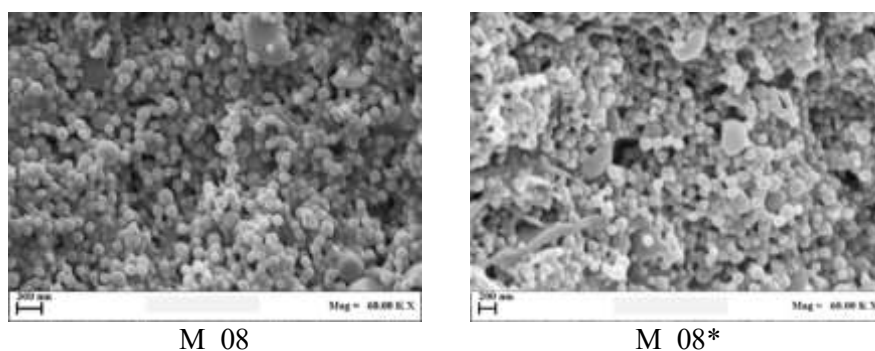
**Figure III.22** *FESEM image of M_08 and M_08*, after heptane washing.*

From FESEM image in **Figure III.22**, spherical and not aggregated particles of M_08 were obtained whereas, more coalescent particles were obtained for test M_08*. Therefore, the surfactant had a improved effect also on the particles morphology. The test M_08 matches and oversteps the required target of the company, resulting in MoDTC final loads of 0.52g /g PMMA and for this reason was considering the best result in terms of EE, morphology and recovery.

About 3 grams of produced M_08 capsules were sent to Total.

### III.3.1 Experimental results on MoDTC

*Characterization of MoDTC particles: TEM analysis*

In **Figure III.23**, TEM analysis performed on the M_08 after heptane washing was reported.
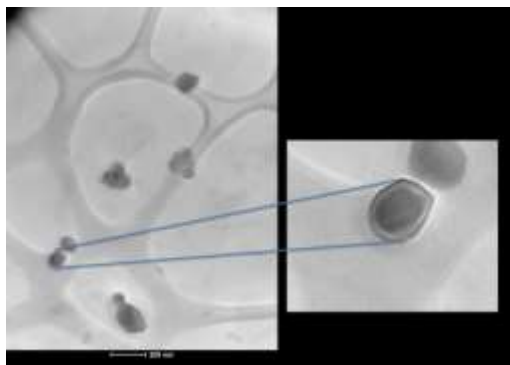
**Figure III.23 TEM analyses on M_08, after heptane washing.**

As reported in the **Figure III.23**, a shell/core structure of the produced particles was evident. In detail, the mean thichness of the polimeric shell and the capsules core size were measured and they were 13 nm and 76 nm respectively.

*Characterization of MoDTC particles: EDX analysis*

In order to attest MoDTC presence in SEE particles produced, EDX analyses were performed to give a chemical characterization of powders..

Using EDX analysis, it is possible to evaluate the chemical elements of the sample: in particular during electron illumination, an electron in the inner shell of the target atom can be ejected from the shell and an electron hole is created. Subsequently, an electron from an outer shell fills the hole, and the difference in the energy between the outer- and inner-shell electrons can be released in the form of X-ray. As the energy of this X-ray is characteristic of the atomic structure of the element from which it is emitted, the elemental composition of the sample can be determined by measuring the quantity and energy of the X-rays emitted from the sample.

In this case, the polymer has a chemical structure in which the constituent atoms are essentially carbon (C) and oxygen (O); on the other hand, the MoDTC has as characteristic atoms sulfur (S) and molybdenum (Mo). For this reason, the simultaneous presence of the various elements (C,O,S and Mo) is indicative of an additive dispersion in the polymer matrix of the sample as reported in **Figure III.24**.
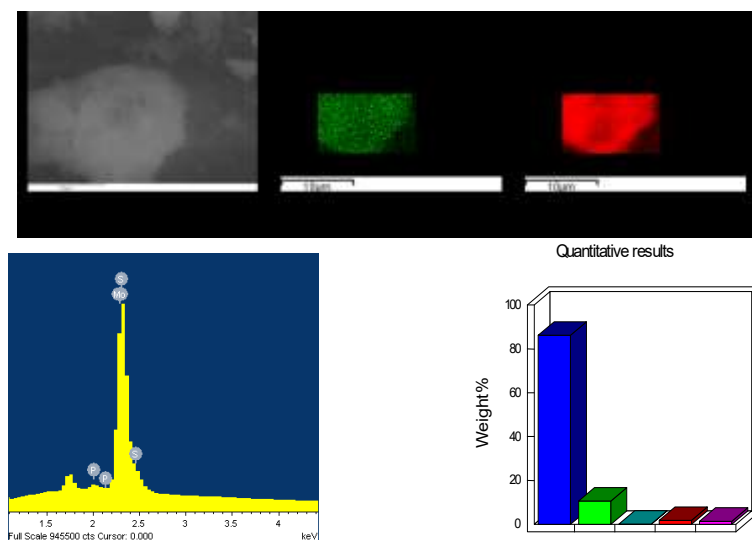
**Figure III.24** *EDX analyses related to M_08 particles, after heptane washing.*

As possible to note from the **Figure III.24**, these analyses confirmed additive presence in produced capsules, since peaks related to S and Mo were clearly evidenced. Furthermore, the key chemical elements were uniformly distributed in the microparticles, confirming the hypothesis that MoDTC was homogenous dispersed in the polymeric matrix at nanometric level, forming microcapsules. However, EDX analyses is not a quantitative analysis. For this information, M_08 batches were sent to Total to perform internal analyses and further studies, that cannot be reported in this thesis.

The particles produced satisfied the targets indicated by Total.

## III.3.2 Use others studied polymers

Feasibility tests of MoDTC encapsulation were also carried out using PMMA at higher Mw (Mw=97000 Da), Polystyrene (PS) and Polycaprolactone (PCL) as polymeric matrix. In particular, Polystyrene is a polymer largely used in self healing applications for its mechanical proprieties of resistance to mechanical stresses and on another hand, polycaprolactone is used in biomedical application and it is often used as an additive for resins to improve their processing characteristics and their end use properties (e.g., impact resistance). In **Table III.5** a summary of tests carried out was reported.

**Table III.6** *Feasibility test of capsules production using PMMA at higher Mw (M_09), polystyrene (PS_00 and PS_01) and polycaprolactone (PCL_00) as polimeric matrix*

| Test | DM±SD [nm] | Theorical cargo [%] | EE [%] |
|------|------------|---------------------|--------|
| M_09 | 224±34 | 41 | ~100 |
| PS_00 | 357±64 | -- | -- |
| PCL_00 | 1110 ± 292 | -- | -- |
| PS_01 | 296 ± 58 | 41 | ~100 |

*PMMA at higher Mw*

Using the optimized condition in the case of PMMA (Mw=18000 Da), another test for MoDTC encapsulation was conducted using the same polymer with a higher molecular weight (Mw=97000 Da).

In the test M_09, particles with mean diameter of 224±34 nm were obtained with EE about 100%. In the **Figure III.25** is reported the SEM image of the obtained powder.
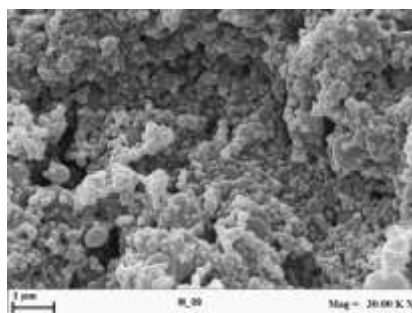


**Figure III.254** *SEM image of the test M_09, using PMMA at high molecular weight*.

As reported from the **Figure III.25**, the sample morphology showed partially coalescent particles. However, 1 gr of this sample was sent to Total because it could be interesting for internal tests.

*Polycaprolactone and Polystyrene*

Fixing a polymer concentration at 5% by weight, two test (PS_00 and PCL_00) were performed for the production of empty capsules. Stable emulsions were obtained in both cases and, as reported in FESEM images of **Figure III.26**, spherical particles with narrow particles size distribution of 357±64 and 1110 ± 292, respectevely for PS_00 and PCL_00 (as in **Table III.5**), were produced.

(a)                                        (b)
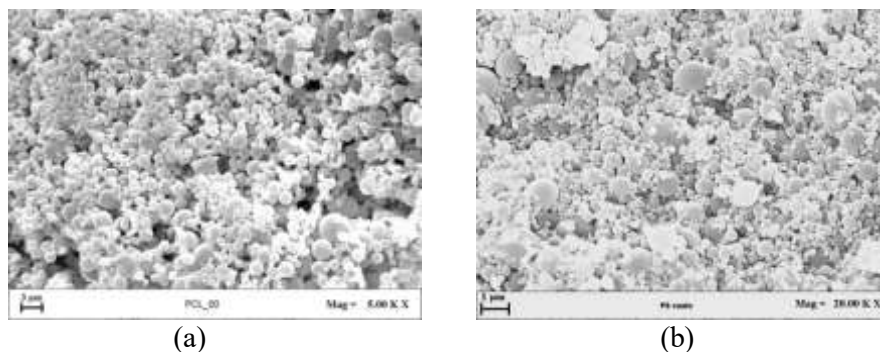
**Figure III.26** *PCL (a) and PS (b) empty produced capsules.*

Feasibility tests on MoDTC cargo was performed using polystyrene as carrier (PS_01 in **Table III.5**): spherical particles were obtained (**Figure III.27a**) and the produced capsules showed a core shell structure (**Figure III.27b**).



(a)

(b)
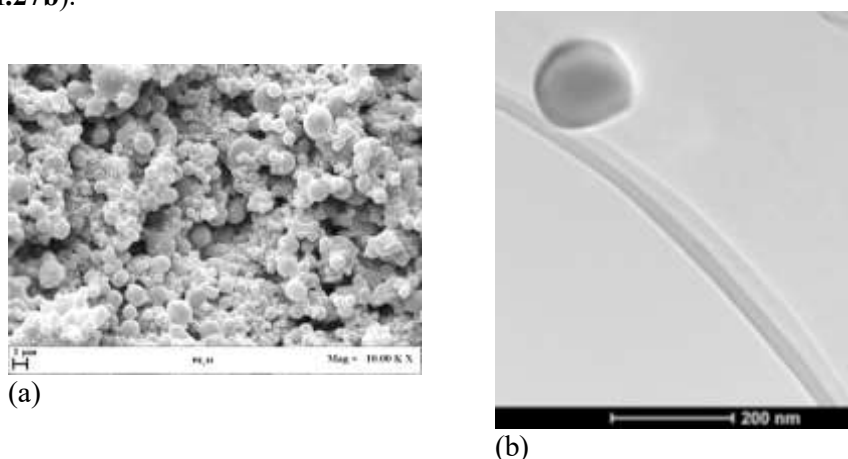
**Figure III.27** *FESEM image of PS_01 (a) and TEM analysis of the produced particles (b).*

However, an optimitation study of encapsulation using these polymers, as reported in the case of PMMA, was not performed because problem of dispersability of these capsules in Total base oil.

## III.5   Conclusions experimentation proposed by Total

Therefore in summary, the goal was successfully achieved: both additives were encapsulated in the targets required by the company and an accurate characterization of the solid state was performed.

Spherical capsules with AM and MoDTC good loading efficiency were successfully produced for the first time using SEE technology. The morphology and presence of the additive in the capsules was demonstrated

using solid state characterizations such as FESEM, UV-vis, TEM and EDX. Tests of oil dispersibility was also carried out in laboratory scale.

For each optimized product, different batches were produced for further analyses, directly performed by Total.

However, internal tests show a poor dispersion of the capsules for a long time, with consequent problems for the motors. These results are already reported in other Total competitors patents, using capsules produced using different techniques. Therefore, a possible future optimization may be aimed at optimizing the dispersion of SEE produced capsules in oil by means of surface modifications that make them stable in oil base suspension for a long time.

# Chapter IV
# Encapsulation of health-monitoring agent in PMMA microcapsules using SEE process

## IV.1   Introduction

Structural parts in the aerospace and automotive field undergo a progressive deterioration over time, caused by a wide variety of environmental factors and operational loads. Drastic and/or protracted load exposure may produce a damage build-up process; therefore, it is necessary to monitor the structural integrity. Load-bearing materials, for safety issues, require not only routine inspections; but, also the use of techniques for continuous monitoring, allowing an estimation of their modifications as a function of time, and a timely warning of a dangerous condition, using real-time data (Abdo, 2014). Structural health monitoring (SHM) concerns the process of activating damage detection and a characterization strategy for engineering structures. In particular, SHM aims at developing new methodologies to determine the structural integrity of aeronautical components. It is worth noting that the growing use of composite materials for which the damage originates and evolves in a different way than in the homogeneous ones, requires new techniques aimed at assessing the performance of the most crucial components to be developed. Several process strategies have been proposed. Conductive nanoparticles based on Carbon, incorporated in coatings or bulk materials have been proposed to confer self-sensing to the materials and for the damage monitoring at nano/micro-scale level (Vertuccio et al., 2018, Lu et al., 2017, Spinelli et al., 2018). Another approach is related to capsule-based strategies in which a chromophore is contained that is capable of revealing the damage. Song et al. (Song et al., 2019) reported the development of an extrinsic, self-healing coating system that shows no fluorescence from the intact coating, a yellowish fluorescence in cracked regions and greenish fluorescence in the

healed regions, thus allowing separate monitoring of cracking and healing of coatings. The best results in the auto repair process have been obtained thanks to healing systems that respond to a mechanical stimulus (White et al., 2001, Bleay et al., 2001). The different systems developed are glass fibers (Farhain Salehuddin et al., 2019), microvascular networks (Farhain Salehuddin et al., 2019), supramolecular interactions (Farhain Salehuddin et al., 2019, Guadagno et al., 2018) and microcapsules (Hucker et al., 1999, Bond et al., 2011, Williams et al., 2007, Ni et al., 2002, Zhu et al., 2015, Guadagno et al., 2010, Raimondo et al., 2016, Mariconda et al., 2015, Raimondo et al., 2015). In this context, the need for producing microcapsules in an easily green scalable process is relevant.

Microencapsulation is a technique widely used to produce controlled release systems in many fields, from pharmaceutical to food and agriculture and in recent times applied to the field of self-healing materials (Zhu et al., 2015, J. Zuidam and Nedovic, 2010, Fang and Bhandari, 2010). Polymeric microcapsules can increase the resistance to the breaking of the matrix; but, also, can act as a reserve containing a healing agent (Zhu et al., 2015, Guadagno et al., 2010). Yang J. et al. (Yang et al., 2008) studied the encapsulation of a repairing liquid agent (isophorone diisocyanate, IPDI) by interfacial polymerization in a stable aqueous emulsion with a polyurethane shell formed between the aqueous phase and the oil phase. These authors studied the effect of stirring speed on the size and morphology of microcapsules; at low stirring speeds, the shell wall was not uniform and thick, whereas, for speeds larger than 900 rpm, capsules with uniform and thick walls were obtained (Yang et al., 2008). White et al. (White et al., 2001) employed the polymerization in situ, to obtain microcapsules containing dicyclopentadiene (DCPD) as the repairing agent and poly urea-formaldehyde with a copolymer, obtained from ethylene and maleic anhydride, as the shell. The obtained capsules had average diameters of 200 µm and smooth and uniform surfaces. Guadagno et al., (Guadagno et al., 2016, Guadagno et al., 2014b, Guadagno et al., 2014a) following the studies of White et al. (White et al., 2001), changed the formulation of the emulsion and encapsulated 5-ethylidene-2-norbornene (ENB). The microcapsules obtained had smaller diameters and more wrinkled surfaces than those produced by White et al. (White et al., 2001). The capsules, heated up to 180 °C, showed good thermal and chemical stability (Guadagno et al., 2016).

Using the solvent evaporation technique, Li Q. et al. (Li et al., 2013b, Li et al., 2013a) produced microcapsules loaded with a repairing epoxy liquid agent, DGEBA, for self-healing applications. In detail, Li Q. et al. (Li et al., 2013b) measured the effect of some parameters (agitation speed, temperature and core-shell weight ratio) on the morphology and size of the microcapsules produced. In particular, they studied the effect of three evaporation temperatures (20°C, 60°C and 80°C) on the particle size and morphology and proved that high evaporation temperature showed a negative effect on

the morphology of the microcapsules. The amount of holes on the surface seemed to increase when the boiling temperature increased. This effect was due to the faster evaporation of the solvent from the microcapsule shell at 60°C and 80°C (Li et al., 2013b).

Conventional encapsulating techniques used for self-healing applications show some limitations such as difficulties in controlling system size and a large number of purification steps are required due to the presence of toxic organic solvents.

In the current scientific literature, encapsulation techniques for self-healing materials that use supercritical fluids have not yet been reported. Supercritical fluids, mainly supercritical carbon dioxide (SC-CO$_2$), are currently being proposed for a wide range of particle formations and design processes (Adschiri and Yoko, 2018, Campardelli and Reverchon, 2017, Di Capua et al., 2017, Franco et al., 2018, Campardelli et al., 2019, Baldino et al., 2019, Trucillo et al., 2019b). The lower viscosity and the higher diffusivity of supercritical fluids improve the mass transfer that is often the limiting factor of several conventional processes. Among all the encapsulation processes, Supercritical Emulsions Extraction (SEE-C) seems to be particularly promising because it combines conventional emulsion processes with the unique properties of supercritical fluids, to produce tailored micro/nanocarriers (Della Porta and Reverchon, 2008)..

Therefore, the objective of this work is to overcome the limits of conventional processes (e.g. repeatability, stability in the time, solvent residue) in health-monitoring microcapsules production, through the use of the supercritical emulsion extraction technique. Using the SEE technique and operating in a continuous layout (SEE-C), the possibility of microencapsulating the health-monitoring agent formed by a bifunctional epoxy precursor and epoxy reactive diluent with a chromophore has been investigated. We assumed that the structural health monitoring (SHM) would be favored when the encapsulated agent has low viscosity and, therefore, the ability to flow more easily to fill the gaps into the micro cracks, once the microcapsules are ruptured. In detail, SHM function is conferred to the materials by a chromophore solubilized in the fluid agent, within the microcapsules, that forms the fluid "core" of the microcapsule. When damage occurs, the chromophore should be released together with the health-monitoring agent in the damaged region allowing the visualization of the region interested by damage. In our case, it is worth noting that the chemical composition chosen for the health-monitoring agent is also able to promote healing reactions. As epoxy reactive diluent the use of a low-viscosity aliphatic reactive diluent 1,4-Butanediol diglycidyl ether (BDE) was proposed. BDE can act simultaneously as a viscosity modulator and as an active component in the curing reaction of the epoxy systems, by virtue of its chemical structure. Indeed, the solidification is due to a crosslinking reaction activated by the contact of oxirane rings of the DGEBA and BDE

components with a mixture of aliphatic amines already present in the coating (the specific reaction is a polyetherification). Hence, BDE was added to the epoxy resin DGEBA, characterized by the high viscosity value of 12.5 Pa.s (Gan and Shahabudin, 2019), to lower its viscosity. It is important to note that the choice of the core material greatly influences the stability of the microcapsules and an optimal ratio by weight between resin and diluent guarantees the right level of viscosity allowing to meet the criteria required for SHM polymeric coatings, also including the self-healing function. Therefore, to well perform their function, microcapsules for coating employment have to meet the following requirements: 1) to remain intact during storage, coating formulation, and application; 2) contain a sufficient amount of chemicals with fast reaction kinetics; 3) readily provide the rupture when the coating is damaged; 4) exhibit a good adhesion with the hosting polymer coating; 5) do not compromise mechanical properties of the coating. Concerning the choice of the bifunctional epoxy precursor DGEBA, it is worth noting that it is a bifunctional epoxy precursor that can be crosslinked in milder conditions (lower temperature) than trifunctional or tetrafunctional epoxy precursors. In particular, the fluid health-monitoring agent can repair the paint through crosslinking reactions. This work was focused on the study of the new microencapsulation process and if the obtained microcapsules could provide an efficient method for monitoring damages in the coating. All data related to the multifunctionality of the coating, including the simultaneously self-healing ability, will be published in a forthcoming work in preparation. Here, different oil-oil-water (O1/O2/W) emulsion formulations have been tested varying the amount of solubilized polymer (PMMA) in the external oily phase (O2) and the concentration of epoxy resin and dye in the internal oil phase (O1). The same emulsions have also been processed using the conventional solvent evaporation (SE) to compare the results of both techniques, in terms of particle size distribution, powder stability in the time and encapsulation efficiency. The calorimetric response has been analyzed using differential scanning calorimetric analysis (DSC), the effect on chemical groups and on the interactions between the components present in the microcapsules has been investigated using Fourier Transform Infrared Spectroscopy (FT-IR) analysis. Energy Dispersive X-ray (EDX) tests have been performed on the obtained particles and on the paint in which they have been dispersed, to carry out first impact tests.

**Materials**

Carbon dioxide, $CO_2$, purity 99.9% was provided by Morlando Group (Naples, Italy). Ethyl acetate (EA) of purity 99.9% was supplied from Carlo Erba Reagents (Milan, Italy). Poly-methyl methacrylate (PMMA MW: 15,000 g/mol, Sigma-Aldrich, Italy), Tween 80 (Sigma-Aldrich, Italy) were used as received. The bifunctional epoxy precursor DGEBA and the epoxy

reactive diluent 1,4-Butanediol diglycidyl ether (BDE) were purchased from Sigma-Aldrich (Italy). As a chromophore, the Solvent Red 242 (Fast Colour LPP) was used. Aerowave 3003 which is a water-based, 2-component, amine-based epoxy was obtained from AkzoNobel Aerospace Coatings. The Curing Solution 6007 used in combination with Aerowave 3003 epoxy primer was also purchased from AkzoNobel Aerospace Coatings. Figure IV.1 shows the chemical formulas of the epoxy components DGEBA and BDE and the Solvent Red 242.
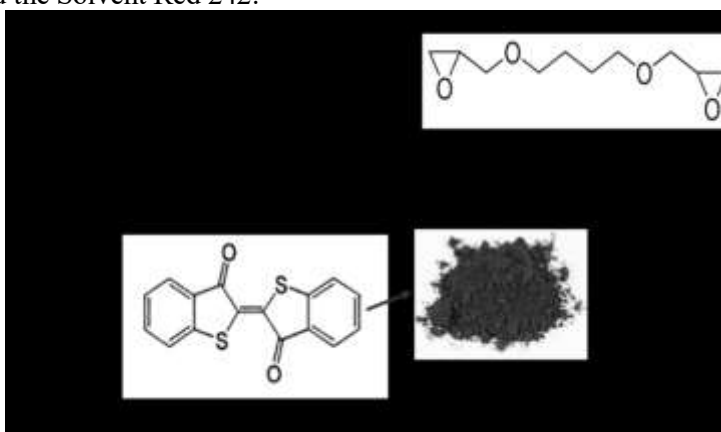


**Figure IV.1** *Chemical formulas of the epoxy components DGEBA and BDE and fluorescent dye Solvent Red 242.*

## Preparation of the health-monitoring liquid epoxy formulation (DGEBA+BDE+Solvent Red 242)

The health-monitoring liquid epoxy formulation, using in microcapsules preparation, was obtained by mixing a bifunctional epoxy resin (DGEBA) with a reactive diluent (BDE), respectively at a weight percentage of 75%: 25%, in an oil bath at 40 °C, in order to guarantee an appropriate mixing homogeneity. The dye, Solvent Red 242, was then added to the fluid mixture (DGEBA+BDE), at 1% (or 3%, 5%, and 10%) w/w with respect to the epoxy components DGEBA and BDE. Then, the dye was homogeneously mixed with a magnetic stirrer until its complete solubilization in the epoxy mixture.

### Emulsion Formulation

Epoxy formulation (O1) at different concentrations was dispersed in an oily phase (O2) consisting of the organic solvent (ethyl acetate, EA) in which PMMA at fixed concentration was dissolved. The primary O1/O2 emulsion was obtained using an ultrasound probe (model S-450D, Branson Ultrasonics Corporation, Danbury, CT) at a fixed amplitude (30%) for a

given time (30 s for 3 times). Using a high-speed homogenizer (model L4RT, Silverson Machines Ltd., Waterside, Chesham Bucks, United Kingdom) for 5 min at 2800 rpm, the primary O1/O2 emulsion was added to a water phase (W) consisting of EA-saturated aqueous Tween 80 solution (0.6% w/w in water).

## Solvent evaporation (SE) and Supercritical emulsion extraction (SEE-C)

All emulsions were processed using the traditional technique of solvent evaporation (SE) and continuous Supercritical Emulsion Extraction (SEE-C). This last process was developed by Reverchon and coworkers (Della Porta and Reverchon, 2008, Della Porta et al., 2013, Falco et al., 2012a, Della Porta et al., 2011b). Briefly, SEE-C apparatus consists of an extraction tower, containing packing elements (0.16 in. Pro-Pak, Scientific Development Company, State College, PA) in which supercritical carbon dioxide (SC-CO$_2$) is fed from the bottom using a high-pressure diaphragm pump (SC_P, mod. Milroyal B, Milton Roy, Pont Saint-Pierre, France). The emulsion is pumped from the top of the column using a high-pressure piston pump (L_P, mod. 305, Gilson, Villiers-le-Bel, France). The counter-current flow between emulsion and SC-CO$_2$ favors the extraction of the organic solvent from the emulsion drops that is, then, recovered in a separator put downstream at the top of the column. The particles are continuously recovered from the bottom of the column in an aqueous suspension (Tirado et al., 2019a).

The emulsions were also processed using solvent evaporation (SE); in this case, the emulsion was stirred at 100 rpm for 2 hours at 38 °C, to allow the elimination of the solvent by evaporation. Microcapsules collected from each assay were washed with distilled water and centrifuged for 45 min at 6500 rpm at 4°C (Thermo Scientific, mod. IEC CL30R) and, then, recovered on a membrane filter (Millipore MF membrane filter, Filter type 0.2 μm HA) and dried in air.

## Preparation of the Coated Samples

The coating samples were prepared according to the procedure described below. A formulation consisting of Curing Solution 6007 and Aerowave 3003 epoxy primer, at a weight percentage of 42.53%:57.47% respectively, was properly mixed. PMMA microcapsules containing the Health-Monitoring liquid agent (DGEBA+BDE+Solvent Red 242) were homogeneously dispersed in the previous formulation, at 3 % by wt. with respect to the mixture Curing Solution 6007 and Aerowave 3003 epoxy primer. The complete formulation was applied to the panel string surface using a "K303 MULTICOATER" surface coating applicator. SEE-C microcapsules prepared with a dye concentration of 1% by wt and epoxy

resin concentration at 10 mg/mL, corresponding to sample RES_E3 SEE, have been employed for the preparation of the coated CFRC strips.

The following strips of CFRC coated with the formulated coatings have been prepared:

1.  Strips of CFRC coated with the formulation containing 5% by wt. of microcapsules. The coating has been applied two times on the panel surface which was, then, thermally treated in an oven at 60 ° C for 20 min (Sample 1);

2.  Strips of CFRC coated with a formulation containing 3% by wt. of microcapsules. The coating has been applied two times on the panel surface which was then thermally treated in an oven at 60 ° C for 20 min after each treatment (Sample 2);

3.  Strips of CFRC coated with a formulation containing 3% by wt. of microcapsules. The coating has been applied two times on the panel surface which was then thermally treated in an oven at 60 ° C for 20 min (Sample 3);

4.  Strips of CFRC coated with a formulation containing 10% by wt. of microcapsules. The coating has been applied two times on the panel surface, that was, then, thermally treated in an oven at 60 ° C for 20 min after each treatment (Sample 4);

5.  Strips of CFRC coated with a formulation containing only the mixture Curing Solution 6007 and Aerowave 3003 epoxy primer, in the absence of microcapsules (reference coating sample) applied two times on the panel surface, that was thermally treated in an oven at 60 ° C for 20 min after each treatment (Sample 5).

Samples 1 and 4 show a rough coating due to the high concentration of microcapsules. Sample 3 health-monitoring sheeting showed a less homogeneous feature than sample 2. Therefore, samples 2 and sample 5 (reference coating sample) were chosen to perform preliminary impact tests.

## IV.2   Experimental results

### IV.2.1 Selection of SEE-C process conditions

Process temperature and pressure were fixed at 80 bar, 38 °C; they were used also in previous works, using the same SEE-C apparatus. Experimental conditions were selected to efficiently extract the organic solvent from the emulsion, since a supercritical solution is formed between SC-$CO_2$ and the organic solvent (Falco and Kiran, 2011, Smith et al., 1998). Indeed, high-pressure vapor-liquid equilibria(VLE) of the binary system EA/$CO_2$ were used to select the operating conditions above the mixture critical point (Smith et al., 1998). Moreover, at these operative conditions, water has only slight solubility in SC-$CO_2$ (King et al., 1992, Falco et al., 2013); therefore, water-SC-$CO_2$ interactions were minimized. At the selected conditions, a

maximum difference in density between the emulsion and SC-$CO_2$ is achieved, which favors the interactions of two distinct phases along the column, avoiding flooding phenomena (Falco et al., 2012a). A liquid/gas (L/G) ratio of 0.1 and a $CO_2$ flow rate of 1.4 kg/h were also fixed according to the previous considerations (Falco et al., 2012a). Different emulsion formulations were explored to assure an optimal encapsulation efficiency of the curing agent. All the emulsion formulations, size, distributions, and loadings are summarized in **Table IV.1**.

**Table IV.7** *Different emulsion formulations tested by SEE. Effect of polymer concentration loaded in the oily phase (O2), effect of epoxy resin and dye concentration in the O1 phase, mean size of the obtained droplets and particles, Encapsulation Efficiency (EE) and the technique used to solvent removal are reported*

| Test | Epoxy resin [mg/mL] | Dye [%] | DSD [nm±SD] | PSD [nm±SD] | EE [%] | Process |
|---|---|---|---|---|---|---|
| **RES_E1** | 5 | 1 | 572±11 | 165±18<br>463±12 | 78.9<br>18.1 | SEE-C<br>SE |
| **RES_E2** | 7.5 | 1 | 589±87 | 184±52<br>444±52 | 57.7<br>33.2 | SEE-C<br>SE |
| **RES_E3** | 10 | 1 | 776± 11 | 258±43<br>726±12 | 76.1<br>----- | SEE-C<br>SE |
| **RES_E4** | 7.5 | 1 | 717±10 | 279±52 | 57.0 | SEE-C |
| **RES_E5** | 5 | 1 | 573±77 | 183±15<br>685±10 | 59.4<br>58.3 | SEE-C<br>SE |
| **RES_E6** | 10 | 3 | 722±42 | 257±50 | ~100 | SEE-C |
| **RES_E7** | 10 | 5 | 935±22 | 268 ±60 | ~100 | SEE-C |
| **RES_E8** | 10 | 10 | 1533±19 | 282±11 | ~100 | SEE-C |

## IV.2.2 Effect of epoxy resin concentration

A first set of experiments was carried out at a constant polymer concentration in the O2 phase of the emulsion (equal to 5% by weight) and varying the quantity of resin loaded in the O1 phase. The tests were performed using SEE technology and the conventional solvent evaporation technique (SE). In particular, two tests were performed, (RES_E1) with a resin concentration of 5 mg/mL (33.3% w/w in O1/O2 emulsion) and (RES_E2) with a resin concentration of 7.5 mg/mL (42.8% w/w O1/O2 emulsion). The analyses carried out, show that the emulsions obtained are stable and, as shown in **Table IV.1**; they show an average drop diameter of 572±114 nm for RES_E1 and 589±87 nm for RES_E2, respectively.

Therefore, increasing the quantity of epoxy resin from 33.3% to 42.8% in the O1 phase a slight increase in the average diameter of the drops is obtained.

The capsules produced were, however, very different when the two techniques were used. In **Figure IV.2**, a comparison of the particle size distributions obtained using both methods used is shown.
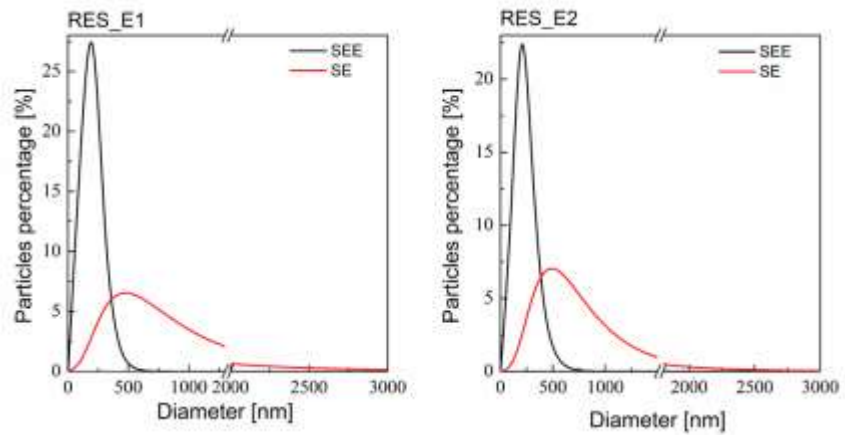


**Figure IV.2** *Comparison of the particle size distribution for RES_E1 and RES_E2 tests produced by SEE and SE, respectively.*

**Figure IV.2** and droplets size distributions in **Table IV.1** display that the particles obtained by SEE show an average diameter of $165 \pm 18$ nm and $184 \pm 52$ nm respectively; whereas, those obtained by conventional technology show an average diameter of $463 \pm 121$ nm for RES_E1 and $444 \pm 52$ nm for RES_E2. Therefore, in both cases, particles with a smaller diameter were obtained using SEE and the distribution curves show also sharper size distribution. The obtained particles were observed also using a scanning electron microscope and the results are reported in **Figure IV.3**. SEM images in **Figures IV.3a** and **IV.3c** show that the particles produced using SEE have a regular spherical morphology; whereas particles obtained using the SE technique are not homogeneous and, as shown in **Figures IV.3b** and **IV.3d**, form a sort of particle network.
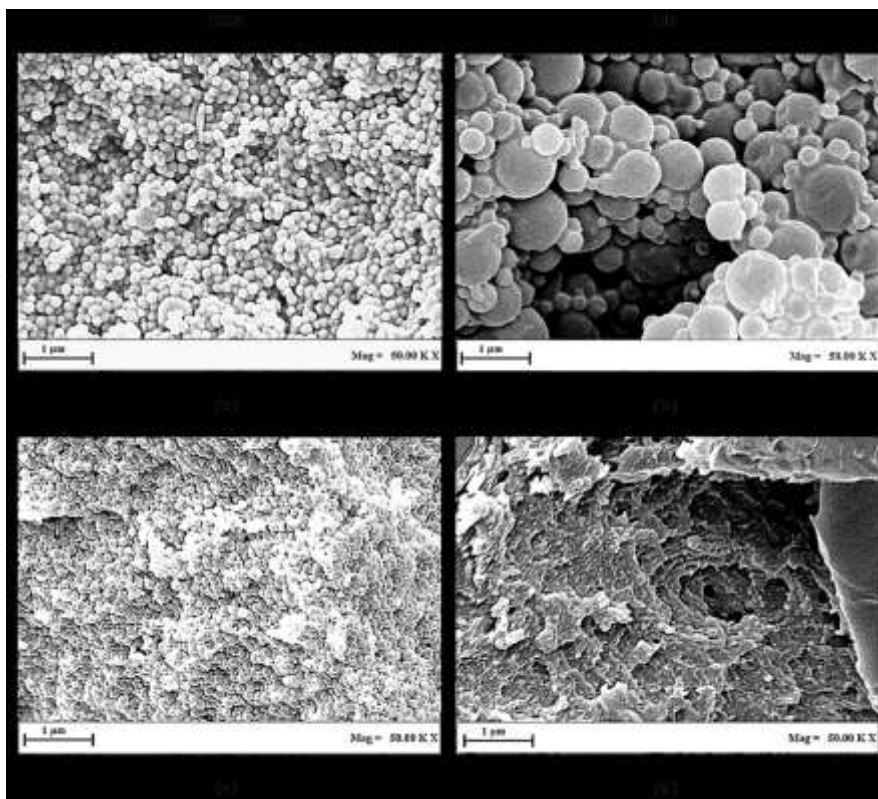
**Figure IV.3** *FESEM images of RES_E1 and RES_E2 experiments, produced by SEE (a, c) and SE technique(b,d).*

The powders were also subjected to UV-vis analysis to determine the quantity of resin entrapped inside the capsules. Encapsulation efficiency of 79% using SEE technique and 18% using conventional method was recorded for the RES_E1 test; whereas, in the test RES_E2 an efficiency of 58% was obtained using the supercritical method, compared to 33% obtained by the SE method. Therefore, using the supercritical solvent extraction technique, it was possible to obtain larger encapsulation efficiencies than the conventional SE method; increasing the initial epoxy resin concentration, this difference was less evident. Moreover, powders obtained using the conventional technique (SE), were glassy, probably due to the presence on the surface of resin that was not encapsulated in the polymer matrix.

To further improve particle stability, it was decided to study the effect of the polymer concentration in the O2 phase of the emulsion.

## IV.2.3 Effect of polymer concentration

A second set of experiments was carried out doubling the concentration of polymer dissolved in the oil phase. In particular, 2 g of PMMA were

dissolved in 20 mL of ethyl acetate (phase O2 of the emulsion), to improve the stability of the emulsions produced and to obtain a larger homogeneity and a better recovery of the particles. Three tests were performed using the SEE-C and SE technologies, varying the concentration of resin within the O1 phase from 20% to 33.3% by weight. The conditions for the formation of the emulsions have been previously described. Stable emulsions were obtained in all cases tested and reducing the quantity of resin in the O2 phase from 33.3% to 20%, droplets with an average diameter of 776± 114 nm, 717±103 nm, and 573±77 nm were obtained respectively (**Table IV.1**) The suspensions were also characterized by DLS to determine the particle size distribution; the results are compared in **Figure IV.4.**
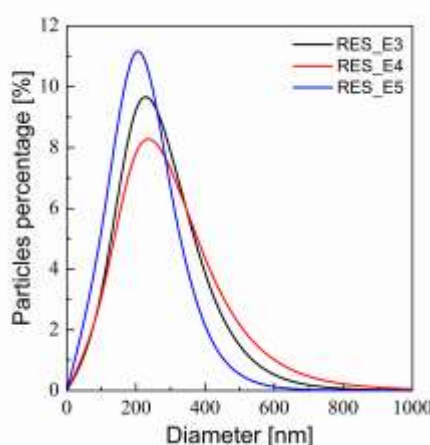


**Figure IV.4** *Comparison of suspension particle size distribution of the test RES_E3, RES_E4, and RES_E5.*

The suspensions obtained using SEE-C, showed an average particle diameter of 258±45 nm, 279±52 nm, and 183±15 nm, respectively. Therefore, increasing the resin concentration in the internal phase from 20% to 33.3%, there was a slight increase in the diameter of the obtained particles, in particular for RES_E4, the largest average diameters were measured. The suspensions obtained using SEE-C were centrifuged and filtered on 0.2 μm porosity membranes and left to dry.

The morphology of the obtained particles was observed using a scanning electron microscope (SEM), the results are shown in **Figure IV.5.**
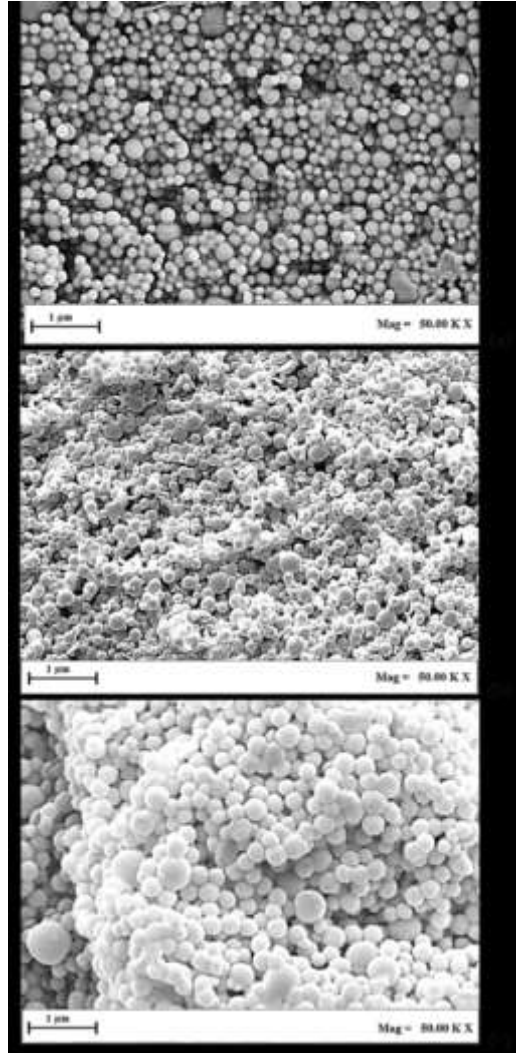
**Figure IV.5** *FESEM images of RES_E3 (a), RES_E4 (b), RES_E5 (c)*

The morphology of particles confirmed the average distribution data of particle diameters reported in **Table IV.1**. Particles were regular, spherical and homogeneous. The emulsions of the tests RES_E3 and RES_E5 were also processed by conventional SE, to have a comparison in this case too. **Figure IV.6** shows the distribution of the suspensions, compared with those produced using SEE-C technology.
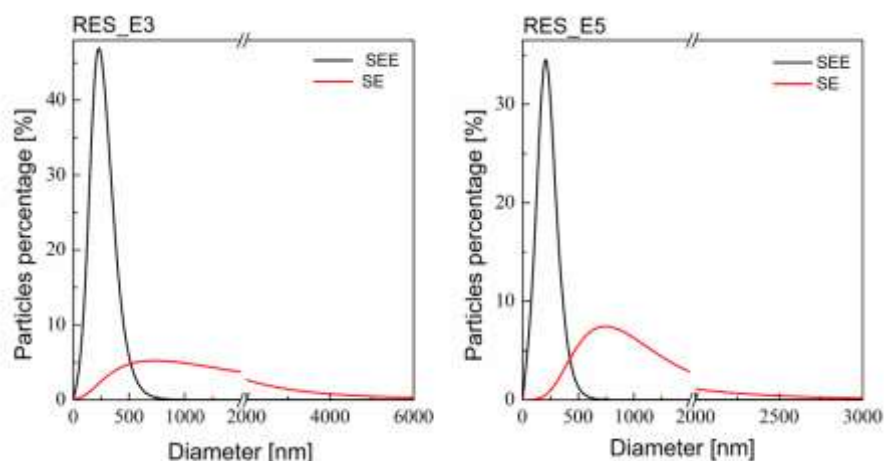
**Figure IV.6** *Comparison of Particles Size Distribution of RES_E3 and RES_E5 produced using the SEE and SE techniques*

As shown in **Table IV.1** and **Figure IV.6**, the particles obtained by SEE-C showed again a smaller diameter and a sharper distribution: an average diameter of 258±43 nm for RES_E3 and 183±15 nm for RES_E5; whereas, the particles produced by SE showed particles size distributions with a mean size of 726±118 nm and 685±103 nm, respectively.

Using SEE-C, a loading efficiency of 76% was measured for the RES_E3 test; whereas, using the conventional technique, this measure cannot be performed due to the poor stability of the sample. In the case of RES_E4 the loading efficiency was 57% and comparable EEs were obtained respectively of 59% using the supercritical process and 58% using a conventional technique for RES_E5 for RES_E5. Therefore, using SEE-C, also higher encapsulation efficiencies were obtained than using SE technique.

### IV.2.4 Effect of dye concentration

An additional set of experiments was performed by increasing the concentration of the dye in the epoxy resin formulation (oil phase, O1). The preparation of the emulsion remained unchanged compared to the previous experiments and in particular, RES_E3 formulation was used; i.e., with a resin concentration of 10 mg / mL, the dye concentration was varied from 1% to 10 %. All the formulations produced were processed using SEE-C technology. In **Figure IV.7**, images of the emulsions obtained at different concentrations are reported and it can be observed that, when the percentage of dye loaded in phase O1 increases, the color of the emulsion produced intensifies, passing from light purple to dark purple.
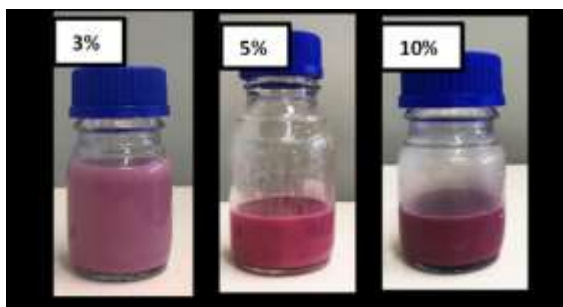
**Figure IV.7** *Emulsions obtained varying the dye concentration*

Homogeneity and stability of the emulsions decreased as the concentration of dye increased. Data in **Table IV.1** show that emulsions with an average drop diameter of $722 \pm 42$ nm, $935 \pm 221$ nm, $1533 \pm 185$ nm, respectively, were obtained increasing the dye concentration from 3% to 10%.
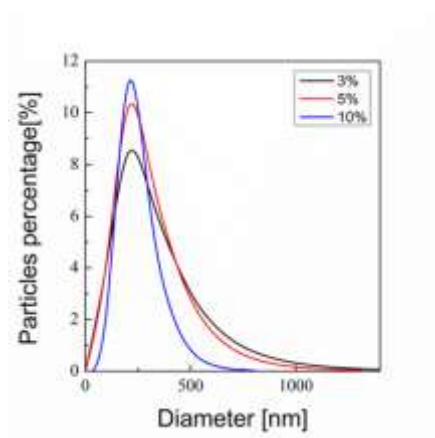


**Figure IV.8** *Comparison of RES_E6, RES_E7, RES_E8 granulometric distributions with varying dye concentration from 3 to 10 %*

Stable suspensions with average particle diameters, of $257 \pm 50$ nm, $268 \pm 60$ nm and $282 \pm 111$ nm respectively were produced, as shown in **Figure IV.8**. The suspensions were centrifuged and filtered on membranes with 0.1 µm porosity and left to dry. **Figure IV.9** shows the color of the powders obtained.

**Figure IV.9** *Powders obtained by varying the dye concentration, color effect*

Powder color ranged from an intense violet using 3% of dye to a dark purple for the 10%. However, using a greater quantity of dye, part of the resin was lost from the polymer matrix and the sample was not homogeneous.

Using a scanning electron microscope (SEM), the morphologies of the obtained powders were studied and results are shown in **Figure IV.10**. SEM images show that the morphology is not very homogeneous. Indeed, there are areas of the sample in which the particles are coalescent and others in which they are spherical, not very regular and partially fused together. This result was probably due to an excessive concentration of dye inside the internal oil phase. Indeed, tests carried out with high dye percentages showed that emulsions were not very stable, with consequent problems related to the processing.
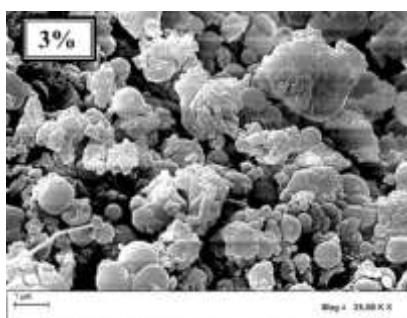


**Figure IV.10** *SEM image of RES_E6 using a dye concentration of 3%*

*IV.2.5 Capsules stability*

Stability analysis in the time was carried out by monitoring the average particle size and morphology. In particular, analyses of the suspensions were repeated for more than 30 days**. Figure IV.11** shows the average size of the particles. In this figure, also the comparison of the analyses for conventional tests (SE) is reported.
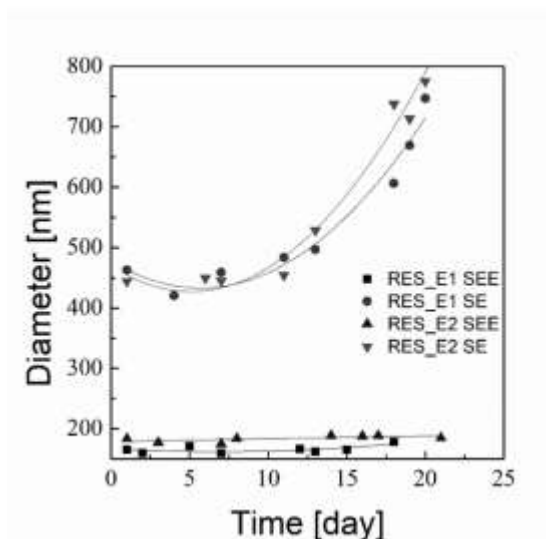
**Figure IV.11** *Stability in the time of produced capsules diameters*

It is possible to observe that capsules obtained using SEE-C show stable average diameters in time; whereas, the capsules obtained using the conventional method show a progressive increase of the average diameter, probably due to the leakage of the resin and the subsequent coalescence of particles. The morphological stability over time was verified by performing SEM analysis on the samples stored at room temperature (**Figure IV.12**), confirming the poor stability of SE particles.
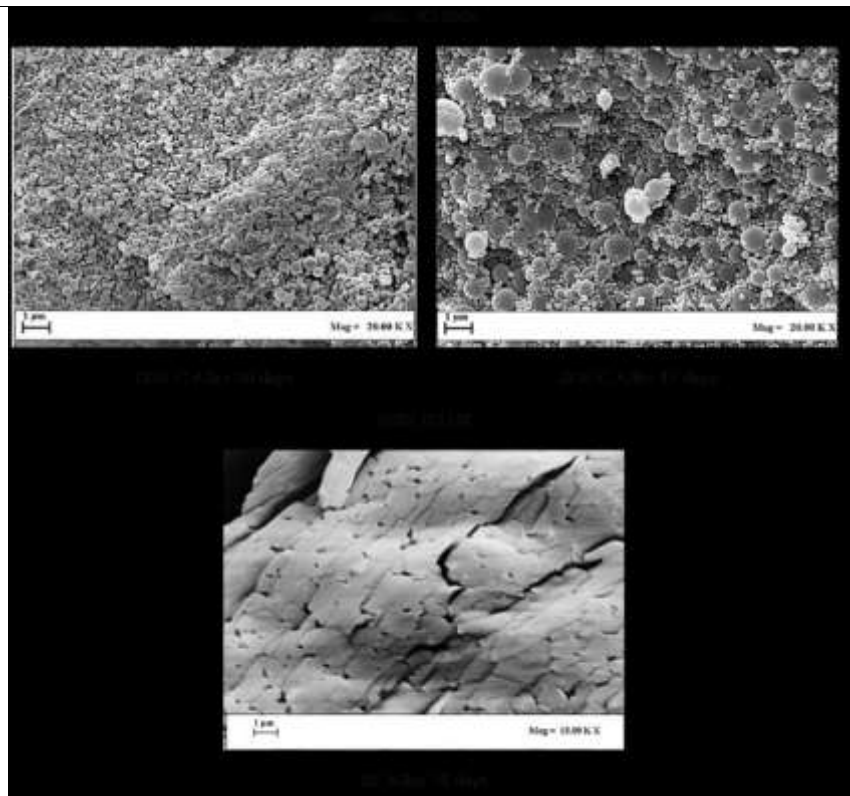
**Figure IV.12** *Analysis of morphological time stability*

The powder obtained by SE completely lost its regular morphology. Probably, the resin was not stably entrapped in the polymer shell and caused the fusion and coalescence of all particles. In **Figure IV.12**, the SEM analyses of RES_E3 are reported after 30 and 45 days. The images show that SEE-C particles maintain their spherical morphology over time, confirming the granulometric analysis.

### IV.2.6 Solid-state characterizations

#### Differential scanning calorimetry (DSC) analysis

To verify that the treated materials did not undergo any structural variation during the process, a differential scanning calorimetry analysis was performed. Thermograms obtained for the powders were compared with those obtained for the untreated polymer. **Figure IV.13** shows the DSC curves of the powders obtained using the SEE and SE, compared with untreated PMMA.
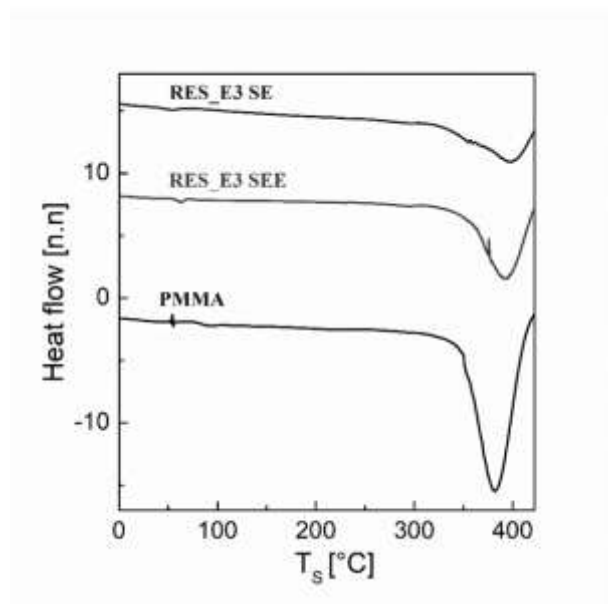
**Figure IV.13** *DSC curves*

Raw PMMA showed a glass transition temperature around 100-110 °C. The powder curves showed a trend similar to that of the raw polymer, demonstrating good thermal stability, and the absence of peaks that lead to assume the presence of non-encapsulated material and therefore resin leaking from the polymer matrix. Therefore, the nanodispersion of the resin in the polymeric matrix led to the formation of an amorphous compound.

*Fourier Transform Infrared (FT-IR) Spectroscopy*

The powders obtained from both techniques were subjected to FT-IR spectroscopy to evaluate the effect of the encapsulation process on chemical groups and the interaction between the components present in the produced microcapsules. The results obtained were compared with those of the raw polymer in **Figure IV.14**.
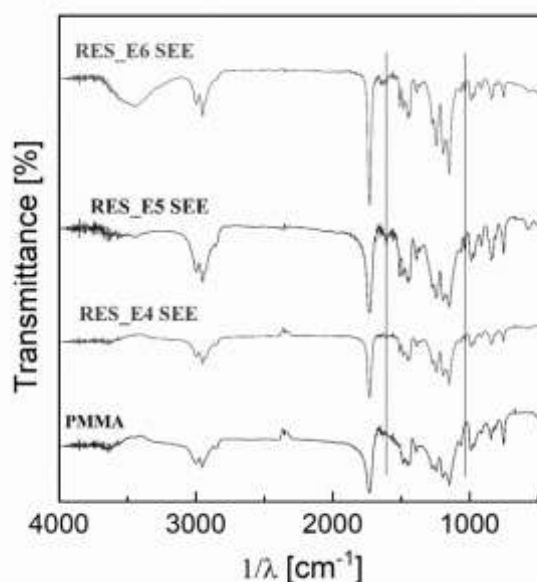
**Figure IV.14** *FT-IR spectroscopy*

It is possible to note the characteristic peaks of the polymer, PMMA shows a C=O (stretch) absorption band at 1730 cm$^{-1}$ and symmetric and asymmetric stretching absorption peaks ---CH$_2$ respectively at 2845 and 2998 cm$^{-1}$. The band at 1200 cm$^{-1}$ represents the O-CH$_3$ stretching vibration. For the produced microcapsules (RES_E4 SEE, RES_E5 SEE and RES_E6 SEE), the absorption peaks at 1607 and 1034 cm$^{-1}$ indicate the presence of C-O-C and epoxide groups, respectively (Li et al., 2013a). Characteristic peaks of both epoxy and PMMA shell appear in the FTIR spectrum of the microcapsules that clearly indicates the encapsulation of epoxy in PMMA microcapsules.

In all the cases analyzed, the characteristic peaks of the processed compounds did not undergo displacements or shifts with respect to the spectrum of the polymer, confirming that the process does not produce a modification of chemical bonds of the processed compounds.

*Energy Dispersive X-ray (EDX) test*

EDX test was performed to individuate a component that could reveal the presence of the resin in the capsules dispersed in the paint. The focus was on sulfur atoms (S) present in the dye chosen for the preparation of the epoxy resin. A first analysis was carried out on capsules produced using a dye concentration of 3% w/w. **Figure IV.15** shows the spectrum of the elements.
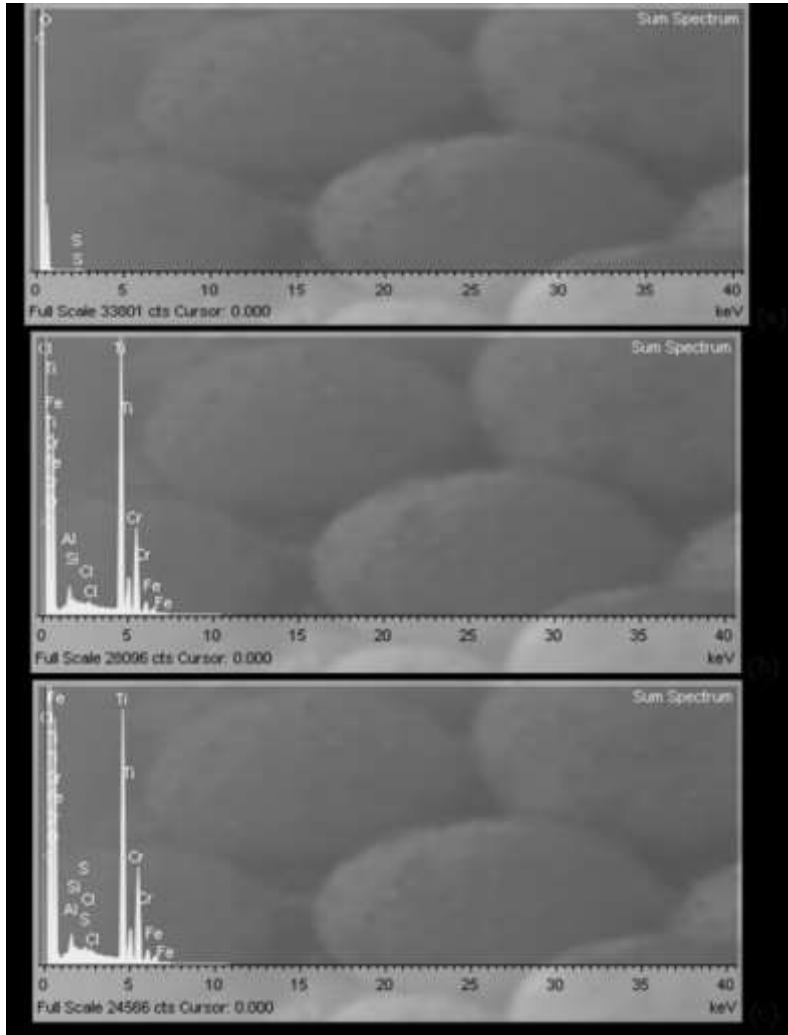
**Figure IV.15** *EDX spectrum of RES_E6 (a), paint (b), paint and capsules (RES_E6) homogeneously distributed (c).*

The spectrum in **Figure IV.15a** clearly shows the presence of sulfur (S), which is attributed to the dye trapped in the polymeric matrix of PMMA. The same analysis was, then, carried out on the paint as it was applied to the carbon fiber panels (**Figure IV.15b**). In this case, the presence of Ti is prevalent, and there is no trace of sulfur. Therefore, the decisive analysis was carried out on the paint in which the capsules were dispersed. The paint containing the capsules with different dye concentration was dispersed on a carbon fiber reinforced panel. In this case, SEE-C microcapsules prepared with a dye concentration of 3% by wt, (RES_E6) and paint were homogeneously distributed on CFRC strips, and the spectrum (**Figure**
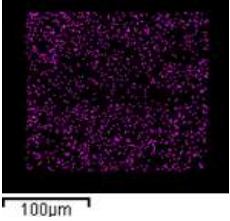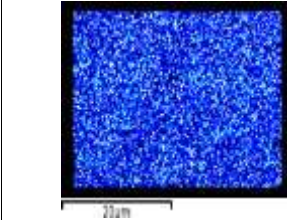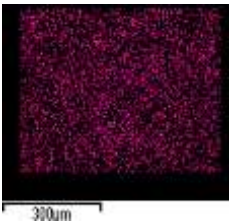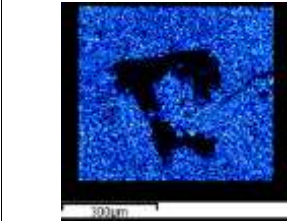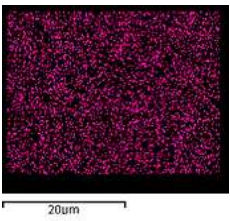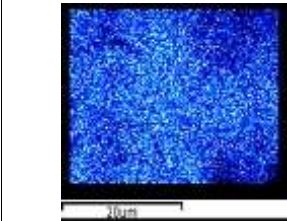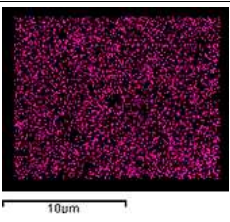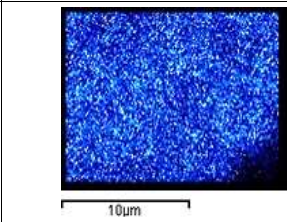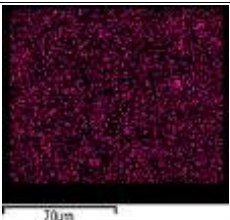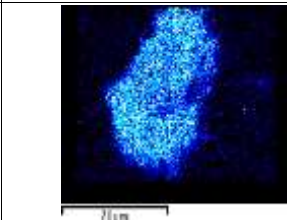
**IV.15c**) was intermediate with respect to the two previous cases, the chemical elements in the paint and in the capsules were clearly visible.

Then, a detailed analysis was conducted on the strip samples prepared as reported in the section

*Preparation of the Coated Samples*

A specific area on the sample was selected and colorimetry of the most significant components was performed. In particular, an identifying color was assigned: magenta for the sulfur (S) and cyan for titanium (Ti). The results are summarized in **Table IV.2**.

**Table IV.8** *EDX images of the analyzed samples*

| | S | Ti |
|---|---|---|
| **Powder (RES_E3 SEE)** | 100µm | ------ |
| **Sample 5 (reference sample)** | ----- |  |
| **Sample 1** | 300µm | 300µm |
| **Sample 2** | 20µm |  |
| **Sample 3** | 10µm | 10µm |
| **Sample 4** | 70µm |  |

The results show that the powders contain sulfur; whereas, the water-based paint shows a significant amount of titanium. Paints with dispersed capsules (Sample 1 to 4) show both elements S and Ti, confirming that the capsules are homogeneously distributed in the examined sample.

*Impact tests*

Impact tests have been carried out to establish the capability of a coating film to stand up to breakage, fracture or splintering on quick deformation, and thus to examine the damaging consequence, if any, due to the microcapsule incorporation on the mechanical property of the coating. Specimens of Carbon Fiber-reinforced Composites were coated with the paint (mixture Curing Solution 6007 and Aerowave 3003 epoxy primer), in which the microcapsules were previously dispersed. The Panels strips were subjected to impact tests performed at two different energies, 3.8 J and 4.5 J, respectively.

The damage generated on the surface of the sample after the impact performed using 4.5 J was not easy identifiable to the naked eye, without the prior knowledge of its position. Therefore, these areas were observed using an optical microscope as reported in the literature protocol (Nair et al., 2017). The preliminary impact test results obtained are shown in **Figure IV.16**. In particular, in this Figure, optical microscopy images a) and b) refer to the reference coating sample in the absence of microcapsules (corresponding to the sample 5 in the paragraph **Preparation of the Coated Samples),** whereas, optical microscopy images c) and d) refer to the sample coated with health-monitoring paint containing 3% by wt of microcapsules (corresponding to the sample 2 in the paragraph **Preparation of the Coated Samples**).
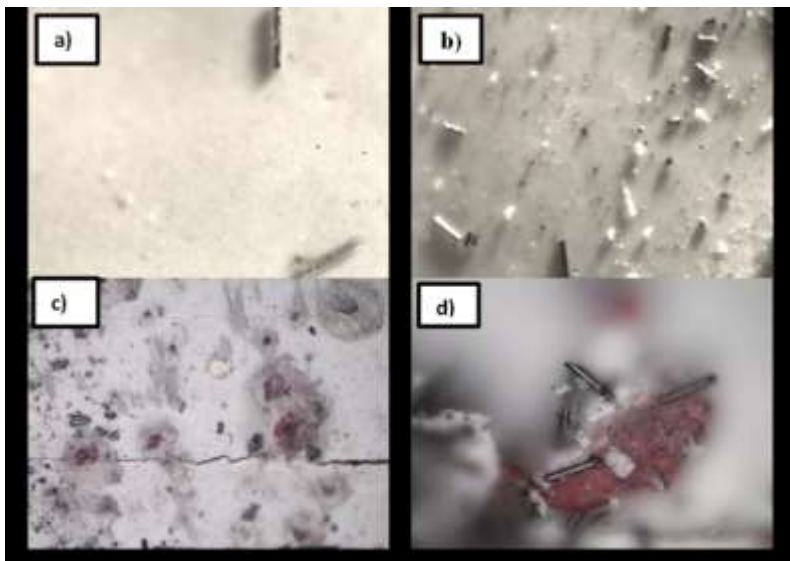
**Figure IV.16** *a) e b) impacted zones of the reference coating sample in the absence of microcapsules (sample 5) (a – magnification 20x, b-magnification 50x) ; c) e d) impacted zone of the sample coated with health-monitoring paint containing 3% by wt. of microcapsules (sample 2) (c – magnification 20x, d-magnification 50x).*

Two impacted zones of the specimen are shown. It is possible to identify fragments of carbon fibers, but no colorimetric changes. In **Figure IV.16c** and **Figure IV.16d**, instead, two impacted zones of a specimen coated with health-monitoring paint loaded with 3% by wt. of microcapsules are shown. In this case, it is possible to note the leakage of the dye, due to the rupture of the microcapsules as a consequence of mechanical stress. It is possible to observe that the monitoring liquid agent into microcracks is released when the coating is damaged and, automatically fixes the microcracks thus proving the effectiveness of both the innovative encapsulation process and the applicative potential of the health-monitoring formulation. Halos of a faint pink color can be identified also to the naked eye, after the impact. Impact tests at lower energy were also performed and no damages were diagnosed.

## IV.3   Conclusion on encapsulation of health-monitoring agent

The SEE-C encapsulation technique proved to be a very effective for producing microcapsules to be used as health monitoring element and potentially for other self-responsive functions.

A comparison between the SEE-C process and solvent evaporation technique was also carried out in term of particle size distribution (PSD), encapsulation efficiencies (EE) and stability in the time (TS) of the produced

particles: SEE-C is more effective in ensuring the essential requirements to impart optical health monitoring function to developed formulations.

Preliminary impact tests performed on carbon fiber reinforced panels coated with an aqueous paint in which SEE-C capsules were previously dispersed, showed a remarkable change in the color of the damaged areas. The panels, subjected to impact tests showed the dye leaking and therefore the capsule breaking in stressed areas.

Experiments are in progress to test the simultaneous self-healing ability of the same coating containing in the matrix microcapsules able to simultaneously confer health monitoring and self-healing capability to the coating.

# Chapter V
# PLA/PLGA micro/nano carriers for the Growth Factors delivery fabricated by Supercritical Emulsion Extraction: release profiles study and cytotoxicity evaluation

## V.1 Introduction

Micro and nano-carriers, with controlled size and suitable encapsulation efficiency, may act as micro-environmental regulators within a 3D bioengineered scaffold, providing a wide range of spatio-temporally controlled bio-molecules delivery (Della Porta et al., 2018; Della Porta et al., 2017). These 3D assembled synthetic matrices can be used for highly predictive in vitro models or to fabricate implantable devices for tissue engineering applications (Ciardulli et al., 2020; Cipollaro et al., 2019; Giordano et al., 2020; Okamoto, 2019). In this context, controlled release systems have recently received extensive attention given their great potential not only in pharmaceutical (Ciaglia et al., 2019; Cricchio et al., 2017; Govoni et al., 2020) but also in biomedical applications within tissue engineering protocols (Della Porta et al., 2015; Govoni et al., 2017; Trucillo et al., 2019). Particularly, growth factors are small biomolecules capable of stimulating cellular growth, proliferation and differentiation (Ren et al., 2020). Therefore, they are largely used in tissue engineering protocols to induce stem cells commitment versus specific phenotype(s). For example, human Growth Differentiation Factor 5 (hGDF-5) induces the expression of genes typically associated to the tendon phenotype (Giordano et al., 2020;

Karthik et al., 2014; Tan et al., 2012) and, for this reason, it is used in pharmacological protocols for tendon healing and repair. On the other hand, human Transforming Growth factor β1 (hTGF-β1) has been widely investigated in the process of chondrogenesis for cartilage healing protocols (Danišovič et al., 2012; Madry et al., 2014).

Poly-lactic-co-glycolic acid (PLGA) and poly-lactic acid (PLA) are FDA approved bioresorbable carriers (Gentile et al., 2014; Makadia and Siegel, 2011) capable of bulk degradation without swelling and with well recognized capacity of ensuring controlled release rate of loaded drugs (Faisant et al., 2006; Faisant et al., 2002; Klose et al., 2006; Siepmann and Siepmann, 2008; Trucillo et al., 2019). Several techniques are available to prepare biopolymer-based micro/nano-carriers, such as spray drying (Miller et al., 2016; Shi et al., 2020) or coacervation (Timilsena et al., 2019), even through, in the specific case of PLA and PLGA processing, the solvent evaporation/extraction of emulsions has been described as optimal given its milder processing conditions compared to spray drying, and easier solvent removal compared to coacervation. Indeed, during the evaporation or extraction of emulsion, the oily droplets dispersed in the water external phase are hardened leading to micro/nano-carriers formation (Freitas et al., 2005; Katou et al., 2008; Nag and Nath, 2018). Despite these two technique being largely recommended, evaporation showed batch to batch reproducibility disturbances (Meng et al., 2004; Miyazaki et al., 2006) and extraction uses relatively large amounts of a second solvent producing the problem of solvent mixtures recovery. Both processes require processing time of several hours and, as a consequence, aggregation phenomena may occur between the droplets, producing carriers with a larger poly-dispersity compared to derived droplets (Ozkan et al., 2019). Another disadvantage lies in the poor encapsulation efficiencies of high water-soluble compounds (Freitas et al., 2005). Indeed, these molecules could spread out or diffuse from the dispersed oily phase into the aqueous continuous phase, and their microcrystalline fragments can deposit on the particulate surface and/or outside of the biopolymer matrix (Freitas et al., 2005). It should also be underlined that, despite the widespread use of solvent evaporation/extraction processes to prepare polymer carriers, there are no standard protocols acquired, and each preparation follows its own set.

Dense carbon dioxide technologies have been proposed to produce micro/nano-particles or biopolymer 3D scaffold for tissue engineering applications (Della Porta et al., 2017). Supercritical Emulsion Extraction (SEE) technology operating in a continuous layout using a counter-current packed tower (Falco et al., 2012) was described for PLA/PLGA carriers fabrication. SEE assured improved performances, such as better batch-to-batch reproducibility (Falco et al., 2013), accurate carrier size control thanks to a fixed droplet shrinkage without aggregation phenomena (Campardelli et al., 2013), lower solvent residue (Campardelli et al., 2012) and controlled

encapsulation efficiency (Della Porta et al., 2016; Gimenez-Rota et al., 2019; Palazzo et al., 2020).

Except for SEE, other supercritical technologies described for particle formation cannot properly work in the case of PLA/PLGA carriers preparation for different reasons: for example, impregnation technology with supercritical fluid cannot be properly applied to PLGA and PLA carriers fabrication because of well-documented polymer foaming (Cabezas et al., 2012). Furthermore, considering Particles from Gas Saturated Solution (PGSS) or Supercritical Assisted Atomization (Di Capua et al., 2018; Palazzo et al., 2019) technologies, the supercritical or dense carbon dioxide come in direct contact with the polymer solution before the expansion step and the subsequent particles precipitation. Particles are then recovered in dried environment that cannot be applied to PLA/PLGA. Indeed, these biopolymers when in contact with dense-$CO_2$, undergo to a reduction of their glass transition temperature that becomes close to the processing temperature of 311-312 K, with consequent particle aggregation or film formation. This behavior is also the reason which mainly prevented the processing of these biopolymers by Supercritical Anti-solvent (SAS) (Chafidz et al., 2018; Franco and De Marco, 2020; Franco et al., 2019); indeed, when PLA/PLGA micronization is attempted by SAS, larger particles aggregates or a continuous film have been always collected (personal communication, data not published).

Furthermore, PGSS, SAA and SAS technologies are not suitable for peptides processing, because of the use of organic solvents to solubilize polymer and peptides which induces their denaturation. This adverse condition is not present when using SEE technology. Indeed, carriers are collected in a liquid environment (water external phase) that prevents the aggregation of any particles and the growth factors are well preserved within the internal water phase before droplet drying (Govoni et al., 2017; Govoni et al., 2020). Moreover, given the Joule-Thomson effect consequent to the expansion of carbon dioxide, the water suspension is always maintained refrigerated in the collection vessel.

However, despite the large investigation on SEE carriers formulation in term of size distributions (Tirado et al., 2019) and drug loading optimization (Gimenez-Rota et al., 2019), to date few investigations described the cytotoxicity of the produced particles. Particularly, in vitro cytotoxicity tests, including cell viability and cells proliferation studies are considered important screening assays, capable of evaluating the reaction of living cells to the implant and to assess safety characteristics of the produced carriers. Up to now, very few cytotoxicity characterizations have been described for the micro/nano materials fabricated by dense gases, while several assays have been performed for carriers fabrication using conventional technologies (Derman et al., 2017; Grasel et al., 2019; Kang et al., 2008). Different cell models can be used to assess the cytotoxic activity of biomaterials. For

example, Chinese Hamster Ovary cells (CHO-K1) are primary cells well-recognized to be in mitosis, and, therefore, they may provide indications on genotoxicity (Santoro et al., 2005). Human-Peripheral Blood Mononuclear Cells (hPBMCs), isolated from human healthy donors can provide indications of the immune reaction to the biopolymer devices and can better mimic in vivo conditions (Di Pietro et al., 2020; Santoro et al., 2008).

Following all these considerations, several emulsion formulation protocols with different surfactant amounts were tested and, then, processed by SEE using both PLA and PLGA with different molecular weights or co-polymer ratios to fix carrier size and distribution. Then, two different human recombinant growth factors (hGDF-5 and hTGFβ1) were added in the formulation to provide data about the drug loading and related release profiles. Cytotoxicity was monitored using two different cell types, from animal and human sources, namely CHO-K1 and hPBMCs, and a comparison was made with carriers obtained by conventional solvent evaporation. These data are extremely important for carrier's use in in vitro and in vivo protocols and to provide a better characterization of the safety of the SEE fabricated carriers.

## Materials

Poly-Lactic-Acid (PLA, RESOMER 203H (Mw 18,000-24,000 Da, indicated as low Mw-PLA), Evonik Industries, Essen, DE) and Poly-lactic-co-Glycolic-Acid (RESOMER 504H, ratio 50:50 Mw 38,000-54,000 Da, indicated as high Mw-PLGA and RESOMER 752H, ratio 75:25, Mw 4,000-15,000 Da, indicated as low Mw-PLGA, Evonik Industries, Essen, DE) were used as received. $O_2$ (99.9%, Morlando Group, Naples, IT).

Polyvinyl alcohol (PVA, Mol wt: 30,000–55,000, Aldrich Chemical Co., Milan, IT), Bovine Serum Albumin (Sigma-Aldrich, Milan, IT), human Serum Albumin (≥98%, HSA, Aldrich Chemical Co., Milan, IT), Tween 80 (Sigma-Aldrich, Milan, IT), Ethyl Acetate (EA, 99.9%, Aldrich Chemical Co., Milan, IT), recombinant hGDF-5 (PeproTech; UK), recombinant hTGF-β1 (PeproTech; UK), glucose (Sigma-Aldrich, Milan, IT), PBS 1X (Corning Cellgro, Manassas, VA, USA), Minimum Essential Medium Alpha (α-MEM) (Corning Cellgro, Manassas, VA, USA), Enzyme Linked Immunosorbent Assay (ELISA, Cloud-Clone Corp., USA), Ficoll-Hypaque gradient density (Sigma-Aldrich, Milan, IT), Roswell Park Memorial Institute (RPMI, Life Technologies Inc., USA), fetal bovine serum (FBS) (Life Technologies Inc.), L-glutamine (Life Technologies Inc., USA), penicillin/streptomycin (Life Technologies Inc., USA), 3-(4,5-Dimethylthiazol-2-yl)-2,5-diphenyl-tetrazolium bromide (MTT, Sigma-Aldrich, Milan, IT), dimethyl sulfoxide (DMSO, Sigma-Aldrich, Milan, IT).

**Emulsions preparation**

Emulsions were obtained using a ratio of 1:19:80 *water-oil-water* ($w_1/o/w_2$). Oily phase was prepared solubilizing a given amount of polymer, whereas a variable amount of PBS solution (1X) containing HSA (1% w/v) and PVA (0.06% w/w) was used as water internal phase. Recombinant hTGF-β1 was reconstituted in citric acid (pH 3) to a final concentration of 1 μg/μL, while hGDF-5 was reconstituted in Milli-Q water at the same concentration.

$w_1$ was mixed with the oily phase to form a primary $w_1/o$ emulsion by sonication with a digital ultrasonic probe operating at 30% of its amplitude (mod. S-450D; Branson Ultrasonic Corp. Danbury, Connecticut, USA). Whereas, when growth factors were added, the inner water phase was mixed with the oily phase by vortexing (mod. Velp Scientifica, Monza, IT) at maximum speed for 30 sec.

The primary emulsion was then slowly added into EA-saturated aqueous Tween80 solution by high-speed stirring (mod. L4RT, Silverson Machines Ltd., Waterside, CheshamBucks, UK). Surfactant amount in the external water phase was varied from 0.1 to 0.6% w/w. In some cases, 15% w/w of glucose was added in the water external phase. Temperature of 10°C was assured during emulsion phase mixing. All emulsions were processed by SEE immediately after their preparation.

It should also be underlined that PLA and PLGA carriers are not amenable to conventional sterilization methods such as ethanol washing, gamma irradiation or steam because of biopolymer oxidation (Athanasiou et al., 1996) and further degradation of peptide payload. To overcome these challenges, a specific SEE operational protocol was set. Carriers, collected from each run, were always washed in sterile conditions with a penicillin/streptomycin (1% w/v) and amphotericin (1% w/v) solution to ensure removal of the surfactant and a cell culture-grade preparation, centrifuged for 50 min at 6500 rpm at 4° C (model IEC CL30R Thermo Scientific, Rodano, Milan, IT), recovered by using a membrane filtration (filter 0.2 μm HA Millipore, Sigma Aldrich, Milan, IT). All experiments were repeated twice (N=2).

**Solvent evaporation protocol**

Solvent evaporation (SE) technique was performed to compare the outcomes of conventional and supercritical techniques starting from the same emulsion. In the case of SE, emulsions were stirred at 100 rpm for 3 hours at a temperature of 38°C in a sterile controlled environment, to allow solvent elimination by evaporation. Carriers collected from each assay were washed and centrifuged following the same protocol described above after for SEE process.

## V.2    Experimental results

### V.2.1 Emulsion Formulation Optimization

The surfactant of the external water phase was varied to optimize the carriers size and distribution. The extremely low amount of growth factor used in the internal water phase was assumed not to exert any influence on carrier's morphology and size. Two different growth factors were loaded only in the emulsion formulations previously optimized, to observe their encapsulation efficiency and release profiles as well as carriers cytotoxicity. A summary of all tested compositions and the obtained results in terms of mean diameter, polydispersity and loading are summarized in **Table V.I.**

**Table V.9** *A summary of the best emulsion formulations processed SEE technology. Internal water phase was always added with human Serum Albumin (1 % w/w); the proteins was used as growth factors stabilizer*.

| Polymer | Tween 80 % w/w | Emulsion composition | DSD (±SD) nm | PSD (±SD) nm | SF % | Load µg/g | EE % |
|---|---|---|---|---|---|---|---|
| low Mw-PLA | 0.1% | **w1**: 0.5mL W+0.06% PVA | 1792±254 | 634±88 | 65 | -- | -- |
| | 0.3% | **o**: 1 g PLA in 19.5 mL EA. | 1613±335 | 285±45 | 82 | -- | -- |
| | 0.6% | **w2**: 80 mL of EA$_{sat}$-W + Tween80 | 819±110 | 220±41 | 73 | -- | -- |
| low Mw-PLGA, 75:25 | 0.1% | **w1**: 0.5mL W+0.06% PVA | 5554±555 | 342±90 | 94 | -- | -- |
| | 0.3% | **o**: 1 g PLGA in 19.5 mL EA. | 2417±283 | 261±39 | 89 | -- | -- |
| | 0.6% | **w2**: 80 mL of EA$_{sat}$-W + Tween80 | 1388±259 | 205±32 | 85 | -- | -- |

PLA/PLGA micro/nano carriers for the Growth Factors delivery fabricated by Supercritical Emulsion Extraction: release profiles study and cytotoxicity evaluation

*… continued **Table V.I***

| Polymer | Tween 80 % w/w | Emulsion composition | DSD (±SD) nm | PSD (±SD) nm | SF % | Load µg/g | EE % |
|---|---|---|---|---|---|---|---|
| **low Mw-PLA plus ihGDF-5** | 0.6% | **w1**: 0.5mL W+0.06% PVA+**10 µg ihGDF-5** **o**: 1 g PLA in 19.5 mL EA. **w2:** 80 mL of EAsat-W+Tween80 | 858±47 | 189±25 | 78 | 2.3 | 23 |
| **low Mw-PLGA 75:25 plus ihGDF-5** | 0.6% | **w1**: 0.5mL W+0.06% PVA +**10 µg ihGDF-5** **o**: 1 g PLGA in 19.5 mL EA. **w2:** 80 mL of EA sat-W+Tween80 | 1653±63 | 193±19 | 88 | 2.2 | 22 |
| ***Mixing by sonicated plus mixing 2800 rpm for 6 min*** | | | | | | | |
| **high Mw-PLGA 50:50 plus hGDF-5** | 0.1% | **w1**: 250 uL PBS +0.06% w/w PVA plus **5 µg hGDF-5** **o**: 500 mg polymer in 5 mL EA. **w2**: 50 mL of EAsat-W + 15% w/w glucose | 3391±1196 | 2073±94 | 84 | 3.2 | 64 |

*… continued* **Table V.I**

| Polymer | Tween 80 % w/w | Emulsion composition | DSD (±SD) nm | PSD (±SD) nm | SF % | Load µg/g | EE % |
|---|---|---|---|---|---|---|---|
| **high Mw-PLGA 50:50 plus hTGF-β1** | 0.1% | **w₁**: 250 uL PBS + 0.06% w/w PVA + **10 µg hTGF-β1**  **o**: 500 mg polymer in 5 mL EA.  **w₂**: 50 mL of EAsat-W + 15% w/w glucose | 4736±2368 | 3287±1002 | 93 | 7 | 70 |

***Mixing by vortex and emulsifier 2000 rpm for 5 min***

Fixing the polymer concentration at 5% w/w in the oily phase, the amount of surfactant in the external phase of the emulsion was varied from 0.1% to 0.6% w/w. These tests were performed using low Mw-PLA or PLGA (75:25) and mixing the secondary emulsions at 2800 rpm for 6 min. In these conditions, PLA emulsions had an average droplets diameter of 1792±254 nm, 1613±335 nm and 819±110 nm, respectively, and the related particles showed mean size of 634±88 nm, 285±45 nm and 220±41 nm, when increased surfactant concentration of 0.1%, 0.3% and 0.6% w/w, respectively, were used. A similar trend was observed using low Mw-PLGA, obtaining droplets sizes from 5554±555nm to 1388±259 nm at increased Tween 80 concentration values; related carriers had a mean size of 342±90 nm and 205±32 nm, respectively (see carrier size and SEM images in **Figure V.1 and V.2**). The average diameter of droplets and carriers decrease when the concentration of surfactant increases. These data are in agreement with those previously reported (Tirado et al., 2019b), confirming that higher surfactant concentrations lead to a higher number of micelles, which may stabilize smaller droplets in emulsion, and produce smaller particles. Lowering the surfactant concentration beyond 0.1% w/w of Tween 80, agglomerated droplets/particles were observed especially in the case of PLA, due to emulsion instability probably induced by extremely low amount of micelles. This observation is in agreement with (Bouissou et al., 2006).

**(a)**



**(b)**
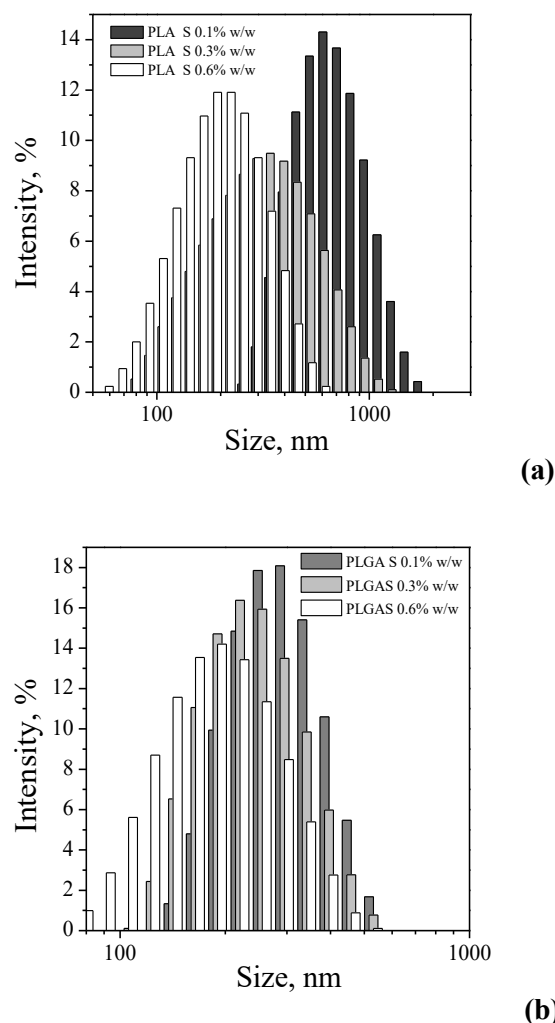
**Figure V.1** *Influence of the surfactant content in the water external phase on carrier size distribution obtained using low Mw-PLA (a) and low Mw-PLGA (75:25) (b). Fixing the polymer concentration in the oily phase and other emulsion formulation parameters, a reduction of carriers mean size was observed with the increase of surfactant concentration in the external water phase.*
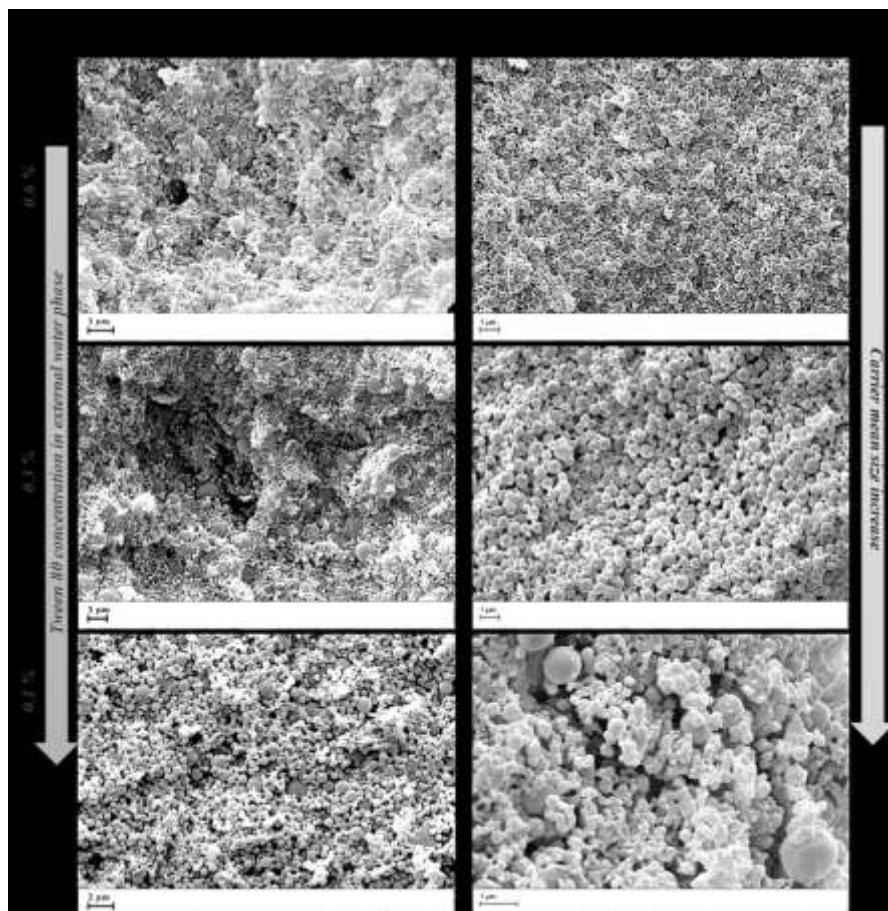
**Figure V.2** *FE-SEM images of carriers fabricated using emulsion formulated at increasing surfactant concentrations in the external water phase from 0.1 to 0.6% w/w. Low Mw-PLA (a) and low Mw-PLGA (75:25) (b). Fixing the all other parameters, increasing the surfactant concentration a general reduction of mean droplets size was obtained in emulsion assuring carriers mean size reduction.*

Shrinkage was always observed between the droplets and the solid particles in all experiments performed (see **Table V.1**). In detail, Shrinkage Factor (SF) ranges between 94-65% were measured when Tween 80 concentration was varied from 0.1 to 0.6%. Generally, when fixing the polymer concentration in the oily phase (i.e., oily phase viscosity), a larger shrinkage was observed in the emulsions with a lower surfactant concentration. This observation can be explained considering that when lower amount of surfactant is used in the external water phase, it allows the formation of a reduced number of micelle and, therefore, a larger droplets are formed in emulsion. Conversely, higher surfactant concentration stabilize smaller droplets; therefore, despite the lower droplets shrinkage, smaller

carrier mean size are obtained (Tirado et al., 2019b). The size of carriers (and the related droplets shrinkage) can be also influenced by the different molecular weight of polymer used in the oily phase formulation which determines the oily phase viscosity. Therefore, the use of low Mw-PLA can be responsible for the different shrinkage values compared to that of the two PLGA used (co-polymer ratio of 75:25 and 50:50) both with higher molecular weight (Gimenez-Rota et al., 2019).

Following the data on carrier size and distribution, the surfactant concentration of 0.6% w/w was selected for preliminary test of growth factor encapsulation using both low Mw-PLA and low Mw-PLGA (75:25) biopolymers. In these cases, emulsions with a droplet mean size of 858±47 nm and 1653±63 nm were obtained and related carriers with a mean size of 189±25 nm and 193±19 nm, respectively, were fabricated. The SFs were also coherent with previous data, confirming that the presence of hGDF-5, had no effect on emulsions stability and processing (see also **Table V.1)**.

Preliminary tests of hGDF-5 encapsulation were performed using the inactive epitope of growth factor (ihGDF-5) given high cost of the active recombinant form. However, the differences between the two epitopes were not relevant from the process point of view.

The explored emulsion formulation conditions were good in terms of carrier morphology and size control but ensured low encapsulation efficiencies which were of about 20%, with hGDF-5 loading of 2.3 and 2.2 µg/g, respectively (see **Table V.1**).

Furthermore, from the literature emerged that active peptides encapsulation requires milder conditions in terms of mixing times and velocity during the emulsion formulation. Moreover, the use of vortex (instead of ultrasound) was strongly recommended for emulsion phase mixing to avoid peptide denaturation. Indeed, the sonication can induce changes in the structural and thermal properties of proteins and increases the enthalpy of denaturation due to protein aggregation (Chandrapala et al., 2011). Following these considerations, the emulsion preparation protocol was modified and the primary emulsion was obtained using vortex at maximum speed for 30 sec. In these conditions, all preliminary runs leaded to encapsulation efficiency even lower than 20% (data not shown).

To improve encapsulation performance, we decided to fabricate larger particles and to reduce the osmotic gradient from external phase to internal water phase. To increase carrier sizes the surfactant concentration was reduced at 0.1 %w/w in the external water phase and the rotational speed of emulsifier was dowgraded to 2000 rpm for 5 min. Furthermore to obtain an osmotic gradient, which was supposed to improve growth factor entrapment efficiency (Zhang and Zhu, 2004), PBS 1X solution was adopted as inner water phase (Nihant et al., 1994), whereas, external water phase was prepared using 0.1% w/w of Tween 80 plus glucose (15% w/w).

Additionally, PLGA co-polymer ratio of 50:50 with higher molecular weight (3,8000-54,000 Da) was selected, to increase oily phase dynamic viscosity, that may also help the encapsulation efficiency (Tirado et al., 2019b). Adopting these new conditions, larger droplet mean sizes were obtained with the consequent increase of derived carriers that showed a size of 2073±94 and 3287±1002 nm, respectively. However, the encapsulation efficiency was increased to 70%, with carriers loading of 3.2 µg/g for hGDF-5 and 7 µg/g for hTGF-β1 (see **Table V.1** and **Figure V.3**), respectively.
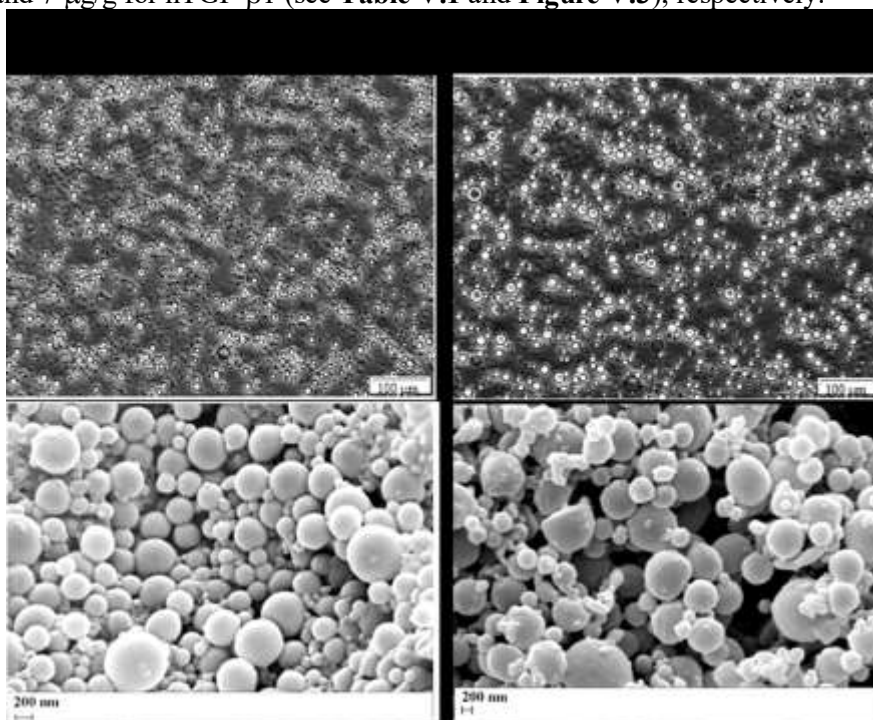


**Figure V.3** *Optical images of emulsions and SEM images of related carriers loaded with growth factors; high Mw-PLGA (50:50) loaded with Active hGDF-5 (a) and hTGFβ1 (b).*

## V.2.2 Comparison between SEE and SE

Using high Mw-PLGA (50:50) and fixing the emulsion composition (see **Table V.2**), the same system was processed by both SEE and SE techniques. SEE technology allowed the formation of carriers with a smaller size (843±226 nm) and distribution, when compared to the ones obtained by SE (1780±1001 nm), as also illustrated in **Figure V.4**.
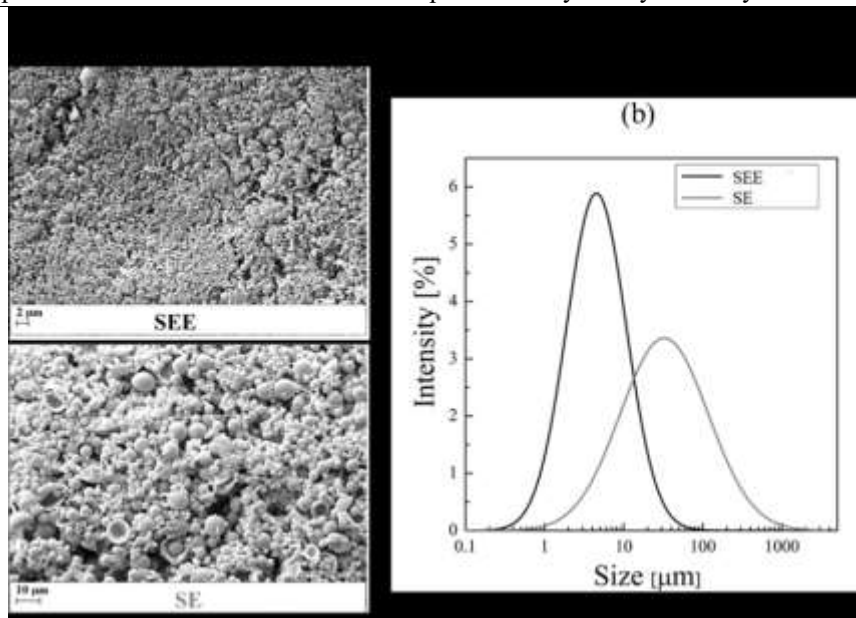
**Figure V.4** *SEM images and Particle Size Distributions of high Mw-PLGA (50:50) empty carriers fabricated using the same emulsion processed with different technologies: Supercritical Emulsion Extraction (SEE) and traditional solvent evaporation (SE) techniques, respectively. Larger carriers size and distribution was observed in the case of particles obtained by SE.*

The results confirms previous data (Falco et al., 2012a, Falco et al., 2013) and it was explained by droplets aggregation (Ostwald maturation) during SE, which lead to larger carriers size. This phenomenon is prevented by SEE process due to the fast elimination of the solvent in the oily phase and consequent rapidly polymer hardening.

## V.2.3 Release Profile study

The release profiles are related to the amounts of peptide (ng) released from 100 mg of carriers; in the case of PLGA/hTGF-β1 (**Figure V.5a**), a typical biphasic delivery profile was observed, with an initial burst release followed by a more controlled secondary release phase. The burst release of 35 ng was followed by a sustained release of about 40/50 ng/day for the following 9/10 days; then, a further drug release of about 20 ng/day was observed for the following 25 days. The initial burst effect could represent the release of the growth factor entrapped on the surface of the carrier, while the drug delivery during the second phase of release (after Day 13) likely results from polymer degradation, a typical characteristic of these PLGA systems (Siepmann and Siepmann, 2008).

In the case of hGDF-5 loaded carriers, loading of 3.2 μg/g (high-MW PLGA 50:50) and 2.3 μg/g (low MW PLA), respectively, provided similar release profile over 25 days into α-MEM medium at 37°C (**Figure V.5b**), ensuring about 1.5 ng/mL released each day for the first 25 days. This linear release profile with the absence of burst effect may result from the different nature of growth factor or its lower amount loaded (about 1/3 with respect to the loaded hTGF-β1). Moreover, despite the larger hydrophobicity of PLA/hGDF-5 carriers with respect to the PLGA(hGDF-5 ones, they showed a similar profile; this behavior must be explained taking into account the different carriers sizes of about 2 μm for PLGA and of 0.2 μm for PLA. It is also worth of note that the inactive hGDF-5 epitope loaded in the PLA carriers has no effect with regards the release study.
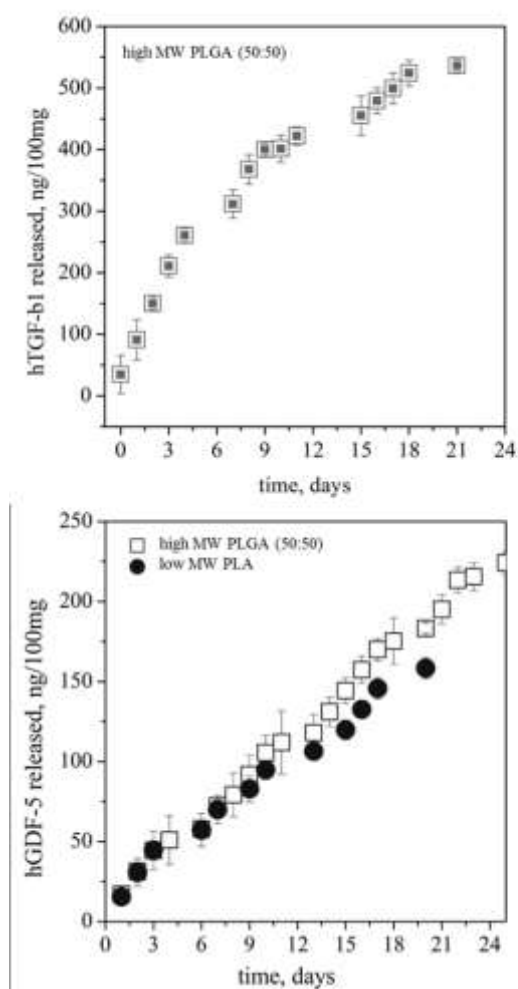
**Figure V.5** *Release profiles of growth factors measured in α-MEM at 37°C up to 25 days. The data are expressed as amounts (ng) released from 100 mg of carriers: hTGF-β1 from high-Mw PLGA (50:50) carriers (a); ihGDF-5 and hGDF-5, respectively, from high-MW PLGA (50:50) and low-MW PLA carriers (b).*

## V.2.4 Cytotoxicity studies

The cytotoxicity of carriers was determined using CHO-K1 cells. Cells were incubated for 24 and 48h using 10μg/uL, 5μg/uL, 2.50μg/uL and 1.25μg/uL concentrations of carriers (unloaded and loaded with growth factors, **Figure V.6**) and their viability was analyzed using MTT assay.

Carriers were designed with different loadings to be enclosed within a 3D environment and commit stem cells towards a specific phenotype, the concentrations were selected according to the amounts required within the 3D environment (Trucillo et al., 2019a).
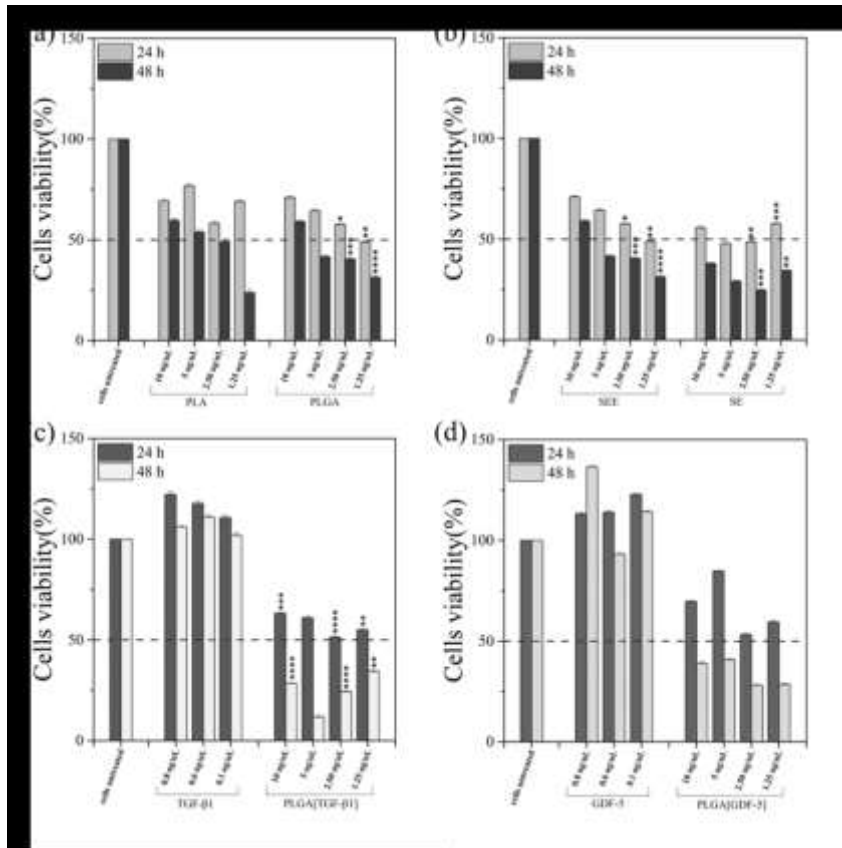


**Figure V.6** *Carriers cytotoxicity evaluated using Chinese Hamster Ovary cell line (CHO-K1) that were treated with empty and loaded PLA and PLGA carriers for 24h and 48h: (a) empty PLA and PLGA carriers; (b) empty high-Mw PLGA carriers, fabricated with SEE and SE techniques; (c) free hTGF-β1 and hTGF-β1 loaded high-Mw PLGA carriers; (d) free hGDF-5 and hGDF-5 loaded PLGA carriers. The histograms report the mean percentage of viable cells compared to controls (untreated cells, 100%). The experiments were analyzed by two-tailed Student's t-test, * $p \leq 0.05$, **$p < 0.01$, ***$p < 0.001$ and ****$p \leq 0.0001$; n=3.*

At 24h, at the lowest concentrations, cell viability decreased up to a maximum of 50% with PLGA unloaded treatments, while PLA treatments turned out to be less toxic. Furthermore, the higher concentrations of both carriers seem to be less toxic reaching the highest (but not statistically

significant) cell viability at 10µg/uL, whereas cell viability reached about 60% at 48h. Similarly, PLGA carriers seemed to affect cell viability at lower concentrations but not at higher ones (**Figure V.6a**). Moreover, at all-time points explored, PLGA carriers fabricated with conventional SE seemed to exhibit more cytotoxicity than SEE PLGA carriers, originated from the same emulsion, as illustrated in **Figure V.6b**. This effect may result from the reduced presence of organic solvent residue in the carriers fabricated with the SEE technique (Della Porta et al., 2011a). On the other hand, the treatment with pure growth factors used as controls, at the concentrations of 0.8 µg/uL; 0.6 µg/uL; 0.1 µg/uL, did not affect cell viability, stimulating cell viability and proliferation, (**Figure V.6c-d**). Indeed, at 24 and 48h, all hTGFβ-1 treatments increased cell viability compared to untreated cells. The treatment of proliferating CHO-K1 cells with hTGFβ-1/PLGA carriers exhibited a cytotoxic effect which in any case, did not exceed the effect observed for the empty carriers used at the same concentrations (**Figure V.6c**). This suggests that the effect probably resulted from PLGA and not to the carriers loaded with hTGFβ-1. Similar results were obtained by treating cells with pure hGDF-5. Particularly, at 24h, the concentration of 0.1 µg/uL induced the highest percentage of cell viability. At 48h, the highest percentage of cell viability was obtained after pure hGDF-5 treatment at a concentration of 0.8 µg/uL. The concentration of pure growth factors were chosen based on loading efficiency of carriers.

From the reported data, it emerges that the higher cytotoxicity was induced by lower concentrations of carriers; possibly a result of an interference of the carrier material with specific cellular receptors and/or internal proteins involved in cell viability and proliferation together with a better internalization of carriers, when diluted. Efficient internalization of carriers by cells has been already reported by Ciaglia et al. where the increasing granular appearance of gated monocytes supports the uptake of carriers. We can hypothesize that CHO-K1 cells might phagocyte carriers, affecting the relative viability (Ciaglia et al., 2019).

The cytotoxicity of low-Mw-PLA and high-Mw-PLGA carriers loaded with hGDF-5 was also established with hPBMCs isolated from healthy donors to provide further evidence on the toxicity of the encapsulated carriers directly on human differentiated cells. To this aim, cells were incubated for 24 and 48h with decreasing concentrations of unloaded and hGDF5-loaded carriers, and viability analyzed by MTT assay as in the CHO cell system. No cytotoxicity was detected in hPBMCs versus controls at both 24 and 48 h of treatment with empty carriers (see **Figure V.7a**), even though PLA carriers seemed to induce a larger increase of cell viability compared to PLGA carriers. However, for both materials, lower concentrations significantly improved cell viability suggesting a better uptake of the carriers with a significant enhancement of cell metabolism as already suggested in other studies of drug cytotoxicity (Prota et al., 2011).

Comparable results were found by treating hPBMCs with hGDF-5 loaded PLGA or PLA carriers (see Figure V.7b). However, conversely to CHO cells, we showed that both PLGA and PLA carriers did not negatively affect cell survival, and instead they appeared to improve this cell parameter. This suggests that empty and loaded carriers, especially at lower concentrations, could stimulate cell proliferation by acting as mitogens or, given the use of MTT assay based on mitochondrial reduction of tetrazolium salt (MTT) to insoluble formazan crystals, carriers could improve mitochondrial metabolism. Therefore, the observed effects could be explained by either a stimulating effect on mitochondrial activity of the carriers and hGDF-5 or by a more general action of these compounds on hPBMCs survival, ultimately leading to an improvement of hPBMCs metabolism. These data are in agreement with those already reported by Da Silva et al. who investigated PLA carriers cytotoxicity on hPBMCs, and showed an increase of cell viability of about 70% (Da Silva et al., 2019).
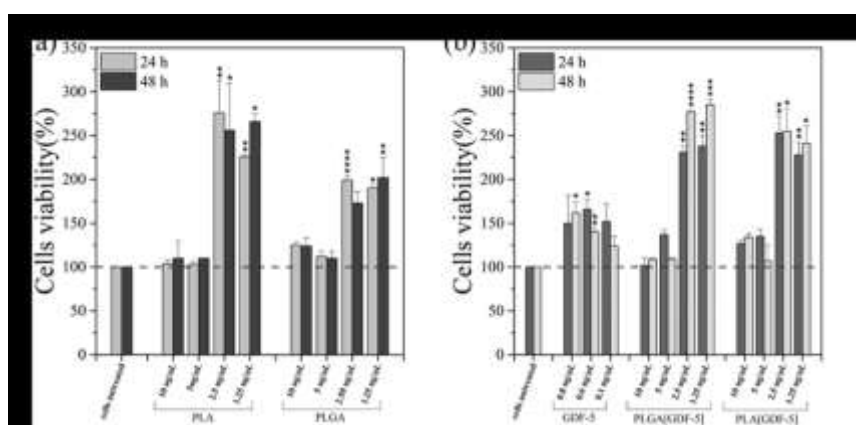


**Figure V.7** *Carrier cytotoxicity was evaluated using human peripheral blood mononuclear cells (hPBMCs) that were treated with decreasing amounts of empty and loaded low-Mw PLA and high-Mw PLGA carriers for 24h and 48h: (a) empty low-Mw PLA and high-Mw PLGA carriers; (b) free hGDF-5 and hGDF-5 loaded carriers. The histograms report the mean percentage of viable cells compared to controls (untreated cells, 100%). The experiments were analyzed by two-tailed Student's t-test * $p \leq 0.05$, **$p < 0.01$, ***$p < 0.001$ and **** $p \leq 0.0001$; n=3.*

## V.3 Conclusion and perspectives

SEE technology can successfully encapsulate peptides such as growth factors into PLGA or PLA carriers providing at the same time an advanced control of carrier's size and morphology, ensuring a sustained growth factor release over 25 days.

SEE-fabricated carriers do not present intrinsic toxicity: they can be safely introduced within biomedical devices structures as they are unlikely to pose a risk for human health. The reported in the present investigation open new perspectives for the use of SEE fabricated carriers for the development of 3D bioengineered microenvironments where biological molecules can be released under controlled conditions stimulating tissue regeneration and healing.

# Chapter VI
# Encapsulation of nutraceutical compounds using SEE technique

## VI.1    Introduction

β-Carotene (β-CA) is widely used in the food, cosmetic and pharmaceutical industries, as natural photo protector colorant and antioxidant (Franceschi et al., 2010). β-CA has a high free radical scavenging and antioxidant activity due to their multiple conjugated double bonds; moreover, it is the major precursor of vitamin A (Ribeiro et al., 2007, Cocero et al., 2009). Others biological effects of β-CA are: decrease of cancer risks enhancing immune responses (Franceschi et al., 2010), stimulation of gap-junctional communication (Nesaretnam et al., 2000), protection from arterial disease (Mezzomo et al., 2012) and induction of a light barrier avoiding cell damaging (Gonnet et al., 2010). Concerning food applications, its inclusion in food matrix allows to obtain the so-called functional or nutraceutical food; moreover, carotenoids are also used as colorants to recover the colour lost during food processing and storage (Mori and Anarjan, 2018).

Astaxanthin (AXT) belongs to the xanthophyll family of carotenoids and the presence of a terminal hydroxyl and ketones in the ionone rings causes esterification ability, antioxidant activity, and greater polar configuration of these compounds compared to other carotenoids (Meyers and Bligh, 1981). Currently there is no established nutritional recommendation regarding AXT daily intake, even though most studies reported beneficial results from a dosage of 4 mg/day (Seabra and Pedrosa, 2010). This amount is the equivalent contained in roughly 206 g of shrimp, including shells (Seabra and Pedrosa, 2010, Khalid and Barrow, 2018). The recommended daily intake could also improve blood parameters, since at daily doses from 6 mg to 8 mg, AXT is reported to decrease the oxidation of the low-density lipoprotein (LDL) cholesterol and prevent it from becoming atherogenic (artery clogging) (Khalid and Barrow, 2018).

Despite the several applications, these molecules are very susceptible to degradation under temperature, light and oxygen and highly hydrophobic and difficult to disperse in water (Ribeiro et al., 2007). For this reason, to improve the bioavailability and enhance water dispersion, they are often micronized (Ribeiro et al., 2007, Chu et al., 2008), co-precipitated with protein (Cocero et al., 2009) or encapsulated.

Different polymers were studied as carrier for β-CA encapsulation such as, tapioca starch, malto-dextrin or oleoresin all using spray drying technology (Loksuwan, 2007, Rodríduez-Huezo et al., 2004, Faria et al., 2010), or casein using solid lipid nanoparticles (SLNs) protocol and galactan by evaporation technology (Pan et al., 2007, Trombino et al., 2009). The co-encapsulation with other antioxidant excipients, such as α-tocopherol (α-TOC) and ascorbic acid can provide a better protective effects on oxidation (Zhang and Omaye, 2000). α-TOC, also known as vitamin E, is a fat-soluble highly potent antioxidant, abundant in vegetable oils or wheat germs; it is widely used by the pharmaceutical, cosmetic and food industries because of its clinical and preservative applications (Tucker and Townsend, 2005, Tomassi and Silano, 1986). RA is a polyphenol with important biological activities, such as anti-inflammatory, antiagregant and antioxidant (Panya et al., 2012). Several biopolymer-based micro/nanocarriers can be designed to preserve a bioactive compound by preventing its degradation (Nesaretnam et al., 2000). Recently, there has been an increasing interest in the development of food-grade carrier systems for encapsulation and protection of nutraceuticals in order to enhance their stability (Mezzomo et al., 2012).

Poly-lactic acid (PLA) and poly-lactic-co-glycolic acid (PLGA) are biocompatible and biodegradable polymers which have recently been the subject of extensive investigation (Nair and Laurencin, 2007, Zhang et al., 2006a, Lademann et al., 2007, Stevanović et al., 2007)18,19,20]. β-CA and carotenoids loading into PLA and PLGA biopolymers have been already proposed by different fabrication technologies for micro and nano-capsules preparation (Stevanovic and Uskokovic, 2009). Ethyl cellulose is an innocuous hydrophobic polymer and its lack of toxicity and stability during storage has allowed its use as a food additive in the European Union, labelled as E 462 (Younes et al., 2018); making it suitable for designing sustained and food-grade matrices.

The emulsification-evaporation method (Astete et al., 2007, Prabha and Labhasetwar, 2004, Song et al., 2006, Sahoo and Labhasetwar, 2005), spontaneous emulsification solvent diffusion method (SESD) (Zhang et al., 2006a), nanoprecipitation method (Ribeiro et al., 2007, Govender et al., 1999) are all widely used in preparing microcarriers of various sizes. Each of these methods employs a similar first step, where a drug solution is emulsified in a water solution to form an oil-in-water dispersion (o-w). If appropriate, the drug to be encapsulated may also be dispersed as a solid powder in an organic polymer solution, or co-dissolved in a common solvent

with the polymer. The solution or dispersion is then processed according to one of the aforementioned methods. During the solid carriers formation using emulsification-evaporation and nano-precipitation approaches, organic solvents such as dichloromethane and chloroform are usually employed. To meet the requirement for the pharmaceutical use, residual solvents should be completely removed from fabricated micro and nano-systems (Cheng et al., 2008).

The use of dense gas, such as Supercritical Carbon Dioxide (SC-$CO_2$) is an alternative to almost all the conventional processes because it is possible to work at near-ambient temperatures, avoiding the degradation of thermolabile substances; SC-$CO_2$ also provides an inert medium suitable for processing oxidable substances.

In this research work, the β-CA encapsulation in polyesters such as, poly-lactide (PLA) or poly-L-lactide-co-glycolide (PLGA) is proposed using SEE technique to preserve the molecule and improve its shelf-life. The co-encapsulation with other natural antioxidants, such as α-TOC and Rosmarinic Acid (RA), is also described to improve capsules shelf-life and antioxidant activity. The possibility of fabricate carriers with different sizes in the micro and nano range was also explored and the related encapsulation efficiency and antioxidant activity was tested. The products shelf-life was monitored by UV exposure for 10 days and after storage for 2 years. The combination of β-CA with other antioxidants wase also tested in order to understand the different formulations stability and their biological activity and demonstrate the versatility of the SEE technology in producing complex formulation for several applications.

Moreover the possibility of microencapsulating AXT in ethyl cellulose using the SEE technique was studied. Different emulsion formulations were tested by varying the concentrations of surfactant in the aqueous phase and the amount of solubilized polymer in the oily phase. The influence of these parameters were monitored on the morphology of the microcapsules size and distribution, as well as on the efficiency of AXT encapsulation. The antioxidant activity of the produced particles was also measured using a DPPH assay.

**Materials**

$CO_2$ (99.9%, Morlando Group, Naples, Italy), chloroform anhydrous (CL), methanol (ME), acetone (AC), ethanol (ET), acetonitrile (ACN), acetic acid (ACE), ethyl acetate (EA) all of purity 99.9% were supplied from Carlo Erba Reagents (Milan, Italy). Water (HPLC grade), glycerol (GLY, purity 99%, Aldrich Chemical Co.), sorbitan monolaurate (Span 20 Sigma-Aldrich), Tween 80 (Sigma-Aldrich), β-carotene (β-CA, Aldrich Chemical Co), α-Tocoferol (α-TOC, Sigma-Aldrich), Rosmarinic acid (RA, 96% Sigma-Aldrich), astaxanthin (AXA, ≥ 98 %, Sigma-Aldrich, Italy), poly-lactic acid

(PLA, MW: 60000 g/mol, Resomer RG 708H Boehringer Ingelhein), poly-lactic-co-glycolic acid (PLGA, 75:25 MW: 20000 g/mol, Resomer RG 752S, Boehringer), ethyl cellulose (viscosity 100 cps in 40/40 toluene/ethanol, 455 kDa, Sigma-Aldrich, Italy), 1,1-diphenyl-2-picrylhydrazine (DPPH, 97% Sigma-Aldrich), (±)-6-hydroxy-2,5,7,8-tetramethylchromane-2-carboxylic acid (Trolox, 97 %, Sigma-Aldrich, Italy) were used as received.

**Emulsions preparation**

To encapsulate β-CA, α-TOC and RA, several double o1/o2/w emulsions were formulated with a composition ratio of 4:16:80 w/w/w. The internal o1 phase contained the active principles solved into CL with 0.06% Span 20; the second oily phase, o2, was formed by EA with a given amount of biopolymer dissolved (0.4 to 0.8 g of PLA or PLGA). For emulsions formulation, the inner phase o1, was mixed with the second oily phase o2 to form the o1/o2 emulsion by ultrasonication (mod. S-450D, Branson Ultrasonics Corporation, Danbury, CT, USA). The o1/o2 emulsion was, then, immediately added into a known amount of EA-saturated aqueous Tween 80 solution (0.6%, w/w of Tween) with the high-speed stirrer (model L4RT, Silverson Machines Ltd., Waterside, Chesham Bucks, United Kingdom) for a time ranges between 4-6 min and at with stirring ranges of 2800-3600 rpm.

Different formulations of RA alone into 1g of PLA were also prepared. In this case w1/o1/w2 emulsions were formulated with a ratio of 1:19:80 w/w/w. Different proportions of ETOH:$H_2O$ (0.06% PVA) as solvent of the internal phase w1 were tested. o2 contained 1 g of PLA into EA; whereas, the external w2 phase was of EA-saturated aqueous Tween 80 solution (0.6%, w/w of Tween).

Some runs were performed fixing the water phase composition at 80% (w/w) glycerol and 20% (w/w) distilled water plus 0.6% (w/w) of Tween 80; the overall ratio o/w was always maintained at 20/80 for all the emulsion prepared. PLGA amount in the oily phase was fixed at 1 g, while the β-C concentration was fixed at 6 mg/g.

In the case of AXA, oil in water (O/W) emulsions with a mass ratio of 20:80 were used. The oily phase was prepared by dissolving ethyl cellulose in ethyl acetate at concentrations of 1.0 %. The water phase was obtained with ethyl acetate-saturated water solution and Tween 80 at concentration of 0.1 % w/w. Emulsions were obtained by high-speed stirrer operating at 3200 rpm for 4 min. AXA was added in the oily phase by sonication at 30 % of amplitude for 1.5 min.

## VI.2    Experimental results for β-CA encapsulation

### *VI.2.1 SEE-C encapsulation of β-CA and α-TOC in PLA and PLGA carriers*

Different emulsion formulations were explored in order to assure both micro and nano-carrier fabrication with a good β-CA encapsulation efficiency. All the emulsion formulations, size, distribution and loading are summarized in **Table VI.1**.

**Table VI.10** *Different emulsion formulations tested by SEE-C. Biopolymer and antioxidants loaded in the oily phase, mean size of the obtained droplets and particles with standard deviation. Encapsulation Efficiency (EE) and Antioxidant Loading (AL) in mg per g of polymer.*

| Polymer in EA ($o_2$) g | Antiox in CL ($o_1$) | Droplets size (mm) | Carrier size (mm) | (EE) % | AL (mg/g) |
|---|---|---|---|---|---|
| | | PLA | | | |
| 0.4 | β-CA | 2.1±0.5 | 1.5±0.5 | 68 | 6.8 |
| 0.4 | β-CA α-TOC | 2.1±0.5 | 1.5±0.5 | 72 | 5.0 |
| 0.4 | β-CA α-TOC | 1.2±0.1 | 0.3±0.07 | 62 | 6.2 |
| 0.4 | β-CA α-TOC RA | 1.4±0.2 | 0.5±0.09 | 35 | 3.5 |
| | | PLGA | | | |
| 0.4 | β-CA | 2.4±0.6 | 1.6±0.6 | 22 | 2.1 |
| 0.8 | β-CA α-TOC | 2.1±0.6 | 2.0±0.6 | 52 | 2.6 |
| 0.8 | β-CA α-TOC | 1.2±0.1 | 0.3±0.07 | 62 | 3.1 |
| 0.8 | β-CA α-TOC RA | 1.3±0.2 | 0.5±0.1 | 53 | 2.7 |
| 1 * | β-CA α-TOC | 7.8±0.9 | 4.3±0.7 | 82 | 25 |

In the case of PLA, 400 mg of biopolymer were always solubilized in the oily phase, obtaining micro-carriers of 1.5± 0.5 μm with 68% of EE. When α-TOC was included in the formulation along with β-CA, the microcapsules mean diameter did not changed and the EE was improved up to 72%. The same formulation with 400 mg of biopolymer in the oily phase was also tested for PLGA; in this case, micro-carriers with mean size of 1.6± 0.6 μm were obtained but with a poor EE of only 22%; the use of α-TOC in the

formulation did not improved the result observed. When, the amount of PLGA in the oily phase of emulsion was increased to 800 mg, microcarriers of 2± 0.6 µm were obtained with an improved EE of 52%. A shrinkage was always observed between the droplets and the solid particles in all experiments performed (Della Porta et al., 2011b). Nevertheless, in the case of emulsion formulations with PLA the SF was almost always of 24%; whereas, for PLGA a reduced shrinkage factor was observed of 37% and 10%, respectively when 400 to 800 mg of biopolymer were solubilized in the oily phase.

In order to reduce the droplet mean sizes and, therefore, to fabricate smaller carriers in the nanometer range, the rotation per minute of the emulsifier was increased during emulsion preparation. For both PLA (load in oily phase of 400 mg) and PLGA (load in oily phase of 800 mg) the droplets mean sizes were reduced to 1.3±0.1 mm and 1.2±0.1 mm, respectively, and the resulting carriers mean diameters were of 0.3±0.07 mm and 0.3±0.1 mm, respectively, after SEE processing. The EE data were measured between 60 and 62%. PSDs of the micro and nano-carriers fabricated using both PLA and PLGA are in **Figure VI.1**.



(a)  (b)
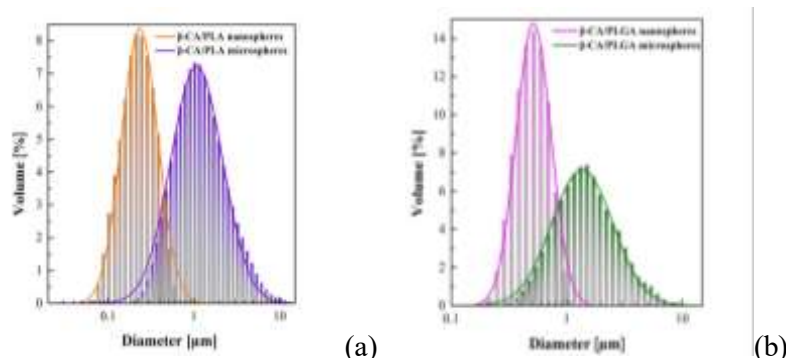
**Figure VI.1** *Particle Size Distribution (PSD) of PLA (a) and PLGA (b) micro- and nano-carriers fabricated by SEE. The possibility of carriers size varying from nano to micro scale, modifying the emulsion formulations was demonstrated for both biopolymers carriers.*

The emulsion optical microscope images and the SEM images of the micro and nano-carriers produced are illustrated in **Figure VI.2 a-d** and in **Figure VI.3 a-d**. Well shaped devices were always fabricated by SEE with narrow distribution.
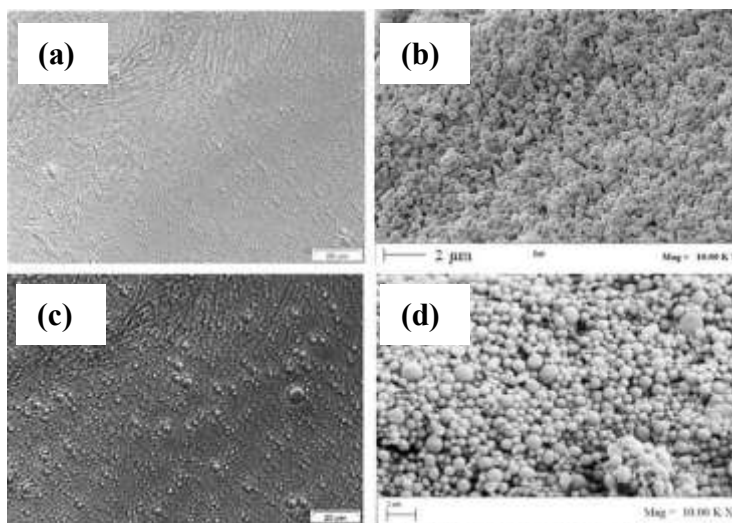
**Figure VI.2** *Optical microscope images of emulsions (a, c) and SEM images of nano (b) and micro-carriers (d) of PLA loaded with β-CA and α-TOC. Nano-carriers with a mean size of 0.3 ±0.1 μm (loading 6.2 mg/g) and micro-carriers with a mean size of 1.5 ±0.5 (loading 6.8 mg/g) were fabricated by SEE.*
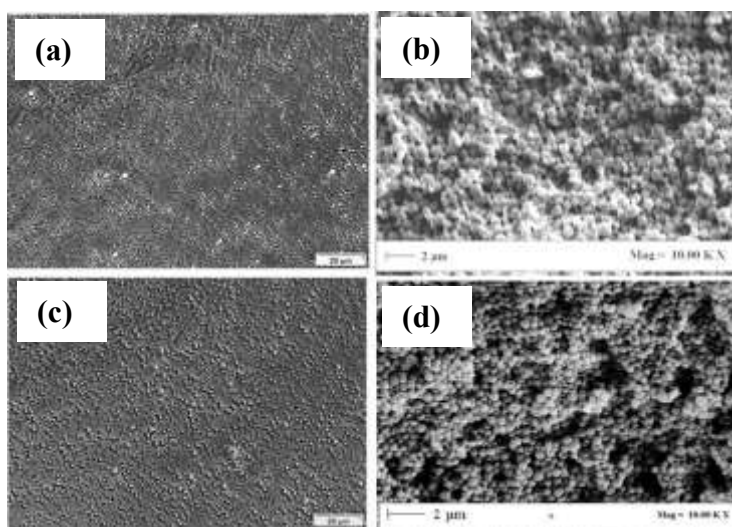


**Figure VI.3** *Optical microscope images of emulsions (a, c) and SEM images of micro (b) and nano-carriers (d) of PLGA loaded with β-CA and α-TOC. Micro-carriers with a mean size of 2 ±0.6 mm (loading 2.6 mg/g) and nano-carriers of 0.5 ±0.1 mm with (loading 2.7 mg/g) were fabricated by SEE.*

The improved EE observed in the PLGA carriers when the amount of polymer was doubled in the oily phase, may be due to the extremely low

molecular weight of PLGA used in this work. Indeed, the molecular weight of PLA used was 3 times higher with respect the one of PLGA; therefore, the dynamic viscosity of the two oily phase solutions could be extremely different, even if the same amount of biopolymer was dissolved in it. This large difference in oily phases dynamic behaviour may strongly influence the capability of drug holding in the oily phase during the emulsion preparation (phases sonication and stirring) and, therefore, it may explain the necessity of a double amount of PLGA in the oily phase to assure a better drug encapsulation efficiency. However, further investigation involving the experimental measurement of dynamic viscosity for the oily phase solutions in relation of the amount of polymer solubilized within and its molecular weight should provide a better understanding of the described behaviour.

## VI.2.2 RA encapsulation into PLA and PLGA

Several runs were performed to test the RA encapsulation; then, it was co-encapsulated with $\beta$-CA and a-TOC. The first set of experiments used a $w_1/o/w_2$ double emulsion where RA was solved in the aqueous internal phase ($w_1$). For the emulsion formulations the proportion of ET:WATER in the internal water phase was varied together with RA concentrations. All the conditions explored are described in **Table VI.2**.

**Table VI.11** *Different emulsion formulations processed by SEE-C. The oily phase was formed of EA with 1 g of PLA; the external water phase was always of saturated water with 0.6% w/w of Tween 80.*

| RA loaded (mg) | Composition of $w_1$ (1 mL) | Polymer in EA ($o_2$) | EE % |
|---|---|---|---|
| 20 | 20:80 EtOH:H2O | PLA | 3.8 |
| 100 | EtOH | PLA | 2.1 |
| 37 | 20:80 EtOH:H2O | PLA | 1.3 |
| 20 | 30:70 EtOH:H2O | PLA | 3.5 |
| 10 | 100 H2O | PLA | 3.5 |
| 150 | -- | PLA | - |
| 150 | -- | PLGA | - |

In all cases, very low EE were experienced ranging between 1.3% to 3.9%. The results seemed almost in contrast with the ones reported by

several authors that described RA encapsulation efficiencies of 60-78% in both poly-caprolactone and carboxy-methyl cellulose, respectively, when emulsions were treated with conventional evaporation/extraction processes (Carvalho et al., 2005). Taking into account the SEE operative conditions used (80 bar and 37°C), the very low encapsulation efficiency obtained for RA cannot be simply due to the RA solubility in SC-$CO_2$ (Carvalho et al., 2005); i.e., in these conditions RA cannot be solubilized by carbon dioxide and only higher pressures/temperature values are required. Nevertheless, considering the presence of the high pressure mixture EA-$CO_2$ formed in the column during the oily phase extraction, the RA solubilisation it is reasonable and possible. Indeed, in the literature, it is largely reported that the system EA-SC-$CO_2$ generates an expanded liquid (Della Porta et al., 2006) at pressure and temperature conditions used for SEE processing; this mixture can extract the RA before or meanwhile the biopolymer is hardened. Further investigations were performed in order to modify the overall system compositions and gain RA encapsulation; emulsion type $o_1/o_2/w$ using β-CA and α-TOC (with Span 20 0.06%), with both PLA and PLGA were tested and even if nano-carriers with a mean diameter of 0.5±0.09 mm and 0.5±0.1 nm respectively were obtained, the RA EE% obtained was no higher than 5%. Additionally, in the case of PLA processing, the inclusion of RA in the emulsion formulation, caused a further reduction of other drugs encapsulation (for example β-CA EE% was reduced from 62% to 35%). When the co-encapsulation was performed into PLGA carriers, RA EE was of 12% and β-CA EE was maintained at 53%. A better understanding of the behaviour observed can be possible with an accurate and more deep knowledge of the behaviour of the quaternary mixture ($CO_2$, EA, RA+β-CA) at high pressure. Indeed, we hypothesized that the quaternary system formed at the pressures and temperatures conditions tested (80 bar and 38°C) has a miscibility hole very sharp or not large enough to prevent the drugs co-extraction. The behaviour, described as "*co-extraction effect*" may limit the application of SEE technology in the encapsulation of compounds with high solubility in the high-pressure mixture formed during the oily phase extraction.

## *VI.2.3 SEE processing of emulsions with glycerol-water phase*

Some runs were performed fixing the water phase composition at GLY:WATER 80:20 with 0.6% (w/w) of Tween 80; the overall ratio *o/w* was always maintained at 20/80 for all the emulsion prepared. Using GLY in the water phase, acetone can be used as solvent of the oily phase, due to the immiscibility hole described in the ternary diagrams reported in **Figure VI.4b**. PLGA amount in the oily phase was fixed at 1 g, while the β-C loading was fixed at 30 mg/g. From the optical image of the emulsion droplets in **FigureVI.4a** it is possible to observe the presence of crystals of

β-CA in the oily saturated phase. For this reason, the emulsion can be more correctly described as *solid-oil-water s/o/w*.
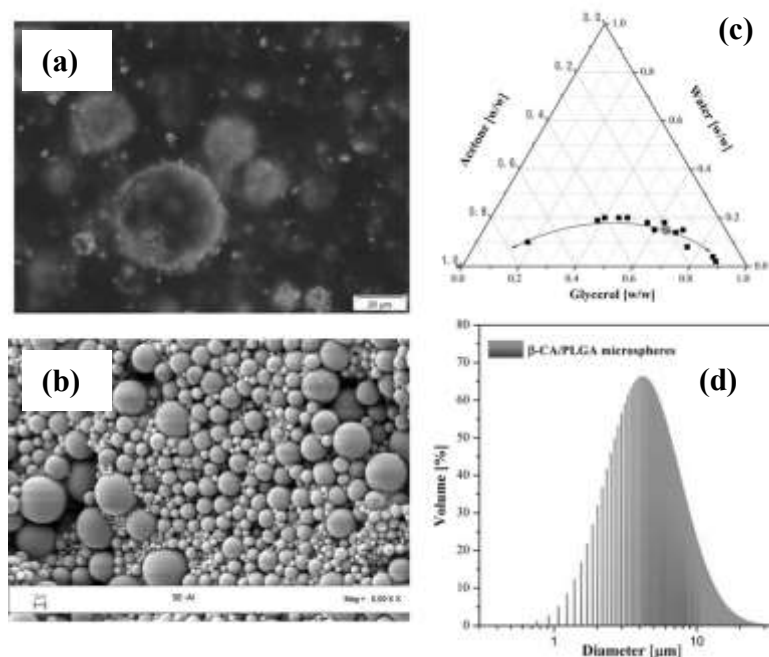


**Figure VI.4** *Optical microscope images of the emulsions (a) and SEM images of the related micro-capsules (b) produced by SEE using an o-w emulsions (20/80) AC:GLY/WATER. The emulsion composition is represented in the ternary diagram (c). Particle Size Distribution (PSD) of PLGA micro-capsules fabricated is also reported (d); mean size of 4.3 mm with β-CA loading of 30 mg/g.*

In **Figure VI.4c-d** a SEM image of the fabricated carriers is also reported with the PSD that showed a mean size of 4.4±0.7 mm; encapsulation rate of 82% has been also reported. SEE pressure and temperature conditions used, were of 80 bar and 40°C with an L/G ratio of 0.3; however, difficulties in SEE process managing have to be reported because of the high viscosity of the GLY-WATER phase that caused severe column blockage, preventing a good plant operation.

## VI.2.3 Shelf life study

Shelf life studies were proposed. Firstly, it was quantified the remaining β-CA into all PLA and PLGA nano-capsules containing β-CA and β-CA+α-TOC after its exposure to the light; the control test with pure β-CA was also

performed. Results are illustrated in **Figure VI.5a**. The 83% of pure β-CA degrades after 3 days of UV exposure, while only the 21.7% and 16.8%, respectively, of the encapsulated drug degraded when loaded in PLA and PLGA nano-capsules. After 10 days of UV exposure, pure β-CA was completely degraded; whereas, 4% and 2.6% of drug was still monitored, when encapsulated into PLA and PLGA, respectively. If β-CA was co-encapsulated with α-TOC, the remaining active drug was of 22% and 30% in PLA and PLGA, respectively after 10 days. This result is in agreement with several authors which reported the beneficial combination of α-TOC presence to prevent degradation of the carotenoid (Scita, 1992). Indeed, the co-encapsulation of β-CA with α-TOC has been reported to block the oxygen radicals chain reaction, prolonging its shelf life in colloidal lipid particles of fat-in-water dispersions (Boon et al., 2010, Santos et al., 2012, Tarver, 2008, Brito-Oliveira et al., 2017). In the second shelf life study, the remaining β-CA was quantified after 2 years of storage in the dark at 4°C when co-encapsulated with α-TOC in both PLA and PLGA nano-capsules. As we can see from **Figure VI.5b,** only the 53% of the active degraded in PLA and the 63% one when encapsulated in PLGA. Both studies confirmed a better protection against oxidation for β-CA and good performances of the carriers fabricated by SEE; the best nano-carrier formulation seemed to be the ones with β-CA/α-TOC in PLGA.
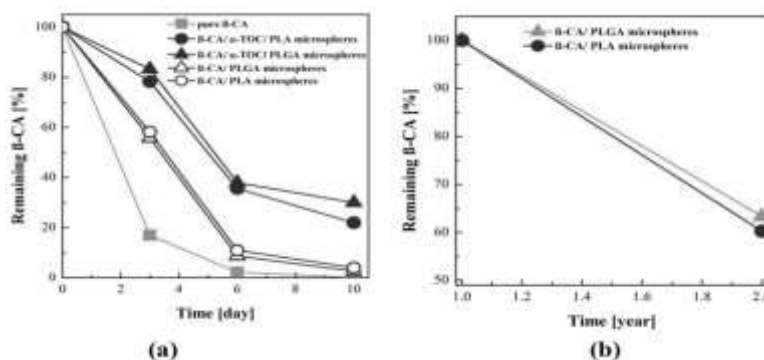


**Figure VI.5** *Shelf-life studies results. Pure β-CA and encapsulated β-CA degradation tendencies along time after its exposure to UV radiation (UV length 259 nm) for one hour during ten days (a); encapsulated β-CA degradation tendencies along two years after its storage at 4 ℃ in the dark (b).*

## VI.2.4 Antioxidant activity

In order to measure the functionality of the micro and nano-capsules, their antioxidant activity was assayed against DPPH radical. According to β-

CA calibration curve and the loading in each carriers tested, the theoretical antioxidant activity of micro and nano-capsules was measured and compared. The antioxidant activity of PLA and PLGA nano-capsules was first monitored after 2 years of storage, as illustrated in **Figure VI.6a**.
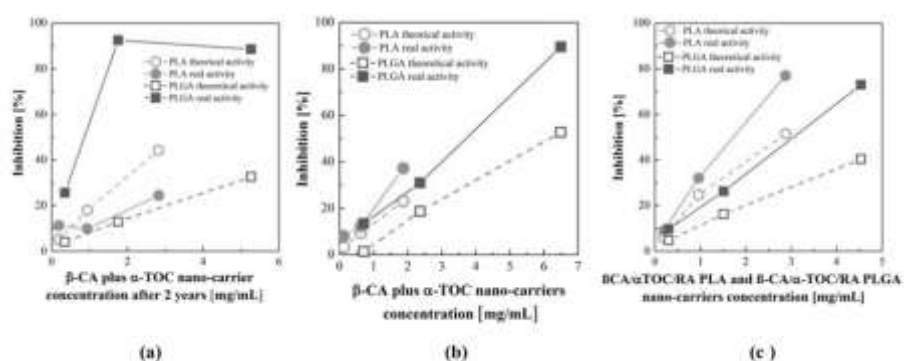


**Figure VI.6** *Antioxidant activity theoretical vs real. PLA and PLGA nano-capsules loaded with β-CA and α-TOC, after 2 years (a); loaded with β-CA and α-TOC, after fabrication (b); loaded with β-CA, α-TOC and RA, after fabrication (c).*

For PLA formulation, the activity measured was lower than expected (IC50$_{expected}$ 3.2 mg/mL vs IC50$_{measured}$ 6.7mg/mL) because of a higher β-CA degradation in these carriers; whereas for PLGA carriers the performance was better, confirming the lower degradation of β-CA in the system after two years with an activity maintained at IC$_{50}$ 2.3 mg/mL. From **Figure VI.6a**, although the theoretical antioxidant activity of PLA nano-capsules seemed higher than the ones of PLGA capsules, it is only due to the higher loading of β-CA in the PLA system. This difference could be also a consequence of a higher content of the co-encapsulated α-TOC (26.78% into PLA vs 52.97% into PLGA). Looking at the real activity, and in accordance with the shelf life results, PLGA seemed to be the more protecting biopolymer, preserving the β-CA activity along the time.

PLA and PLGA antioxidant activity was also measured immediately after their formulation for both PLA and PLGA nano-capsules. β-CA+ α-TOC theoretical IC50 according to their loading (6.2 mg/g and 3.1 mg/g, respectively) was of 2.7 mg/mL and 5.6 mg/mL; however, the measured antioxidant activity was always higher and of 1.8 mg/mL and 3 mg/mL, respectively, as reported (in percentage) in **Figure VI.6b**. When RA was included in the formulation, a higher theoretical IC50 was expected, and 6.3 mg/mL and 4.2 mg/mL for PLA and PLGA nano-carriers was measured; however, their antioxidant activity was lower than the equivalent PLA and PLGA carriers without RA because of the overall reduction of β-CA loading. Nevertheless, as described in **Figure VI.6c**, the measured activity is higher

than the expected, when carriers with the co-encapsulation of the three bio-actives are tested. This is probably due to the combination of the three actives (β-CA+α-TOC+RA) even if they are entrapped at an overall lower concentration. β-CA/a-TOC/PLA capsules showed a superior antioxidant activity with an $IC_{50}$ against the free radical DPPH of 1.8 mg/mL.

## VI.3    Experimental results for AXA encapsulation

Taking into account the best nanocarriers fabricated in term of size and morphology using EC as polymer (reported in Chapter III) and considering that the surfactant and polymer expenditure could determine the costs of the particles production process, the surfactant concentration of Tween 80 was studied. Futhermore, the effect of stirring condition on emulsion formulation was evaluated. Data of produced tests are report in **Table VI.3.**

On the other hand, the low solubility of AXT in the organic phase, conditioned the amount of polymer to obtain a higher AXT/polymer ratio. Taking into account that the maximum solubility of AXT in ethyl acetate was 0.25 mg AXT/g solvent; and that 100 mL of emulsion processed by SEE-C contained 19.8 g of ethyl acetate; it meant a maximum amount of 4.95 mg of AXT in the formulation. Consequently, using 1% polymer in the organic phase led to a mass ratio AXT/Ethyl cellulose of 25 mg/g. This is already a quite small ratio; using higher polymer content would mean reducing this ratio even more. As a result of this circumstance, the proportion of polymer in the organic phase was finally fixed at 1 % to carry out the encapsulation.

**Table VI.12** *Encapsulation study of Axastanthin, varyng Tween 80 concentration (AXA 0.1- AXA 0.2) and stirring effect (AXA 0.1-AXA 0.1 bis)*

| TEST | Tween 80 (w/w) | DSD (nm) | PSD (nm) | EE (%) |
|---|---|---|---|---|
| **AXA 0.1** | 0.1% | 585±102 | 429±59 | 80 |
| **AXA 0.2** | 0.2% | 452±63 | 219±10 | 42 |
| **AXA 0.1 bis** | 0.1% | 495±34 | 366±32 | 84 |

Fixing the polymer concentration at 1% of weight, two effects were studied, the surfactant used and the stirring condition form emulsion formulation. As can see from **Table VI.3**, when the surfactant concentration increases, a decrease in the average diameter of the particles obtained were observed. Particles with an average diameter of about 429 ± 59 nm and 219 ± 10.5 nm were obtained for the AXA 0.1 and AXA 0.2 test, respectively.

However, as can be observed from **Table VI.3** and **Figure VI.7a,** the test AXA 0.2 showed a wider distribution compared to the AXA 0.1 test which show a PdI of 0.276. Spherical particles were obtained in both tests as reported in **Figure VIa** and **Figure VIb**, even if the AXA 0.1 showed a more regular morphology than AXA 0.2. Probably the increase of surfactant allowed the formation of smaller particles but with more difficult recover; in fact, during the membrane filtration process they tend to co-exist with each other. EE of 80 % and 42 % were obtained respectively, confirming AXA 0.1 as the best formulation.

In a further analysis it was decided to investigate the operating condition of the emulsion formation. The same AXA 0.1 emulsion was produced using a 150 mL becker and therefore reducing the axial distance between the emulsifier and the beaker in the emulsion formation phase (AXA 0.1 bis). As can be seen from **Table VI.3**, this operative parameter influenced the PSD of produced capsules, indeed smaller particles with mean diameter of 366±32 nm were obtained respect to the test AXA 0.1. The comparison of produced particle size distribution were reported in **Figure VI.6**. Reducing the volume of the beaker in which the emulsion was prepared, a closer particle size distribution was obtained. In this case, encapsulation efficiency of 84 % was achieved.
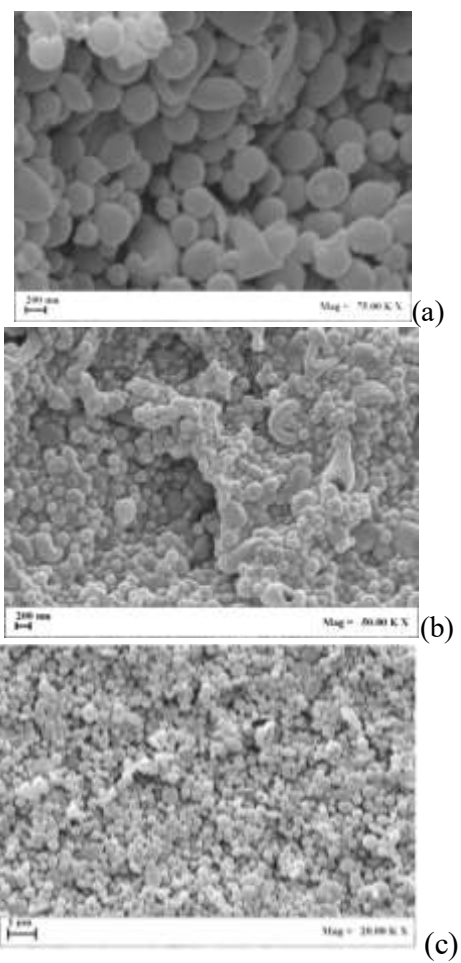
**Figure VI.7** *SEM images of astaxanthin in ethyl cellulose carriers. AXA0.1 (a), AXA 0.2 (b) and AXA 0.1bis(c).*

(a)                                                    (b)
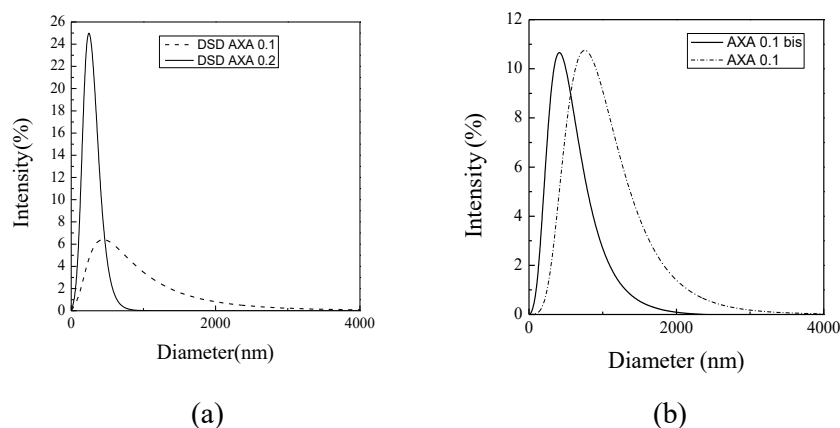
**Figure VI.8** *Comparison of particles size distribution of test varying the Tween concentration (a) and the stirring effect (b)*

Accordingly, the loading ratio AXT/polymer was 21 mg/g. Taking into account the studies that reported beneficial results from a daily intake of 4 mg (Seabra and Pedrosa, 2010), it would be enough for a person to etake 190 mg/day of the powder obtained in this work to promote health benefits. This is a relatively small amount, considering that a person would need to consume from 600 g of salmon to reach the recommended consumption.

The encapsulation efficiency achieved in this work was within the highest range of values reported in the literature using other techniques. Indeed, by using conventional technologies, Gomez-Estaca et al. (Gomez-Estaca et al., 2016), reached an AXT (from shrimp waste) encapsulation efficiency of almost 60% by complex coacervation with gelatine. Alternatively, Lee et al., (Lee et al., 2011) found a maximum AXT encapsulation efficiency of 31 % (extract from Xanthophyllomyces dendrorhous) within calcium alginate gel beads by ionic gelation. Using supercritical fluid technologies, Mezzomo et al., (Mezzomo et al., 2012) encapsulated an AXT-rich extract from shrimp residue in Hi-Cap 100 (a modified starch) operating at 10 MPa, 313 K, 4.0 kg CO2 $h^{-1}$ and 4 mL $min^{-1}$ by using SEE. These authors reported an AXT encapsulation efficiency of 83%. Another work (Machado Jr et al., 2014) investigated the effectiveness of SC-CO$_2$ for the encapsulation of AXT (extracted from Haematococcus pluvialis) in the co-polymer poly-3-hydroxybutyrate-co-3-hydroxyvalerate (PHBV) using the Solution Enhanced Dispersion by Supercritical Fluids (SEDS) technique and dichloromethane as organic solvent. These authors reached an encapsulation efficiency of 48 %.

## VI.3.1 Antioxidant activity

The antioxidant capacity of loaded particles with AXT was measured using radical scavenging assays with DPPH, the results were reported in **Table VI.4**.

**Table VI.13** *Scavenging activity of AXA tests. The calculated scavenging activity (SA) was compared with SA of pure compound also considering EE value.*

| Test | SA (%) | SA tq (%) |
|---|---|---|
| AXA 0.1 | 11.6 | 13.2-10.6 |
| AXA 0.1 bis | 6.7 | 13.2-4.1 |
| AXA 0.2 | 12.3 | 13.2-11.1 |

As can be seen from **Table VI.4**, the percentage of inhibition of the encapsulated samples (SA) is always included in the scavenging activity range which takes into account the pure compound and the percentage of inhibition of the same calculated on the basis of the encapsulation efficiency of each sample. Therefore, it is possible to state that the samples produced show good antioxidant activity.This means that the AXT maintained its antioxidant activity and did not significantly deteriorate during the SEE-C processing and encapsulation, thanks to the low temperature and the very short residence time within the high-pressure column, as well as the non-oxidizing atmosphere of the $CO_2$.

## VI.4    Conclusion

The Supercritical Emulsion Extraction (SEE-C) allowed the formulation of β-CA/PLA and β-CA/PLGA carriers with a wide range of sizes from nano up to micro scale and with high EEs. The biopolymer capsules demonstrated to provide drug protection from UV radiation and along two years of storage, improving drug shelf life. α-TOC co-encapsulations gives an extra protection to β-CA degradation in both oxidizing conditions; whereas, PLGA encapsulation gave better preservation. A SEE limitation was detected for the lack of encapsulation efficiency in the case of molecules extremely soluble in the high-pressure mixture formed during the oily phase extraction.

Using SEE-C was also possible to load within ethyl cellulose a relatively high amount of AXT (21 mg/g) with a high degree of encapsulation (84 %) preserving its antioxidant capacity.

# Conclusions

The aim of this Ph.D. work was the development of new and smart formulations consisting of microcapsules, using supercritical assisted processes for lubricant, self healing, pharmaceutical and nutraceutical applications.

The SEE process was successfully applied to all the studied application fields, demonstrating to be attractive and available from an industrial point of view.

In the framework of the oil gas industry for lubricant formulations, two additives were investigated, as part of the agreement between Total and the Department of Industrial Engineering (DIIN) of the University of Salerno. Differently from the conventional techniques, the SEE process was able to reach the specific targets requested by the Company. Spherical capsules with AM and MoDTC loading up to 90% were successfully produced for the first time using SEE technology. For each optimized product, different batches were produced for further analyses, directly performed by Total.

A future study may be aimed at optimizing the dispersion of SEE produced capsules in base oil by means of surface modifications that make loaded microcapsules stable in suspension for a long time.

SEE-C encapsulation technique proved to be a very effective for producing optical health monitoring microcapsules to be used as element in new smart coating and potentially for other self-responsive functions in aeronautical application. SEE-C produced capsules were dispersed in an aqueous paint used to coat carbon fiber reinforced panels and preliminary impact tests were performed: the panels, subjected to impact tests showed the dye leaking and therefore the capsule breaking in stressed areas

Future development on the same coating are in progress in order to evaluate the ability of the microcapsules to simultaneously confer health monitoring and self-healing capability to the coating.

SEE technology was successfully use to encapsulate peptides such as growth factors into PLGA or PLA carriers providing a good control size and morphology and ensuring a sustained growth factor release over the time.

SEE-fabricated carriers were safely introduced within biomedical devices structures because they have no intrinsic toxicity and are considered safe for health. These results open new perspectives for the use of SEE fabricated carriers for the development of 3D bioengineered microenvironments where biological molecules can be released under controlled conditions stimulating tissue regeneration and healing.

Finally, the SEE technique revealed to be a reliable alternative to conventional processes also in the field of nutraceuticals. For the first time, SEE composite systems based on the dispersion in different carriers of bioactive compounds, such as β-caratotene and astaxanthin, were successfully produced. Defined, spherical capsules with high loading efficiencies up to 80-84% and with preserved antioxidant activity were obtained.

# References

**Primary Sources**

**Secondary Sources**

**Uncategorized References**

ABDO, M. 2014. *Structural Health Monitoring, History, Applications and Future. A Review Book*.

ADAMI, R., LIPAROTI, S., DELLA PORTA, G., DEL GAUDIO, P. & REVERCHON, E. 2017. Lincomycin hydrochloride loaded albumin microspheres for controlled drug release, produced by Supercritical Assisted Atomization. *The Journal of Supercritical Fluids,* 119**,** 203-210.

ADAMI, R., LIPAROTI, S., IZZO, L., PAPPALARDO, D. & REVERCHON, E. 2012. PLA–PEG copolymers micronization by supercritical assisted atomization. *The Journal of Supercritical Fluids,* 72**,** 15-21.

ADAMI, R. & REVERCHON, E. 2012. Composite polymer-Fe3O4 microparticles for biomedical applications, produced by Supercritical Assisted Atomization. *Powder Technology,* 218**,** 102-108.

ADSCHIRI, T. & YOKO, A. 2018. Supercritical fluids for nanotechnology. *The Journal of Supercritical Fluids $V 134***,** 167-175.

ADVANI, S. G. & HSIAO, K. T. 2012. 1 - Introduction to composites and manufacturing processes. *In:* ADVANI, S. G. & HSIAO, K.-T. (eds.) *Manufacturing Techniques for Polymer Matrix Composites (PMCs).* Woodhead Publishing.

AGUILAR, M. R. & SAN ROMÁN, J. 2014. 1 - Introduction to smart polymers and their applications. *In:* AGUILAR, M. R. & SAN ROMÁN, J. (eds.) *Smart Polymers and their Applications.* Woodhead Publishing.

AKIYAMA, H., KANAZAWA, S., OKUYAMA, Y., YOSHIDA, M., KIHARA, H., NAGAI, H., NORIKANE, Y. & AZUMI, R. 2014. Photochemically Reversible Liquefaction and Solidification of Multiazobenzene Sugar-Alcohol Derivatives and Application to Reworkable Adhesives. *ACS Applied Materials & Interfaces,* 6**,** 7933-7941.

ALARCÓN, C. D. L. H., FARHAN, T., OSBORNE, V. L., HUCK, W. T. & ALEXANDER, C. 2005. Bioadhesion at micro-patterned stimuli-responsive polymer brushes. *Journal of Materials Chemistry,* 15**,** 2089-2094.

ALEXANDER, C. & SHAKESHEFF, K. M. 2006. Responsive Polymers at the Biology/Materials Science Interface. *Advanced Materials,* 18**,** 3321-3328.

ALMEIDA, H., AMARAL, H. & LOBÃO, P. 2012. Temperature and pH stimuli-responsive polymers and their applications in controlled and selfregulated drug delivery. *Journal of Applied Pharmaceutical Science,* 2**,** 01-10.

ALVAREZ-LORENZO, C., BROMBERG, L. & CONCHEIRO, A. 2009. Light-sensitive Intelligent Drug Delivery Systems†. *Photochemistry and Photobiology,* 85**,** 848-860.

ANDREEVA, D. V., FIX, D., MÖHWALD, H. & SHCHUKIN, D. G. 2008. Self-Healing Anticorrosion Coatings Based on pH-Sensitive Polyelectrolyte/Inhibitor Sandwichlike Nanostructures. *Adv Mater,* 20**,** 2789-94.

ANIKIN, K., RÖCKER, C., WITTEMANN, A., WIEDENMANN, J., BALLAUFF, M. & NIENHAUS, G. U. 2005. Polyelectrolyte-mediated protein adsorption: fluorescent protein binding to individual polyelectrolyte nanospheres. *The Journal of Physical Chemistry B,* 109**,** 5418-5420.

ASAKA, K. & OGURO, K. 2000. Bending of polyelectrolyte membrane platinum composites by electric stimuli: Part II. Response kinetics. *Journal of Electroanalytical Chemistry,* 480**,** 186-198.

ASTETE, C. E., KUMAR, C. S. & SABLIOV, C. M. 2007. Size control of poly (d, l-lactide-co-glycolide) and poly (d, l-lactide-co-glycolide)-magnetite nanoparticles synthesized by emulsion evaporation technique. *Colloids and Surfaces A: Physicochemical and Engineering Aspects,* 299**,** 209-216.

ATHANASIOU, K. A., NIEDERAUER, G. G. & AGRAWAL, C. M. 1996. Sterilization, toxicity, biocompatibility and clinical applications of polylactic acid/ polyglycolic acid copolymers. *Biomaterials,* 17**,** 93-102.

BABIN, J., LEPAGE, M. & ZHAO, Y. 2008. "Decoration" of Shell Cross-Linked Reverse Polymer Micelles Using ATRP: A New Route to Stimuli-Responsive Nanoparticles. *Macromolecules,* 41**,** 1246-1253.

BAJPAI, A. K., SHUKLA, S. K., BHANU, S. & KANKANE, S. 2008. Responsive polymers in controlled drug delivery. *Progress in Polymer Science,* 33**,** 1088-1118.

BALASUNDRAM, N., SUNDRAM, K. & SAMMAN, S. 2006. Phenolic compounds in plants and agri-industrial by-products: Antioxidant activity, occurrence, and potential uses. *Food Chemistry,* 99**,** 191-203.

BALDINO, L., CARDEA, S., DE MARCO, I. & REVERCHON, E. 2014a. Chitosan scaffolds formation by a supercritical freeze extraction process. *The Journal of Supercritical Fluids,* 90**,** 27-34.

BALDINO, L., CARDEA, S. & REVERCHON, E. 2014b. Supercritical assisted enzymatic membranes preparation, for active packaging applications. *Journal of Membrane Science,* 453**,** 409-418.

BALDINO, L., CARDEA, S. & REVERCHON, E. 2019. A supercritical CO2 assisted electrohydrodynamic process used to produce microparticles and microfibers of a model polymer. *Journal of CO2 Utilization,* 33**,** 532-540.

BLEAY, S. M., LOADER, C. B., HAWYES, V. J., HUMBERSTONE, L. & CURTIS, P. T. 2001. A smart repair system for polymer matrix composites. *Composites Part A: Applied Science and Manufacturing,* 32**,** 1767-1776.

BOKIAS, G., HOURDET, D. & ILIOPOULOS, I. 2000. Positively Charged Amphiphilic Polymers Based on Poly(N-isopropylacrylamide): Phase Behavior and Shear-Induced Thickening in Aqueous Solution. *Macromolecules,* 33**,** 2929-2935.

BOND, I. P., TRASK, R. S. & WILLIAMS, H. R. 2011. Self-Healing Fiber-Reinforced Polymer Composites. *MRS Bulletin,* 33**,** 770-774.

BOON, C. S., MCCLEMENTS, D. J., WEISS, J. & DECKER, E. A. 2010. Factors influencing the chemical stability of carotenoids in foods. *Critical reviews in food science and nutrition,* 50**,** 515-532.

BOUISSOU, C., ROUSE, J. J., PRICE, R. & VAN DER WALLE, C. F. 2006. The Influence of Surfactant on PLGA Microsphere Glass Transition and Water Sorption: Remodeling the Surface Morphology to Attenuate the Burst Release. *Pharmaceutical Research,* 23**,** 1295-1305.

BRAND-WILLIAMS, W., CUVELIER, M. E. & BERSET, C. 1995. Use of a free radical method to evaluate antioxidant activity. *LWT - Food Science and Technology,* 28**,** 25-30.

BRITO-OLIVEIRA, T. C., MOLINA, C. V., NETTO, F. M. & PINHO, S. C. 2017. Encapsulation of Beta-carotene in Lipid Microparticles Stabilized with Hydrolyzed Soy Protein Isolate: Production Parameters, Alpha-tocopherol Coencapsulation and Stability Under Stress Conditions. *Journal of food science,* 82**,** 659-669.

BRUNNER, G. 2009. Counter-current separations. *Journal of Supercritical Fluids,* 47**,** 574-582.

BURNWORTH, M., TANG, L., KUMPFER, J. R., DUNCAN, A. J., BEYER, F. L., FIORE, G. L., ROWAN, S. J. & WEDER, C. 2011. Optically healable supramolecular polymers. *Nature,* 472**,** 334.

CABANE, E., ZHANG, X., LANGOWSKA, K., PALIVAN, C. G. & MEIER, W. 2012. Stimuli-Responsive Polymers and Their Applications in Nanomedicine. *Biointerphases,* 7**,** 9.

CALCAVECCHIO, P., SHOUGH, A. M., NG, M. K. & DRAKE, E. N. 2015. Inverse micellar compositions containing lubricant additives. Google Patents.

References

CAMPARDELLI, R., BALDINO, L. & REVERCHON, E. 2015. Supercritical fluids applications in nanomedicine. *The Journal of Supercritical Fluids,* 101**,** 193-214.

CAMPARDELLI, R., FRANCO, P., REVERCHON, E. & DE MARCO, I. 2019. Polycaprolactone/nimesulide patches obtained by a one-step supercritical foaming + impregnation process. *The Journal of Supercritical Fluids,* 146.

CAMPARDELLI, R. & REVERCHON, E. 2017. Instantaneous coprecipitation of polymer/drug microparticles using the supercritical assisted injection in a liquid antisolvent. *The Journal of Supercritical Fluids,* 120**,** 151-160.

CARVALHO, R. N., MOURA, L. S., ROSA, P. T. V. & MEIRELES, M. A. A. 2005. Supercritical fluid extraction from rosemary (Rosmarinus officinalis): Kinetic data, extract's global yield, composition, and antioxidant activity. *The Journal of Supercritical Fluids,* 35**,** 197-204.

CERRITELLI, S., VELLUTO, D. & HUBBELL, J. A. 2007. PEG-SS-PPS: Reduction-Sensitive Disulfide Block Copolymer Vesicles for Intracellular Drug Delivery. *Biomacromolecules,* 8**,** 1966-1972.

CHAMBIN, O., DUPUIS, G., CHAMPION, D., VOILLEY, A. & POURCELOT, Y. 2006. Colon-specific drug delivery: Influence of solution reticulation properties upon pectin beads performance. *International Journal of Pharmaceutics,* 321**,** 86-93.

CHAMPAGNE, C. P. & FUSTIER, P. 2007. Microencapsulation for the improved delivery of bioactive compounds into foods. *Current Opinion in Biotechnology,* 18**,** 184-190.

CHANDRAPALA, J., ZISU, B., PALMER, M., KENTISH, S. & ASHOKKUMAR, M. 2011. Effects of ultrasound on the thermal and structural characteristics of proteins in reconstituted whey protein concentrate. *Ultrasonics Sonochemistry,* 18**,** 951-957.

CHATTOPADHYAY, P. & GUPTA, R. B. 2003. Supercritical $CO_2$-based formation of silica nanoparticles using water-in-oil microemulsions. *Industrial & Engineering Chemistry Research,* 42**,** 465-472.

CHATTOPADHYAY, P., HUFF, R. & SHEKUNOV, B. Y. 2006. Drug encapsulation using supercritical fluid extraction of emulsions. *Journal of Pharmaceutical Sciences,* 95**,** 667-679.

CHATTOPADHYAY, P., SHEKUNOV, B. Y., YIM, D., CIPOLLA, D., BOYD, B. & FARR, S. 2007. Production of solid lipid nanoparticle suspensions using supercritical fluid extraction of emulsions (SFEE) for pulmonary delivery using the AERx system. *Advanced Drug Delivery Reviews,* 59**,** 444-453.

CHENG, F. Y., WANG, S. P., SU, C. H., TSAI, T. L., WU, P. C., SHIEH, D. B., CHEN, J. H., HSIEH, P. C. & YEH, C. S. 2008. Stabilizer-

142

free poly(lactide-co-glycolide) nanoparticles for multimodal biomedical probes. *Biomaterials,* 29**,** 2104-12.

CHENG, R., MENG, F., DENG, C., KLOK, H.-A. & ZHONG, Z. 2013. Dual and multi-stimuli responsive polymeric nanoparticles for programmed site-specific drug delivery. *Biomaterials,* 34**,** 3647-3657.

CHRISOCHOOU, A., SCHABER, K. & BOLZ, U. 1995. Phase equilibria for enzyme-catalyzed reactions in supercritical carbon dioxide. *Fluid Phase Equilibria,* 108**,** 1-14.

CHU, B.-S., ICHIKAWA, S., KANAFUSA, S. & NAKAJIMA, M. 2008. Stability of protein-stabilised β-carotene nanodispersions against heating, salts and pH. *Journal of the science of food and agriculture,* 88**,** 1764-1769.

CIAGLIA, E., MONTELLA, F., TRUCILLO, P., CIARDULLI, M. C., DI PIETRO, P., AMODIO, G., REMONDELLI, P., VECCHIONE, C., REVERCHON, E., MAFFULLI, N., PUCA, A. A. & DELLA PORTA, G. 2019. A bioavailability study on microbeads and nanoliposomes fabricated by dense carbon dioxide technologies using human-primary monocytes and flow cytometry assay. *International Journal of Pharmaceutics,* 570**,** 118686.

COCERO, M. J., MARTÍN, Á., MATTEA, F. & VARONA, S. 2009. Encapsulation and co-precipitation processes with supercritical fluids: fundamentals and applications. *The Journal of Supercritical Fluids,* 47**,** 546-555.

COMOLLI, N., NEUHUBER, B., FISCHER, I. & LOWMAN, A. 2009. In vitro analysis of PNIPAAm–PEG, a novel, injectable scaffold for spinal cord repair. *Acta biomaterialia,* 5**,** 1046-1055.

CORONEL-AGUILERA, C. P. & SAN MARTÍN-GONZÁLEZ, M. F. 2015. Encapsulation of spray dried β-carotene emulsion by fluidized bed coating technology. *LWT - Food Science and Technology,* 62**,** 187-193.

CUNLIFFE, D., DE LAS HERAS ALARCÓN, C., PETERS, V., SMITH, J. R. & ALEXANDER, C. 2003. Thermoresponsive surface-grafted poly (N− isopropylacrylamide) copolymers: effect of phase transitions on protein and bacterial attachment. *Langmuir,* 19**,** 2888-2899.

DA SILVA, J., JESUS, S., BERNARDI, N., COLAÇO, M. & BORGES, O. 2019. Poly(D,L-Lactic Acid) Nanoparticle Size Reduction Increases Its Immunotoxicity. *Frontiers in Bioengineering and Biotechnology,* 7.

DAI, S., RAVI, P. & TAM, K. C. 2008. pH-Responsive polymers: synthesis, properties and applications. *Soft Matter,* 4**,** 435-449.

DE PAZ, E., MARTÍN, Á., DUARTE, C. M. M. & COCERO, M. J. 2012. Formulation of β-carotene with poly-(ε-caprolactones) by PGSS process. *Powder Technology,* 217**,** 77-83.

DEL BARRIO, J., ORIOL, L., SÁNCHEZ, C., SERRANO, J. L., DI CICCO, A., KELLER, P. & LI, M.-H. 2010. Self-Assembly of Linear−Dendritic Diblock Copolymers: From Nanofibers to Polymersomes. *Journal of the American Chemical Society,* 132**,** 3762-3769.

DELLA PORTA, G., CAMPARDELLI, R., FALCO, N. & REVERCHON, E. 2011a. PLGA Microdevices for Retinoids Sustained Release Produced by Supercritical Emulsion Extraction: Continuous Versus Batch Operation Layouts. *Journal of Pharmaceutical Sciences,* 100**,** 4357-4367.

DELLA PORTA, G., CAMPARDELLI, R. & REVERCHON, E. 2013. Monodisperse biopolymer nanoparticles by Continuous Supercritical Emulsion Extraction. *The Journal of Supercritical Fluids,* 76**,** 67-73.

DELLA PORTA, G., FALCO, N. & REVERCHON, E. 2010. NSAID Drugs Release from Injectable Microspheres Produced by Supercritical Fluid Emulsion Extraction. *Journal of Pharmaceutical Sciences,* 99**,** 1484-1499.

DELLA PORTA, G., FALCO, N. & REVERCHON, E. 2011b. Continuous supercritical emulsions extraction: A new technology for biopolymer microparticles production. *Biotechnology and Bioengineering,* 108**,** 676-686.

DELLA PORTA, G. & REVERCHON, E. 2008. Nanostructured microspheres produced by supercritical fluid extraction of emulsions. *Biotechnology and Bioengineering,* 100**,** 1020-1033.

DELLA PORTA, G., VOLPE, M. C. & REVERCHON, E. 2006. Supercritical cleaning of rollers for printing and packaging industry. *The Journal of Supercritical Fluids,* 37**,** 409-416.

DI CAPUA, A., ADAMI, R. & REVERCHON, E. 2017. Production of Luteolin/Biopolymer Microspheres by Supercritical Assisted Atomization. *Industrial & Engineering Chemistry Research,* 56**,** 4334-4340.

DIMITROV, I., TRZEBICKA, B., MÜLLER, A. H. E., DWORAK, A. & TSVETANOV, C. B. 2007. Thermosensitive water-soluble copolymers with doubly responsive reversibly interacting entities. *Progress in Polymer Science,* 32**,** 1275-1343.

DING, X.-B., SUN, Z.-H., ZHANG, W.-C., PENG, Y.-X., WAN, G.-X. & JIANG, Y.-Y. 2000. Adsorption/desorption of protein on magnetic particles covered by thermosensitive polymers. *Journal of Applied Polymer Science,* 77**,** 2915-2920.

DIPHARE, M. J., PILUSA, J. & MUZENDA, E. The effect of degrading agents and diluents on oil recovery from lithium based waste

lubricating grease. 2013. International Conference on Environment, Agriculture and Food Sciences ….

FAISANT, N., AKIKI, J., SIEPMANN, F., BENOIT, J. P. & SIEPMANN, J. 2006. Effects of the type of release medium on drug release from PLGA-based microparticles: Experiment and theory. *International Journal of Pharmaceutics,* 314**,** 189-197.

FALCO, N. & KIRAN, E. 2011. Volumetric properties of ethyl acetate + carbon dioxide binary fluid mixtures at high pressures. *Journal of Supercritical Fluids - J SUPERCRIT FLUID,* 61.

FALCO, N., REVERCHON, E. & DELLA PORTA, G. 2012a. Continuous Supercritical Emulsions Extraction: Packed Tower Characterization and Application to Poly(lactic-co-glycolic Acid) + Insulin Microspheres Production. *Industrial & Engineering Chemistry Research,* 51**,** 8616-8623.

FALCO, N., REVERCHON, E. & DELLA PORTA, G. 2012b. Continuous Supercritical Emulsions Extraction: Packed Tower Characterization and Application to Poly(lactic-co-glycolic Acid) plus Insulin Microspheres Production. *Industrial & Engineering Chemistry Research,* 51**,** 8616-8623.

FALCO, N., REVERCHON, E. & DELLA PORTA, G. 2013. Injectable PLGA/hydrocortisone formulation produced by continuous supercritical emulsion extraction. *International Journal of Pharmaceutics,* 441**,** 589-597.

FANG, Z. & BHANDARI, B. 2010. Encapsulation of polyphenols – a review. *Trends in Food Science & Technology $V 21***,** 510-523.

FARHAIN SALEHUDDIN, S. M., HAWAJI, M. H., BASHER KHAN, A. S. M., CHE MAN, S. H., WAN ALI, W. K. & BAHARULRAZI, N. 2019. - A Review of Recent Developments: Self-Healing Approaches for Polymeric Materials. *Journal of the Italian Association of Chemical Engineering, -* 72.

FARIA, A. F., MIGNONE, R. A., MONTENEGRO, M. A., MERCADANTE, A. Z. & BORSARELLI, C. D. 2010. Characterization and singlet oxygen quenching capacity of spray-dried microcapsules of edible biopolymers containing antioxidant molecules. *Journal of agricultural and food chemistry,* 58**,** 8004-8011.

FEIL, H., BAE, Y. H., FEIJEN, J. & KIM, S. W. 1992. Mutual influence of pH and temperature on the swelling of ionizable and thermosensitive hydrogels. *Macromolecules,* 25**,** 5528-5530.

FILIPCSEI, G., CSETNEKI, I., SZILÁGYI, A. & ZRÍNYI, M. 2007. Magnetic Field-Responsive Smart Polymer Composites. *Oligomers - Polymer Composites - Molecular Imprinting.* Berlin, Heidelberg: Springer Berlin Heidelberg.

FRANCESCHI, E., CEZARO, A. D., FERREIRA, S. R., KUNITA, M. H., MUNIZ, E. C., RUBIRA, A. F. & OLIVEIRA, J. V. 2010. Co-precipitation of beta-carotene and bio-polymer using supercritical carbon dioxide as antisolvent. *The Open Chemical Engineering Journal,* 4.

FRANCESCHI, E., DE CESARO, A. M., FEITEN, M., FERREIRA, S. R. S., DARIVA, C., KUNITA, M. H., RUBIRA, A. F., MUNIZ, E. C., CORAZZA, M. L. & OLIVEIRA, J. V. 2008. Precipitation of β-carotene and PHBV and co-precipitation from SEDS technique using supercritical CO2. *The Journal of Supercritical Fluids,* 47**,** 259-269.

FRANCO, P., REVERCHON, E. & DE MARCO, I. 2018. Zein/diclofenac sodium coprecipitation at micrometric and nanometric range by supercritical antisolvent processing. *Journal of CO2 Utilization,* 27**,** 366-373.

FREY, W., MEYER, D. E. & CHILKOTI, A. 2003. Thermodynamically reversible addressing of a stimuli responsive fusion protein onto a patterned surface template. *Langmuir,* 19**,** 1641-1653.

GAN, S. N. & SHAHABUDIN, N. 2019. Applications of Microcapsules in Self-Healing Polymeric Materials. *Microencapsulation-Processes, Technologies and Industrial Applications.* IntechOpen.

GANTA, S., DEVALAPALLY, H., SHAHIWALA, A. & AMIJI, M. 2008. A review of stimuli-responsive nanocarriers for drug and gene delivery. *Journal of Controlled Release,* 126**,** 187-204.

GENZER, J. & EFIMENKO, K. 2000. Creating Long-Lived Superhydrophobic Polymer Surfaces Through Mechanically Assembled Monolayers. *Science,* 290**,** 2130-2133.

GIL, E. S. & HUDSON, S. M. 2004. Stimuli-reponsive polymers and their bioconjugates. *Progress in Polymer Science,* 29**,** 1173-1222.

GIMENEZ-ROTA, C., PALAZZO, I., SCOGNAMIGLIO, M. R., MAINAR, A., REVERCHON, E. & DELLA PORTA, G. 2019. β-Carotene, α-tocoferol and rosmarinic acid encapsulated within PLA/PLGA microcarriers by supercritical emulsion extraction: Encapsulation efficiency, drugs shelf-life and antioxidant activity. *The Journal of Supercritical Fluids,* 146**,** 199-207.

GOMEZ-ESTACA, J., COMUNIAN, T. A., MONTERO, P., FERRO-FURTADO, R. & FAVARO-TRINDADE, C. S. 2016. Encapsulation of an astaxanthin-containing lipid extract from shrimp waste by complex coacervation using a novel gelatin–cashew gum complex. *Food Hydrocolloids,* 61**,** 155-162.

GONNET, M., LETHUAUT, L. & BOURY, F. 2010. New trends in encapsulation of liposoluble vitamins. *J Control Release,* 146**,** 276-90.

GOVENDER, T., STOLNIK, S., GARNETT, M. C., ILLUM, L. & DAVIS, S. S. 1999. PLGA nanoparticles prepared by nanoprecipitation: drug loading and release studies of a water soluble drug. *J Control Release,* 57, 171-85.

GRAS, S. L., MAHMUD, T., ROSENGARTEN, G., MITCHELL, A. & KALANTAR-ZADEH, K. 2007. Intelligent Control of Surface Hydrophobicity. *ChemPhysChem,* 8, 2036-2050.

GUADAGNO, L., LONGO, P., RAIMONDO, M., NADDEO, C., MARICONDA, A., SORRENTINO, A., VITTORIA, V., IANNUZZO, G. & RUSSO, S. 2010. Cure Behavior and Mechanical Properties of Structural Self-Healing Epoxy Resins. *Journal of Polymer Science Part B: Polymer Physics,* 48, 2413-2423.

GUADAGNO, L., LONGO, P., RAIMONDO, M., NADDEO, C., MARICONDA, A., VITTORIA, V., IANNUZZO, G. & RUSSO, S. 2011. Use of Hoveyda–Grubbs' second generation catalyst in self-healing epoxy mixtures. *Composites Part B: Engineering,* 42, 296-301.

GUADAGNO, L., RAIMONDO, M., NADDEO, C., LONGO, P. & MARICONDA, A. 2014a. Self-Healing Materials for Structural Applications. *Polymer Engineering & Science,* 54.

GUADAGNO, L., RAIMONDO, M., NADDEO, C., LONGO, P., MARICONDA, A. & BINDER, W. 2014b. Healing efficiency and dynamic mechanical properties of self-healing epoxy systems. *Smart Materials and Structures,* 23, 045001.

GUADAGNO, L., RAIMONDO, M., VIETRI, U., NADDEO, C., STOJANOVIC, A., SORRENTINO, A. & BINDER, W. 2016. Evaluation of the Mechanical Properties of Microcapsule-Based Self-Healing Composites. *International Journal of Aerospace Engineering,* 2016, 1-10.

GUADAGNO, L., VERTUCCIO, L., NADDEO, C., CALABRESE, E., BARRA, G., RAIMONDO, M., SORRENTINO, A., BINDER, W., MICHAEL, P. & RANA, S. 2018. Self-healing epoxy nanocomposites via reversible hydrogen bonding.

GUAMÁN-BALCÁZAR, M. C., MONTES, A., PEREYRA, C. & MARTÍNEZ DE LA OSSA, E. 2019. Production of submicron particles of the antioxidants of mango leaves/PVP by supercritical antisolvent extraction process. *The Journal of Supercritical Fluids,* 143, 294-304.

HANDFORD, C. E., DEAN, M., HENCHION, M., SPENCE, M., ELLIOTT, C. T. & CAMPBELL, K. 2014. Implications of nanotechnology for the agri-food industry: Opportunities, benefits and risks. *Trends in Food Science & Technology,* 40, 226-241.

HARGOU, K., PINGKARAWAT, K., MOURITZ, A. P. & WANG, C. H. 2013. Ultrasonic activation of mendable polymer for self-healing carbon–epoxy laminates. *Composites Part B: Engineering,* 45**,** 1031-1039.

HESKINS, M. & GUILLET, J. E. 1968. Solution Properties of Poly(N-isopropylacrylamide). *Journal of Macromolecular Science: Part A - Chemistry,* 2**,** 1441-1455.

HSU, S. M. 2004. Molecular basis of lubrication. *Tribology International,* 37**,** 553-559.

HSU, S. M. & ZHAO, F. 2017. Microencapsulation of chemical additives. Google Patents.

HU, J. & LIU, S. 2010. Responsive Polymers for Detection and Sensing Applications: Current Status and Future Developments. *Macromolecules,* 43**,** 8315-8330.

HUCKER, M. J., BOND, I. P., FOREMAN, A. & HUDD, J. 1999. Optimisation of hollow glass fibres and their composites. *Advanced Composites Letters,* 8, No.4**,** 181-189.

HUGLIN, M. B. & RADWAN, M. A. 1991. Unperturbed dimensions of a zwitterionic polymethacrylate. *Polymer International,* 26**,** 97-104.

HYUN, J., LEE, W.-K., NATH, N., CHILKOTI, A. & ZAUSCHER, S. 2004. Capture and release of proteins on the nanoscale by stimuli-responsive elastin-like polypeptide "switches". *Journal of the American Chemical Society,* 126**,** 7330-7335.

IONOV, L., HOUBENOV, N., SIDORENKO, A., STAMM, M. & MINKO, S. 2009. Stimuli-responsive command polymer surface for generation of protein gradients. *Biointerphases,* 4**,** FA45-FA49.

ITOH, Y., MATSUSAKI, M., KIDA, T. & AKASHI, M. 2006. Enzyme-Responsive Release of Encapsulated Proteins from Biodegradable Hollow Capsules. *Biomacromolecules,* 7**,** 2715-2718.

J. ZUIDAM, N. & NEDOVIC, V. 2010. *Encapsulation Technologies for Active Food Ingredients and Food Processing*.

JANISZEWSKA-TURAK, E. 2017. Carotenoids microencapsulation by spray drying method and supercritical micronization. *Food Res Int,* 99**,** 891-901.

JEONG, B., BAE, Y. H., LEE, D. S. & KIM, S. W. 1997. Biodegradable block copolymers as injectable drug-delivery systems. *Nature,* 388**,** 860.

JIANG, H. Y., KELCH, S. & LENDLEIN, A. 2006. Polymers Move in Response to Light. *Advanced Materials,* 18**,** 1471-1475.

JIANG, J., QI, B., LEPAGE, M. & ZHAO, Y. 2007. Polymer Micelles Stabilization on Demand through Reversible Photo-Cross-Linking. *Macromolecules,* 40**,** 790-792.

JOYE, I. J., DAVIDOV-PARDO, G. & MCCLEMENTS, D. J. 2014. Nanotechnology for increased micronutrient bioavailability. *Trends in Food Science & Technology,* 40, 168-182.

KAUFFMAN, G. B. 1988. Polymer pioneers: a popular history of the science and technology of large molecules (Morris, Peter J.T.). *Journal of Chemical Education,* 65, A301.

KAWAGUCHI, S. & ITO, K. 2005. Dispersion Polymerization. *In:* OKUBO, M. (ed.) *Polymer Particles: -/-.* Berlin, Heidelberg: Springer Berlin Heidelberg.

KHALID, N. & BARROW, C. 2018. Critical review of encapsulation methods for stabilization and delivery of astaxanthin. 1.

KIM, S. Y. & LEE, S. C. 2009. Thermo-responsive injectable hydrogel system based on poly (N-isopropylacrylamide-co-vinylphosphonic acid). I. Biomineralization and protein delivery. *Journal of applied polymer science,* 113, 3460-3469.

KIMURA, T., AGO, H., TOBITA, M., OHSHIMA, S., KYOTANI, M. & YUMURA, M. 2002. Polymer Composites of Carbon Nanotubes Aligned by a Magnetic Field. *Advanced Materials,* 14, 1380-1383.

KING, M. B., MUBARAK, A., KIM, J. D. & BOTT, T. R. 1992. The mutual solubilities of water with supercritical and liquid carbon dioxides. *The Journal of Supercritical Fluids,* 5, 296-302.

KLUGE, J., FUSARO, F., CASAS, N., MAZZOTTI, M. & MUHRER, G. 2009a. Production of PLGA micro- and nanocomposites by supercritical fluid extraction of emulsions: I. Encapsulation of lysozyme. *The Journal of Supercritical Fluids,* 50, 327-335.

KLUGE, J., FUSARO, F., MAZZOTTI, M. & MUHRER, G. 2009b. Production of PLGA micro- and nanocomposites by supercritical fluid extraction of emulsions: II. Encapsulation of Ketoprofen. *Journal of Supercritical Fluids,* 50, 336-343.

KOCAK, G., TUNCER, C. & BÜTÜN, V. 2017. pH-Responsive polymers. *Polymer Chemistry,* 8, 144-176.

KOERNER, H., PRICE, G., PEARCE, N. A., ALEXANDER, M. & VAIA, R. A. 2004. Remotely actuated polymer nanocomposites—stress-recovery of carbon-nanotube-filled thermoplastic elastomers. *Nature Materials,* 3, 115.

KOO, A. N., LEE, H. J., KIM, S. E., CHANG, J. H., PARK, C., KIM, C., PARK, J. H. & LEE, S. C. 2008. Disulfide-cross-linked PEG-poly(amino acid)s copolymer micelles for glutathione-mediated intracellular drug delivery. *Chemical Communications,* 6570-6572.

KUMAR, A., SRIVASTAVA, A., GALAEV, I. Y. & MATTIASSON, B. 2007. Smart polymers: Physical forms and bioengineering applications. *Progress in Polymer Science,* 32, 1205-1237.

LADEMANN, J., RICHTER, H., TEICHMANN, A., OTBERG, N., BLUME-PEYTAVI, U., LUENGO, J., WEISS, B., SCHAEFER, U.

F., LEHR, C.-M. & WEPF, R. 2007. Nanoparticles–an efficient carrier for drug delivery into the hair follicles. *European Journal of Pharmaceutics and Biopharmaceutics,* 66**,** 159-164.

LAFKA, T.-I., SINANOGLOU, V. & LAZOS, E. S. 2007. On the extraction and antioxidant activity of phenolic compounds from winery wastes. *Food Chemistry,* 104**,** 1206-1214.

LAI, N., QIN, X., YE, Z., PENG, Q., ZHANG, Y. & MING, Z. 2013. Synthesis and Evaluation of a Water-Soluble Hyperbranched Polymer as Enhanced Oil Recovery Chemical. *Journal of Chemistry,* 2013**,** 11.

LEE, J.-S., PARK, S.-A., CHUNG, D. & LEE, H. G. 2011. Encapsulation of astaxanthin-rich Xanthophyllomyces dendrorhous for antioxidant delivery. *International journal of biological macromolecules,* 49**,** 268-273.

LI, G., SONG, S., GUO, L. & MA, S. 2008. Self-assembly of thermo- and pH-responsive poly(acrylic acid)-b-poly(N-isopropylacrylamide) micelles for drug delivery. *Journal of Polymer Science Part A: Polymer Chemistry,* 46**,** 5028-5035.

LI, H., YU, G.-E., PRICE, C., BOOTH, C., HECHT, E. & HOFFMANN, H. 1997. Concentrated Aqueous Micellar Solutions of Diblock Copoly(oxyethylene/oxybutylene) E41B8: A Study of Phase Behavior. *Macromolecules,* 30**,** 1347-1354.

LI, P., ZHU, J., SUNINTABOON, P. & HARRIS, F. W. 2002. New Route to Amphiphilic Core−Shell Polymer Nanospheres: Graft Copolymerization of Methyl Methacrylate from Water-Soluble Polymer Chains Containing Amino Groups. *Langmuir,* 18**,** 8641-8646.

LI, Q., KIM, N. H., HUI, D. & LEE, J. H. 2013a. Effects of dual component microcapsules of resin and curing agent on the self-healing efficiency of epoxy. *Composites Part B: Engineering,* 55**,** 79-85.

LI, Q., MISHRA, A., KIM, N. H., KUILA, T., LAU, K. T. & LEE, J. 2013b. Effects of processing conditions of poly(methylmethacrylate) encapsulated liquid curing agent on the properties of self-healing composites. *Composites Part B Engineering,* 49**,** 6-15.

LIM, H. S., HAN, J. T., KWAK, D., JIN, M. & CHO, K. 2006. Photoreversibly Switchable Superhydrophobic Surface with Erasable and Rewritable Pattern. *Journal of the American Chemical Society,* 128**,** 14458-14459.

LIU, F. & URBAN, M. W. 2010. Recent advances and challenges in designing stimuli-responsive polymers. *Progress in Polymer Science,* 35**,** 3-23.

LIU, J.-H. & CHIU, Y.-H. 2010. Behaviors of self-assembled diblock copolymer with pendant photosensitive azobenzene segments.

*Journal of Polymer Science Part A: Polymer Chemistry,* 48**,** 1142-1148.

LIU, L., YANG, J.-P., JU, X.-J., XIE, R., YANG, L., LIANG, B. & CHU, L.-Y. 2009. Microfluidic preparation of monodisperse ethyl cellulose hollow microcapsules with non-toxic solvent. *Journal of Colloid and Interface Science,* 336**,** 100-106.

LIU, X.-Y., MU, X.-R., LIU, Y., LIU, H.-J., CHEN, Y., CHENG, F. & JIANG, S.-C. 2012. Hyperbranched Polymers with Thermoresponsive Property Highly Sensitive to Ions. *Langmuir,* 28**,** 4867-4876.

LOK, K. & OBER, C. 2011. Particle Size Control in Dispersion Polymerization of Polystyrene. *Canadian Journal of Chemistry,* 63**,** 209-216.

LOKSUWAN, J. 2007. Characteristics of microencapsulated β-carotene formed by spray drying with modified tapioca starch, native tapioca starch and maltodextrin. *Food hydrocolloids,* 21**,** 928-935.

LU, S., TIAN, C., WANG, X., CHEN, D., MA, K., LENG, J. & ZHANG, L. 2017. Health monitoring for composite materials with high linear and sensitivity GnPs/epoxy flexible strain sensors. *Sensors and Actuators A: Physical,* 267**,** 409-416.

LUTOLF, M. P., LAUER-FIELDS, J. L., SCHMOEKEL, H. G., METTERS, A. T., WEBER, F. E., FIELDS, G. B. & HUBBELL, J. A. 2003. Synthetic matrix metalloproteinase-sensitive hydrogels for the conduction of tissue regeneration: engineering cell-invasion characteristics. *Proc Natl Acad Sci U S A,* 100**,** 5413-8.

MA, M., GUO, L., ANDERSON, D. G. & LANGER, R. 2013. Bio-Inspired Polymer Composite Actuator and Generator Driven by Water Gradients. *Science,* 339**,** 186-189.

MACHADO JR, F. R., REIS, D. F., BOSCHETTO, D. L., BURKERT, J. F., FERREIRA, S. R., OLIVEIRA, J. V. & BURKERT, C. A. V. 2014. Encapsulation of astaxanthin from Haematococcus pluvialis in PHBV by means of SEDS technique using supercritical CO2. *Industrial Crops and Products,* 54**,** 17-21.

MARICONDA, A., LONGO, P., AGOVINO, A., GUADAGNO, L., SORRENTINO, A. & RAIMONDO, M. 2015. Synthesis of ruthenium catalysts functionalized graphene oxide for self-healing applications. *Polymer,* 69**,** 330-342.

MARTÍN, A. & COCERO, M. J. 2008. Micronization processes with supercritical fluids: Fundamentals and mechanisms. *Advanced Drug Delivery Reviews,* 60**,** 339-350.

MARTIN, L., LIPAROTI, S., DELLA PORTA, G., ADAMI, R., MARQUÉS, J. L., URIETA, J. S., MAINAR, A. M. & REVERCHON, E. 2013. Rotenone coprecipitation with

biodegradable polymers by supercritical assisted atomization. *The Journal of Supercritical Fluids,* 81**,** 48-54.

MARTÍNEZ RIVAS, C. J., TARHINI, M., BADRI, W., MILADI, K., GREIGE-GERGES, H., NAZARI, Q. A., GALINDO RODRÍGUEZ, S. A., ROMÁN, R. Á., FESSI, H. & ELAISSARI, A. 2017. Nanoprecipitation process: From encapsulation to drug delivery. *International Journal of Pharmaceutics,* 532**,** 66-81.

MATRAY, E., BOUFFET, A. & GONNEAUD, C. 2015. Additives for transmission oils. Google Patents.

MATSUMOTO, S., CHRISTIE, R. J., NISHIYAMA, N., MIYATA, K., ISHII, A., OBA, M., KOYAMA, H., YAMASAKI, Y. & KATAOKA, K. 2009. Environment-Responsive Block Copolymer Micelles with a Disulfide Cross-Linked Core for Enhanced siRNA Delivery. *Biomacromolecules,* 10**,** 119-127.

MCBRIDE-WRIGHT, M., MAITLAND, G. C. & TRUSLER, J. M. 2015. Viscosity and density of aqueous solutions of carbon dioxide at temperatures from (274 to 449) K and at pressures up to 100 MPa. *Journal of Chemical & Engineering Data,* 60**,** 171-180.

MENDES, P. M. 2008. Stimuli-responsive surfaces for bio-applications. *Chemical Society Reviews,* 37**,** 2512-2529.

MENESES, M. A., CAPUTO, G., SCOGNAMIGLIO, M., REVERCHON, E. & ADAMI, R. 2015. Antioxidant phenolic compounds recovery from Mangifera indica L. by-products by supercritical antisolvent extraction. *Journal of Food Engineering,* 163**,** 45-53.

MENG, H. & LI, G. 2013. A review of stimuli-responsive shape memory polymer composites. *Polymer,* 54**,** 2199-2221.

MEYERS, S. P. & BLIGH, D. 1981. Characterization of astaxanthin pigments from heat-processed crawfish waste. *Journal of Agricultural and Food Chemistry,* 29**,** 505-508.

MEZZOMO, N., DE PAZ, E., MARASCHIN, M., MARTÍN, Á., COCERO, M. J. & FERREIRA, S. R. 2012. Supercritical anti-solvent precipitation of carotenoid fraction from pink shrimp residue: Effect of operational conditions on encapsulation efficiency. *The Journal of Supercritical Fluids,* 66**,** 342-349.

MINAMI, I. 2017. Molecular science of lubricant additives. *Applied Sciences,* 7**,** 445.

MISHRA, D. K., JAIN, A. K. & JAIN, P. K. 2013. A review on various techniques of microencapsulation. *Int J Pharm Chem Sci,* 2**,** 962-968.

MITCHELL, K., NEVILLE, A., WALKER, G. M., SUTTON, M. R. & CAYRE, O. J. 2018. Synthesis and tribological testing of poly(methyl methacrylate) particles containing encapsulated organic friction modifier. *Tribology International,* 124**,** 124-133.

152

MORGAN, P. W. & KWOLEK, S. L. 1959. Interfacial polycondensation. II. Fundamentals of polymer formation at liquid interfaces. *Journal of Polymer Science,* 40**,** 299-327.

MORGAN, S. E. & MCCORMICK, C. L. 1990. Water-soluble polymers in enhanced oil recovery. *Progress in Polymer Science,* 15**,** 103-145.

MORI, H., HIRAO, A., NAKAHAMA, S. & SENSHU, K. 1994. Synthesis and Surface Characterization of Hydrophilic-Hydrophobic Block Copolymers Containing Poly(2,3-dihydroxypropyl methacrylate). *Macromolecules,* 27**,** 4093-4100.

MORI, Z. & ANARJAN, N. 2018. Preparation and characterization of nanoemulsion based β-carotene hydrogels. *Journal of food science and technology,* 55**,** 5014-5024.

MURTHY, P. S. & NAIDU, M. M. 2012. Recovery of Phenolic Antioxidants and Functional Compounds from Coffee Industry By-Products. *Food and Bioprocess Technology,* 5**,** 897-903.

NAIR, L. S. & LAURENCIN, C. T. 2007. Biodegradable polymers as biomaterials. *Progress in polymer science,* 32**,** 762-798.

NAIR, N. S., DASARI, A., YUE, Y. C. & NARASIMALU, S. 2017. Failure Behavior of Unidirectional Composites under Compression Loading: Effect of Fiber Waviness. *Materials,* 10.

NATH, N. & CHILKOTI, A. 2003. Fabrication of a reversible protein array directly from cell lysate using a stimuli-responsive polypeptide. *Analytical chemistry,* 75**,** 709-715.

NESARETNAM, K., LIM, E. J., REIMANN, K. & LAI, L. C. 2000. Effect of a carotene concentrate on the growth of human breast cancer cells and pS2 gene expression. *Toxicology,* 151**,** 117-126.

NI, W., CHENG, Y.-T. & GRUMMON, D. S. 2002. Recovery of microindents in a nickel–titanium shape-memory alloy: A "self-healing" effect. *Applied Physics Letters,* 80**,** 3310-3312.

NIHANT, N., SCHUGENS, C., GRANDFILS, C., JÉRÔME, R. & TEYSSIÉ, P. 1994. Polylactide Microparticles Prepared by Double Emulsion/Evaporation Technique. I. Effect of Primary Emulsion Stability. *Pharmaceutical Research,* 11**,** 1479-1484.

NOBUHIKO, Y., JUN, N., TERUO, O. & YASUHISA, S. 1993. Regulated release of drug microspheres from inflammation responsive degradable matrices of crosslinked hyaluronic acid. *Journal of Controlled Release,* 25**,** 133-143.

PAN, X., YAO, P. & JIANG, M. 2007. Simultaneous nanoparticle formation and encapsulation driven by hydrophobic interaction of casein-graft-dextran and β-carotene. *Journal of colloid and interface science,* 315**,** 456-463.

PANYA, A., KITTIPONGPITTAYA, K., LAGUERRE, M. L., BAYRASY, C., LECOMTE, J. R. M., VILLENEUVE, P., MCCLEMENTS, D. J. & DECKER, E. A. 2012. Interactions between α-tocopherol and

rosmarinic acid and its alkyl esters in emulsions: synergistic, additive, or antagonistic effect? *Journal of agricultural and food chemistry,* 60**,** 10320-10330.

PARASURAMAN, D. & SERPE, M. J. 2011. Poly (N-Isopropylacrylamide) Microgel-Based Assemblies for Organic Dye Removal from Water. *ACS Applied Materials & Interfaces,* 3**,** 4714-4721.

PARK, J.-Y. & SHIM, J.-J. 2003. Emulsion stability of PMMA particles formed by dispersion polymerization of methyl methacrylate in supercritical carbon dioxide. *The Journal of Supercritical Fluids,* 27**,** 297-307.

PERIGNON, C., ONGMAYEB, G., NEUFELD, R., FRERE, Y. & PONCELET, D. 2015. Microencapsulation by interfacial polymerisation: membrane formation and structure. *J Microencapsul,* 32**,** 1-15.

PHILIPPOVA, O. E. & KHOKHLOV, A. R. 2010. Smart polymers for oil production. *Petroleum Chemistry,* 50**,** 266-270.

PIACENTINI, E. 2016. Coacervation. *In:* DRIOLI, E. & GIORNO, L. (eds.) *Encyclopedia of Membranes.* Berlin, Heidelberg: Springer Berlin Heidelberg.

PRABHA, S. & LABHASETWAR, V. 2004. Nanoparticle-Mediated Wild-Type p53 Gene Delivery Results in Sustained Antiproliferative Activity in Breast Cancer Cells. *Molecular Pharmaceutics,* 1**,** 211-219.

PRASERTMANAKIT, S., PRAPHAIRAKSIT, N., CHIANGTHONG, W. & MUANGSIN, N. 2009. Ethyl Cellulose Microcapsules for Protecting and Controlled Release of Folic Acid. *AAPS PharmSciTech,* 10**,** 1104.

PRIAMO, W. L., DE CEZARO, A. M., BENETTI, S. C., OLIVEIRA, J. V. & FERREIRA, S. R. S. 2011. In vitro release profiles of β-carotene encapsulated in PHBV by means of supercritical carbon dioxide micronization technique. *The Journal of Supercritical Fluids,* 56**,** 137-143.

PROSAPIO, V., REVERCHON, E. & DE MARCO, I. 2015. Coprecipitation of Polyvinylpyrrolidone/β-Carotene by Supercritical Antisolvent Processing. *Industrial & Engineering Chemistry Research,* 54**,** 11568-11575.

PROTA, L., SANTORO, A., BIFULCO, M., AQUINO, R., MENCHERINI, T. & RUSSO, P. 2011. Leucine enhances aerosol performance of Naringin dry powder and its activity on cystic fibrosis airway epithelial cells. *International journal of pharmaceutics,* 412**,** 8-19.

RAIMONDO, M., DE NICOLA, F., VOLPONI, R., BINDER, W., MICHAEL, P., RUSSO, S. & GUADAGNO, L. 2016. Self-repairing CFRPs targeted towards structural aerospace applications. *International Journal of Structural Integrity,* 7.

154

RAIMONDO, M., LONGO, P., MARICONDA, A. & GUADAGNO, L. 2015. Healing agent for the activation of self-healing function at low temperature. *Advanced Composite Materials,* 24**,** 519-529.

RECHARLA, N., RIAZ, M., KO, S. & PARK, S. 2017. Novel technologies to enhance solubility of food-derived bioactive compounds: A review. *Journal of Functional Foods,* 39**,** 63-73.

REVERCHON, E., ADAMI, R., CAMPARDELLI, R., DELLA PORTA, G., DE MARCO, I. & SCOGNAMIGLIO, M. 2015. Supercritical fluids based techniques to process pharmaceutical products difficult to micronize: Palmitoylethanolamide. *The Journal of Supercritical Fluids,* 102**,** 24-31.

REVERCHON, E., ADAMI, R., CARDEA, S. & PORTA, G. D. 2009. Supercritical fluids processing of polymers for pharmaceutical and medical applications. *The Journal of Supercritical Fluids,* 47**,** 484-492.

REVERCHON, E. & DELLA PORTA, G. 2003. Micronization of antibiotics by supercritical assisted atomization. *The Journal of Supercritical Fluids,* 26**,** 243-252.

RIBEIRO, S. M. R., QUEIROZ, J. H., DE QUEIROZ, M. E. L. R., CAMPOS, F. M. & SANT'ANA, H. M. P. 2007. Antioxidant in mango (Mangifera indica L.) pulp. *Plant Foods for Human Nutrition,* 62**,** 13-17.

RIZVI, S. Q. 2003. Additives and additive chemistry. *In Fuels and Lubricants Handbook: Technology, Properties, Performance, and Testing***,** 199-248.

RODRÍDUEZ-HUEZO, M., PEDROZA-ISLAS, R., PRADO-BARRAGÁN, L., BERISTAIN, C. & VERNON-CARTER, E. 2004. Microencapsulation by spray drying of multiple emulsions containing carotenoids. *Journal of Food Science,* 69**,** 351-359.

SABIRZYANOV, A. N., IL'IN, A. P., AKHUNOV, A. R. & GUMEROV, F. M. 2002. Solubility of Water in Supercritical Carbon Dioxide. *High Temperature,* 40**,** 203-206.

SAHOO, S. K. & LABHASETWAR, V. 2005. Enhanced antiproliferative activity of transferrin-conjugated paclitaxel-loaded nanoparticles is mediated via sustained intracellular drug retention. *Molecular pharmaceutics,* 2**,** 373-383.

SALGADO-RODRíGUEZ, R., LICEA-CLAVERíE, A. & ARNDT, K. F. 2004. Random copolymers of N-isopropylacrylamide and methacrylic acid monomers with hydrophobic spacers: pH-tunable temperature sensitive materials. *European Polymer Journal,* 40**,** 1931-1946.

SALONEN, A., LANGEVIN, D. & PERRIN, P. 2010. Light and temperature bi-responsive emulsion foams. *Soft Matter,* 6**,** 5308-5311.

SANTORO, A., BIANCO, G., PICERNO, P., AQUINO, R. P., AUTORE, G., MARZOCCO, S., GAZZERRO, P., LIOI, M. B. & BIFULCO, M. 2008. Verminoside- and verbascoside-induced genotoxicity on human lymphocytes: Involvement of PARP-1 and p53 proteins. *Toxicology Letters,* 178**,** 71-76.

SANTOS, D. T., MARTÍN, Á., MEIRELES, M. A. A. & COCERO, M. J. 2012. Production of stabilized sub-micrometric particles of carotenoids using supercritical fluid extraction of emulsions. *The Journal of Supercritical Fluids,* 61**,** 167-174.

SCITA, G. 1992. Stability of beta-carotene under different laboratory conditions. *Methods Enzymol,* 213**,** 175-85.

SEABRA, L. M. A. J. & PEDROSA, L. F. C. 2010. Astaxanthin: structural and functional aspects. *Revista de Nutrição,* 23**,** 1041-1050.

SENSHU, K., KOBAYASHI, M., IKAWA, N., YAMASHITA, S., HIRAO, A. & NAKAHAMA, S. 1999. Relationship between Morphology of Microphase-Separated Structure and Phase Restructuring at the Surface of Poly[2-hydroxyethyl methacrylate-block-4-(7'-octenyl)styrene] Diblock Copolymers Corresponding to Environmental Change. *Langmuir,* 15**,** 1763-1769.

SHAMSIJAZEYI, H., MILLER, C. A., WONG, M. S., TOUR, J. M. & VERDUZCO, R. 2014. Polymer-coated nanoparticles for enhanced oil recovery. *Journal of Applied Polymer Science,* 131.

SHARMA, S., KAUR, P., JAIN, A., RAJESWARI, M. R. & GUPTA, M. N. 2003. A smart bioconjugate of chymotrypsin. *Biomacromolecules,* 4**,** 330-336.

SHENOY, D., LITTLE, S., LANGER, R. & AMIJI, M. 2005. Poly(Ethylene Oxide)-Modified Poly($\beta$-Amino Ester) Nanoparticles as a pH-Sensitive System for Tumor-Targeted Delivery of Hydrophobic Drugs: Part 2. In Vivo Distribution and Tumor Localization Studies. *Pharmaceutical Research,* 22**,** 2107-2114.

SHIRAISHI, Y., MIYAMOTO, R. & HIRAI, T. 2009. Spiropyran-Conjugated Thermoresponsive Copolymer as a Colorimetric Thermometer with Linear and Reversible Color Change. *Organic Letters,* 11**,** 1571-1574.

SIEPMANN, J. & SIEPMANN, F. 2008. Mathematical modeling of drug delivery. *International Journal of Pharmaceutics,* 364**,** 328-343.

SMITH, R. L., YAMAGUCHI, T., SATO, T., SUZUKI, H. & ARAI, K. 1998. Volumetric behavior of ethyl acetate, ethyl octanoate, ethyl laurate, ethyl linoleate, and fish oil ethyl esters in the presence of supercritical CO2. *The Journal of Supercritical Fluids,* 13**,** 29-36.

SONG, K. C., LEE, H. S., CHOUNG, I. Y., CHO, K. I., AHN, Y. & CHOI, E. J. 2006. The effect of type of organic phase solvents on the particle size of poly (d, l-lactide-co-glycolide) nanoparticles.

*Colloids and Surfaces A: Physicochemical and Engineering Aspects,* 276**,** 162-167.

SONG, Y. K., LEE, T., KIM, J. C., CHEOL LEE, K., LEE, S.-H., MAN NOH, S. & PARK, Y. I. 2019. Dual Monitoring of Cracking and Healing in Self-healing Coatings Using Microcapsules Loaded with Two Fluorescent Dyes. *Molecules,* 24**,** 1679.

SOVOVA, H., JEZ, J. & KHACHATURYAN, M. 1997. Solubility of squalane, dinonyl phthalate and glycerol in supercritical CO2. *Fluid Phase Equilibria,* 137**,** 185-191.

SPINELLI, G., LAMBERTI, P., TUCCI, V., VERTUCCIO, L. & GUADAGNO, L. 2018. Experimental and theoretical study on piezoresistive properties of a structural resin reinforced with carbon nanotubes for strain sensing and damage monitoring. *Composites Part B: Engineering,* 145**,** 90-99.

STEVANOVIĆ, M., SAVIĆ, J., JORDOVIĆ, B. & USKOKOVIĆ, D. 2007. Fabrication, in vitro degradation and the release behaviours of poly (DL-lactide-co-glycolide) nanospheres containing ascorbic acid. *Colloids and Surfaces B: Biointerfaces,* 59**,** 215-223.

STEVANOVIC, M. & USKOKOVIC, D. 2009. Poly (lactide-co-glycolide)-based micro and nanoparticles for the controlled drug delivery of vitamins. *Current Nanoscience,* 5**,** 1-14.

TARVER, T. 2008. "Just add water": regulating and protecting the most common ingredient. *Journal of food science,* 73**,** R1-R13.

TEMELLI, F. 2018. Perspectives on the use of supercritical particle formation technologies for food ingredients. *The Journal of Supercritical Fluids,* 134**,** 244-251.

THEATO, P. 2011. One is Enough: Influencing Polymer Properties with a Single Chromophoric Unit. *Angewandte Chemie International Edition,* 50**,** 5804-5806.

TIRADO, D. F., PALAZZO, I., SCOGNAMIGLIO, M., CALVO, L., DELLA PORTA, G. & REVERCHON, E. 2019a. Astaxanthin encapsulation in ethyl cellulose carriers by continuous supercritical emulsions extraction: A study on particle size, encapsulation efficiency, release profile and antioxidant activity. *Journal of Supercritical Fluids,* 150**,** 128-136.

TIRADO, D. F., PALAZZO, I., SCOGNAMIGLIO, M., CALVO, L., DELLA PORTA, G. & REVERCHON, E. 2019b. Astaxanthin encapsulation in ethyl cellulose carriers by continuous supercritical emulsions extraction: A study on particle size, encapsulation efficiency, release profile and antioxidant activity. *The Journal of Supercritical Fluids,* 150**,** 128-136.

TOMASSI, G. & SILANO, V. 1986. An assessment of the safety of tocopherols as food additives. *Food and Chemical Toxicology,* 24**,** 1051-1061.

TRENOR, S. R., SHULTZ, A. R., LOVE, B. J. & LONG, T. E. 2004. Coumarins in Polymers: From Light Harvesting to Photo-Cross-Linkable Tissue Scaffolds. *Chemical Reviews,* 104**,** 3059-3078.

TRIPATHI, A. K. & VINU, R. 2015. Characterization of thermal stability of synthetic and semi-synthetic engine oils. *Lubricants,* 3**,** 54-79.

TROMBINO, S., CASSANO, R., MUZZALUPO, R., PINGITORE, A., CIONE, E. & PICCI, N. 2009. Stearyl ferulate-based solid lipid nanoparticles for the encapsulation and stabilization of β-carotene and α-tocopherol. *Colloids and Surfaces B: Biointerfaces,* 72**,** 181-187.

TRUCILLO, E., BISCEGLIA, B., VALDRÈ, G., GIORDANO, E., REVERCHON, E., MAFFULLI, N. & DELLA PORTA, G. 2019a. Growth factor sustained delivery from poly-lactic-co-glycolic acid microcarriers and its mass transfer modeling by finite element in a dynamic and static three-dimensional environment bioengineered with stem cells. *Biotechnology and Bioengineering,* 116**,** 1777-1794.

TRUCILLO, P., CAMPARDELLI, R., SCOGNAMIGLIO, M. & REVERCHON, E. 2019b. Control of liposomes diameter at micrometric and nanometric level using a supercritical assisted technique. *Journal of CO2 Utilization,* 32**,** 119-127.

TUCKER, J. & TOWNSEND, D. 2005. Alpha-tocopherol: roles in prevention and therapy of human disease. *Biomedicine & pharmacotherapy,* 59**,** 380-387.

TURNER, S. R., LUNDBERG, R. D. & WALKER, T. O. 1984. *Drilling fluids based on sulfonated elastomeric polymers.*

URBAN, M. W. 2006. Intelligent Polymeric Coatings; Current and Future Advances. *Journal of Macromolecular Science, Part C,* 46**,** 329-339.

URBAN, M. W. 2009. Stratification, stimuli-responsiveness, self-healing, and signaling in polymer networks. *Progress in Polymer Science,* 34**,** 679-687.

VERTUCCIO, L., GUADAGNO, L., SPINELLI, G., LAMBERTI, P., ZARRELLI, M., RUSSO, S. & IANNUZZO, G. 2018. Smart coatings of epoxy based CNTs designed to meet practical expectations in aeronautics. *Composites Part B: Engineering,* 147**,** 42-46.

WANG, F., LAI, Y.-H. & HAN, M.-Y. 2004. Stimuli-Responsive Conjugated Copolymers Having Electro-Active Azulene and Bithiophene Units in the Polymer Skeleton: Effect of Protonation and p-Doping on Conducting Properties. *Macromolecules,* 37**,** 3222-3230.

WEBSTER, M. N., SHOUGH, A. M., OXLEY, J. D. & MENDEZ, J. L. 2019. Lubricating oil compositions containing microencapsulated additives. Google Patents.

WEVER, D. A. Z., PICCHIONI, F. & BROEKHUIS, A. A. 2011. Polymers for enhanced oil recovery: A paradigm for structure–property relationship in aqueous solution. *Progress in Polymer Science,* 36**,** 1558-1628.

WHITE, S. R., SOTTOS, N. R., GEUBELLE, P. H., MOORE, J. S., KESSLER, M. R., SRIRAM, S. R., BROWN, E. N. & VISWANATHAN, S. 2001. Autonomic healing of polymer composites. *Nature,* 409**,** 794-797.

WILLIAMS, K., BOYDSTON, A. & W BIELAWSKI, C. 2007. Towards electrically conductive, self-healing materials. *Journal of the Royal Society, Interface / the Royal Society,* 4**,** 359-62.

WU, D. Y., MEURE, S. & SOLOMON, D. 2008. Self-healing polymeric materials: A review of recent developments. *Progress in Polymer Science,* 33**,** 479-522.

WU, J.-J., SHEN, C.-T., JONG, T.-T., YOUNG, C.-C., YANG, H.-L., HSU, S.-L., CHANG, C.-M. J. & SHIEH, C.-J. 2009. Supercritical carbon dioxide anti-solvent process for purification of micronized propolis particulates and associated anti-cancer activity. *Separation and Purification Technology,* 70**,** 190-198.

WU, L., WANG, M., SINGH, V., LI, H., GUO, Z., GUI, S., YORK, P., XIAO, T., YIN, X. & ZHANG, J. 2017. Three dimensional distribution of surfactant in microspheres revealed by synchrotron radiation X-ray microcomputed tomography. *Asian Journal of Pharmaceutical Sciences,* 12**,** 326-334.

XIA, F., ZHU, Y., FENG, L. & JIANG, L. 2009. Smart responsive surfaces switching reversibly between super-hydrophobicity and super-hydrophilicity. *Soft Matter,* 5**,** 275-281.

XIN, B. & HAO, J. 2010. Reversibly switchable wettability. *Chemical Society Reviews,* 39**,** 769-782.

XU, C., WU, T., DRAIN, C. M., BATTEAS, J. D., FASOLKA, M. J. & BEERS, K. L. 2006. Effect of Block Length on Solvent Response of Block Copolymer Brushes: Combinatorial Study with Block Copolymer Brush Gradients. *Macromolecules,* 39**,** 3359-3364.

XULU, P. M., FILIPCSEI, G. & ZRÍNYI, M. 2000. Preparation and Responsive Properties of Magnetically Soft Poly(N-isopropylacrylamide) Gels. *Macromolecules,* 33**,** 1716-1719.

YANG, J., KELLER, M. W., MOORE, J. S., WHITE, S. R. & SOTTOS, N. R. 2008. Microencapsulation of Isocyanates for Self-Healing Polymers. *Macromolecules,* 41**,** 9650-9655.

YANG, Y., ZHANG, B., WANG, Y., YUE, L., LI, W. & WU, L. 2013. A Photo-driven Polyoxometalate Complex Shuttle and Its Homogeneous Catalysis and Heterogeneous Separation. *Journal of the American Chemical Society,* 135**,** 14500-14503.

YANG, Y. Y., CHIA, H. H. & CHUNG, T. S. 2000. Effect of preparation temperature on the characteristics and release profiles of PLGA microspheres containing protein fabricated by double-emulsion solvent extraction/evaporation method. *Journal of Controlled Release,* 69**,** 81-96.

YANG, Y. Y., CHUNG, T. S. & NG, N. P. 2001. Morphology, drug distribution, and in vitro release profiles of biodegradable polymeric microspheres containing protein fabricated by double-emulsion solvent extraction/evaporation method. *Biomaterials,* 22**,** 231-241.

YOUNES, M., AGGETT, P., AGUILAR, F., CREBELLI, R., DI DOMENICO, A., DUSEMUND, B., FILIPIČ, M., JOSE FRUTOS, M. & GALTIER, P. 2018. Re-evaluation of celluloses E 460 (i), E 460 (ii), E 461, E 462, E 463, E 464, E 465, E 466, E 468 and E 469 as food additives. *EFSA Journal,* 16**,** e05047.

ZHANG, F., FAN, J.-B. & WANG, S. 2020. Interfacial Polymerization: From Chemistry to Functional Materials. *Angewandte Chemie International Edition,* 59**,** 21840-21856.

ZHANG, H., CUI, W., BEI, J. & WANG, S. 2006a. Preparation of poly (lactide-co-glycolide-co-caprolactone) nanoparticles and their degradation behaviour in aqueous solution. *Polymer degradation and stability,* 91**,** 1929-1936.

ZHANG, J., LIU, H.-J., YUAN, Y., JIANG, S., YAO, Y. & CHEN, Y. 2013. Thermo-, pH-, and Light-Responsive Supramolecular Complexes Based on a Thermoresponsive Hyperbranched Polymer. *ACS Macro Letters,* 2**,** 67-71.

ZHANG, J., LU, X., HUANG, W. & HAN, Y. 2005. Reversible Superhydrophobicity to Superhydrophilicity Transition by Extending and Unloading an Elastic Polyamide Film. *Macromolecular Rapid Communications,* 26**,** 477-480.

ZHANG, J. X. & ZHU, K. J. 2004. An improvement of double emulsion technique for preparing bovine serum albumin-loaded PLGA microspheres. *Journal of Microencapsulation,* 21**,** 775-785.

ZHANG, L., XU, T. & LIN, Z. 2006b. Controlled release of ionic drug through the positively charged temperature-responsive membranes. *Journal of Membrane Science,* 281**,** 491-499.

ZHANG, P. & OMAYE, S. T. 2000. Beta-carotene and protein oxidation: effects of ascorbic acid and alpha-tocopherol. *Toxicology,* 146**,** 37-47.

ZHAO, Q., DUNLOP, J. W. C., QIU, X., HUANG, F., ZHANG, Z., HEYDA, J., DZUBIELLA, J., ANTONIETTI, M. & YUAN, J. 2014. An instant multi-responsive porous polymer actuator driven by solvent molecule sorption. *Nature Communications,* 5**,** 4293.

ZHU, D. Y., RONG, M. Z. & ZHANG, M. Q. 2015. Self-healing polymeric materials based on microencapsulated healing agents: From design to preparation. *Progress in Polymer Science,* 49-50**,** 175-220.

ZHUANG, J., GORDON, M. R., VENTURA, J., LI, L. & THAYUMANAVAN, S. 2013. Multi-stimuli responsive macromolecules and their assemblies. *Chemical Society Reviews,* 42**,** 7421-7435.

ZRÍNYI, M. 2000. Intelligent polymer gels controlled by magnetic fields. *Colloid and Polymer Science,* 278**,** 98-103.